Multidentate coordination and microscopic metal complexation of Cyclo-μ-imidotriphosphate Anions.

Maki, Hideshi

(Degree)
博士 (理学)

(Date of Degree)
2004-03-12

(Date of Publication)
2013-05-31

(Resource Type)
doctoral thesis

(Report Number)
乙2743

(URL)
https://hdl.handle.net/20.500.14094/D2002743

神戸大学博士論文

Multidentate Coordination and Microscopic Metal Complexation of Cyclo-μ-imidotriphosphate Anions.

環状イミド三リン酸イオン群の多座配位及び

微視的錯生成挙動に関する研究

平成16年3月

牧　秀志

Department of Chemical Science and Engineering

Faculty of Engineering

Kobe University

Hideshi Maki

Contents

Chapter 4.

^{27}Al NMR Study on Multidentate Complexation Behavior of Cyclo-μ-imidotriphosphate Anions in Aqueous Solution.

Chapter 5.

^9Be and ^{31}P NMR Analyses on Be^{2+} Complexation With Cyclo-tri-μ-imidotriphosphate Anions in Aqueous Solution.

Chapter 6.

On the Protonation Behavior of Several Monothiophosphate Anions.

Chapter 7.

       General Conclusion

Acknowledgements

CHAPTER 1

General Introduction

A great deal of effort has been made on the complexation behaviors and coordination structures of the cyclic poly aza ligands, *i.e.*, azacrown ethers and cryptands, as cyclic ligands which have oxygen and nitrogen donors. Considerable attention has been given on the effect of the variations of macrocyclic ring size and pendant donor groups, however, the influence of the number of the bridging donor has not so far been investigated. The bridging imino nitrogen atoms in a *cyclo*-tri-μ-imidotriphosphate anion, $cP_3(NH)_3^{3-}$ as can be seen in Fig. 1-1, is easily substituted with a oxygen atom by rapid hydrolysis right after decyclization of the ligand, so the $cP_3(NH)_n^{3-}$ (n = 0-3, Fig. 1-1) ligands can provide opportunity to study the influence of the increasing number of bridging donors on the stability and coordination structures of metal complexes.

Cyclo-triphosphate anion, cP_3^{3-}, contains just P-O-P linkages which is well known as a representative cyclic polyphosphate anion. Considerable number of studies have been made on the complexation mechanisms of cP_3^{3-} anions [1,2], and the complexation mechanisms seem to be not so complicated, because this anion contains only non-bridging oxygen atoms as a coordinating atom. The molecular structures of a series of *cyclo*-μ-imidotriphosphate anions, *i.e.*, $cP_3(NH)_n^{3-}$ (n = 0-3, Fig. 1-1), are rigid in various *cyclo*-phosphate anions. In particular, *cyclo*-tri-μ-imidotriphosphate anions, $cP_3(NH)_3^{3-}$, whose all phosphate units are linked by P-NH-P linkages contains the two types of total six coordination atoms which are non-bridging oxygen atoms and bridging nitrogen atoms, and it seems that electron-crowded donor nitrogen atoms form a specific binding site in the ring center of $cP_3(NH)_3$ molecule. It can be expected that $cP_3(NH)_3^{3-}$ anions coordinate to metal ions more peculiarly than cP_3^{3-} anions, because non-bridging oxygen atoms as well as bridging nitrogen atoms of the anion are able to coordinate to metal ions.

A large number of studies have been carried out on the equlibria of acid-dissociation and metal complexation of inorganic polyphosphate anions because of the fundamental and practical interest. Compared with the studies on polyphosphate molecules with P-O-P linkages[3-10], however, quite a limited number of researches have been carried out on imidopolyphosphate molecules[11-24], which contain P-NH-P linkages in the polymeric structure. Since the

imidopolyphosphate anions contain non-bridging oxygen atoms as well as bridging nitrogen atoms as possible coordinating atoms, and since the molecules with P-NH-P linkage can produce tautomeric structures[21-24], the comparison of the complexation behaviors of the two ligand families, *i.e.*, with P-O-P bond(s) and P-NH-P bond(s) is of particular interest.

The general composition $cP_n(NH)_n{}^{n-}$ with $n = 3, 4,$ are a good example for tautomerism in inorganic compounds as can be seen in Scheme 1-1. Extensive IR and Raman spectroscopic investigations have been conducted to find out in which of the two tautomeric forms, the $cP_3(NH)_3{}^{3-}$ anions exists[25-28]. The polymetaphosphinates can be formally deduced from the *cyclo*-tri- and *cyclo*-tetraphosphoric acid by substitution of all ring oxygens by imido groups. The formal partial substitution of one or two O^{2-} by NH^{2-} in the *cyclo*-tri-μ-imidotriphosphate leads to *cyclo*-mono-μ-imidotriphosphate and *cyclo*-di-μ-imidotriphosphate, *i.e.*, $cP_3(NH)$ and $cP_3(NH)_2$. They are formed during the hydrolysis of the $cP_3(NH)_3{}^{3-}$ ions in aqueous solutions and were mainly characterized by ^{31}P NMR and IR spectroscopy[29-31]. In addition to this the synthesis and thermal behavior of sodium *cyclo*-mono-μ-imidotriphosphate and sodium *cyclo*-di-μ-imidotriphosphate has been described in detail[32].

Sparse works have been reported on the acid dissociation constants of the anions of mono-μ-imidodiphosphate and di-μ-imidotriphosphate and the stability constants of the complexes with mono-μ-imidodiphosphate, di-μ-imidotriphosphate, and *cyclo*-tri-μ-imidotriphosphate anions. However, no systematic work has been carried out on the protonation, tautomeric, and complexation equilibria of the series of these multidentate ligand molecules.

In Chapter 2 and 3, the protonation, tautomeric and complexation equilibria of the trimeric molecules, *i.e.*, cP_3, $cP_3(NH)$, $cP_3(NH)_2$, and $cP_3(NH)_3$, have been re-investigated precisely by use of a potentiometric titration technique together with a ^{31}P NMR method.

The acid-dissociation and metal complexation behaviors of imidodiphosphate anions (Scheme 1-2-I) as well as the ATP analog 5'-adenyl imidodiphosphate anions (Scheme 1-2-II), have been studied[13-19], since the latter ligand has been proven to be a competitive inhibitor of adenosine triphosphatase. Direct coordination of nitrogen atoms of 5'-adenyl imidodiphosphate anions to Mg^{2+} has been suggested[20,21], which might stabilize the imino tautomers. Since a *cyclo*-tri-μ-imidotriphosphate anions (Scheme 1-2-III), $cP_3(NH)_3{}^{3-}$, is composed of three P-NH-P linkages in the cyclic structure, *i.e.*, it contains three nitrogen atoms as well as three oxygen atoms

as possible coordinating atoms, this ligand seems suitable for the coordination study to examine the direct metal coordination with nitrogen atoms of imidopolyphosphate anions. Also, since it has already been indicated by our previous works that combination of metal NMR and ^{31}P NMR measurements provides straightforward information on the microscopic coordination structures of the complexes with these multicoordinating ligand molecules in aqueous solution[33,34].

In Chapter 4, ^{27}Al NMR spectra of Al^{3+}-ligand mixture solutions have been obtained in order to determine of the structures of the complexes. ^{27}Al NMR method has the following advantageous aspects to this study. First, due to 100% isotopic abundance of ^{27}Al nuclei, the sensitivity of ^{27}Al NMR is high. Second, the chemical exchange rate in Al^{3+} complexation system is usually much slower than the ^{27}Al NMR time scale, separated peaks corresponding to the free and complexed species can be obtained in the ^{27}Al NMR spectra. Furthermore, the chemical shift value corresponding to the complexes changes linearly with an increase in the ligand coordination number[33]. Compared with this simplified peak assignment in the ^{27}Al NMR spectra obtained in the systems of Al^{3+}-polyphosphate complexation, the ^{31}P NMR peak assignment is rather complicated due to the ^{31}P-^{31}P spin-spin coupling and the absence of simplified relationship between the chemical shift and the coordination state. These aspects mentioned above enable us to determine the microscopic structures of Al^{3+}-cP$_3$(NH)$_n$$^{3-}$ (n = 0-3) complexes. The concentrations of the free, and the monodentate, didentate, and tridentate ligand complexes can be calculated from the areas of the peaks separated from each other. ^{27}Al NMR spectra of mixture solutions of Al^{3+} and cP$_3$(NH)$_n$$^{3-}$ (n = 0-3) anions have been obtained and are analyzed by peak deconvolution. NMR peak area almost proportional to the number of nuclei, that is, the concentration of a species, and it leads to the quantitative information about a chemical equilibria, *i.e.* the estimation of the successive complex formation constants.

In recent years, beryllium metal has utilized as material for beryllium copper which is excellent in conductivity, corrosion resistance and spring characteristics. However, despite strong carcinogenicity, only few attempts have so far been made at the chemical properties of beryllium compounds and the complexation behavior of Be^{2+} ions in aqueous solutions. In this study, it has been expected that various multidentate complexation behavior such as the direct coordination structure of "hard" Be^{2+} ions to the imino nitrogen atoms which is interested in solution chemistry. Since the ratio of charge/ionic radius of Be^{2+} ions is quite close to Al^{3+} ions, it is of special

interest to study the complexation behavior of the Be^{2+}-$cP_3(NH)_3^{3-}$ system.

In Chapter 5, ^9Be and ^{31}P NMR spectra of the mixture solutions of Be^{2+} cations and $cP_3(NH)_3^{3-}$ anions of various compositions have been obtained and the complexation equilibria are analyzed by a peak deconvolution method and the successive complex formation constants are estimated in order to get the information on the microscopic complexation.

In recent years some studies have been made on monothiophosphate derivatives[35-37]. However, so far the study of the other thiophosphate, *i.e.*, di-, tri-, and tetrathiophosphates, and their derivatives have been scarce. It seems to be a cause that the acid-base properties and the complex formation behavior are hard to observe, since these thiophosphates are easy to hydrolyze in aqueous solution. This study is intended as an investigation of the protonation behaviors of not only a monothiophosphate anion but also di-, tri-, and tetrathiophosphates which are simple analogues of the several thiophosphate derivatives. It is considered that this information is useful for the interpretation of the protonation and the complex formation behavior of these derivatives. In Chapter 6, the protonation constants together with intrinsic chemical shifts of the phosphorus nuclei belonging to the thiomonophosphate anions *i.e.*, monothiomonophosphate anion, PO_3S^{3-}, dithiomonophosphate anion, $PO_2S_2^{3-}$, trithiomonophosphate anion, POS_3^{3-}, and tetrathiomonophosphate anion, PS_4^{3-} have been evaluated by means of the pH titration profiles of ^{31}P NMR chemical shifts of respective phosphorus nuclei. The direction and the magnitude of the shift changes of the respective phosphorus nuclei are compared with each other.
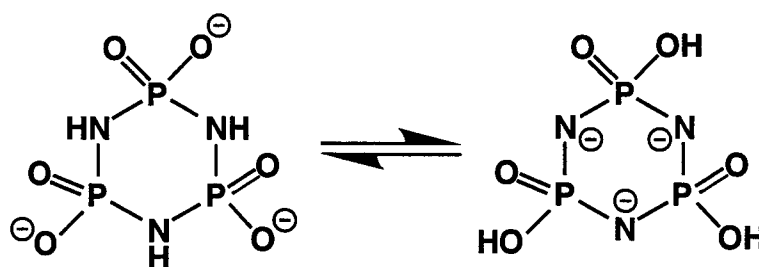
Scheme 1-1

Scheme 1-2

I II III
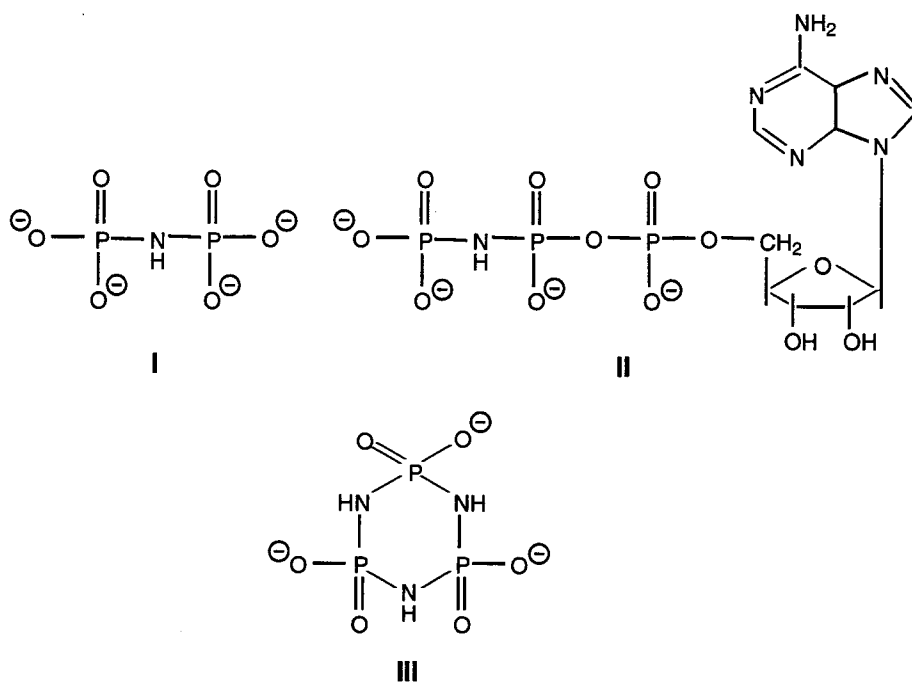
REFERENCES

1. L. G. Sillen and A. E. Martell, in *Stability Constants of Metal-ion Complexes.*, The Chemical Society, London, 1971, Special publication No. 25

2. R. M. Smith and A. E. Martell, in *Critical Stability Constants, Inorganic Complexes*, Plenum Press, New York, 1976, Vol. 4 E. Högfeldt, in *Stability Constants of Metai-ion Complexes, Part A: Inorganic Ligands.* Pergamon Press, Oxford, 1982.

3. R. M. Smith, A. E. Martell, In *Critical Stability Constants, Inorganic Complexes* Plenum Press: New York, 1976 Vol. 4.

4. E. Högfeldt, In *Stability Constants of Metai-ion Complexes, Part A: Inorganic Ligands* Pergamon Press: Oxford, 1982.

5. A. Sigel, H. Sigel, In *Metal Ions in Biological Systems (Interactions of Metal Ions with Nucleotides, Nucleic Acids, and Their Constituents)*, Marcel Dekker, Inc.: New York, 1996 Vol. 32, pp 1-814.

6. A. Sigel, H. Sigel, In *Metal Ions in Biological Systems (Probing of Nucleic Acids by Metal Ion Complexes of Small Molecules)*, Marcel Dekker, Inc.: New York, 1996 Vol. 33, pp 1-678.

7. T. Miyajima, H. Maki, H. Kodama, S. Ishiguro, H. Nariai, I. Motooka, *Phosphorus Res. Bull.*, 6, 281(1996).

8. J. Huskens, A. D. Kennedy, H. Bekkum, and J. A. Peters, *J. Am. Chem. Soc.*, 117, 375(1995).

9. B. Song, R. K. O. Sigel, H. Sigel, *Chem. Eur. J.*, 3, 29(1997).

10. H. Sigel, B. Song, *Met. Ions Biol. Syst.*, 32, 135(1996).

11. T. Miyajima, H. Maki, M. Sakurai, S. Sato, M. Watanabe, *Phosphorus Res. Bull.*, 3, 31(1993).

12. K. Komiya, T. Miyajima, M. Sakurai, S. Sato, M. Watanabe, *Phosphorus Res. Bull.*, 2, 33(1992).

13. M. Komiya, T. Miyajima, S. Sato, M. Watanabe, *Phosphorus Res. Bull.*, 1, 137(1991).

14. L. Riesel, G. Pich, and C. Ruby, *Anorg. Allg. Chem.*, 430, 227(1977).

15. S. Tran-Dinh, M. Roux, M. Ellenberger, *Nucleic Acids Res.*, 2, 1101(1975).

16. R. G. Yount, D. Babcock, W. Ballantyne, D. Ojala, *Biochemistry*, 10, 2484(1971).

17. M. Larsen, R. Willett, R. G. Yount, *Science*, 166, 1510(1969).

18. R. A. Chaplain, B. Frommelt, *Kybernetik*, 5, 1(1968).

19. M. L. Neilsen, R. R. Ferguson, W. S. Coakley, *J. Am. Chem. Soc.*, 83, 99(1961).

20. S. Tran-Dinh, M. Roux, *Eur. J. Biochem.*, 76, 245(1977).

21. M. A. Reynolds, J. A. Gerlt, P. C. Demou, N. J. Oppenheimer, G. L. Kenyon, *J. Am. Chem. Soc.*, 105, 6475(1983).

22. J. A. Gerlt, P. C. Demou, S. Mehdi, *J. Am. Chem. Soc.*, 104, 2848(1982).

23. M. K. Kabachnik, V. A. Gilyarov, E. M. Popov, *Izv. Akad. Nauk SSSR, Ser. Khim.*, 6, 1022(1961).

24. V. V. Kireev, G. C. Kolesnikov, S. S. Titov, *Zh. Obshch. Khim.*, 40, 2105(1970).

25. J. V. pustinger, W. T. Cave, N. L. Nielsen, *Spectrochim. Acta*, 11, 909(1959)

26. D. E. C. Corbridge, E. J. Lowe, *J. Chem. Soc.*, 4555(1954)

27. K. Lunkwitz, E. Steger, *Z. Anorg. Allg. Chem.*, 358, 111(1968)

28. E. Steger, K. Lunkwitz, *J. Mol. Struct.*, 3. 67(1969)

29. W. Wanek, V. Novobilsky, E. Thilo, *Z. Chem.*, 7, 109(1967)

30. A. Narath, F. H. Lohman, O. T. Quimby, *J. Am. Chem. Soc.*, 78, 4493(1956).

31. M. L. Nielsen, J. V. Pustinger, *J. Phys. Chem.*, 68, 152(1964)

32. M. Sakurai, M. Watanabe, *J. Mater. Sci.*, 29, 4897(1994)

33. T. Miyajima, R. Kakehashi, *Phosphorus Res. Bull.*, 1, 101(1991).

34. T. Miyajima, H. Maki, H. Kodama, S. Ishiguro, H. Nariai, I. Motooka. *Phosphorus Res. Bull.*, 6, 281(1996).

35. H. Kanehara, T. Wada, M. Mizuguchi and K. Makino, *Nucleosides and Nucleotides*, **15**, 1169(1996).

36. S. Tawata, S. Taira, H. Kikizu, N. Kobamoto, M. Ishihara and S. Toyama, *Biosci. Biotech. Biochem.*, **61**, 2103(1997).

37. A. Chive, B. Delfort, M. Born, L. Barre, Y. Chevalier and R. Gallo, *Langmuir*, **14**, 5355(1998).
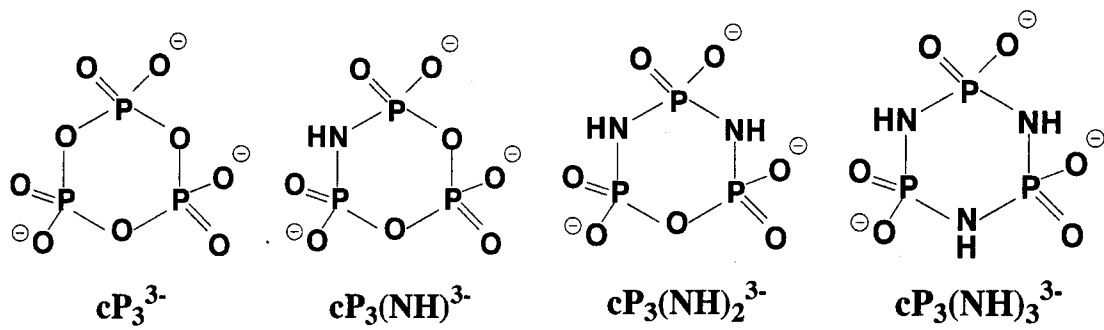
Fig. 1-1 Structures of the *cyclo*-μ-imidotriphosphate anions.

CHAPTER 2

On the protonation equilibria of *cyclo*-μ-imidotriphosphate anions.

ABSTRACT

Protonation equilibria of trimeric cyclic anions, *cyclo*-triphosphate, *cyclo*-mono-μ-imidotriphosphate, *cyclo*-di-μ-imidotriphosphate, and *cyclo*-tri-μ-imidotriphosphate have been investigated potentiometrically at $25 \pm 0.5°C$ under N_2 atmosphere. The first protonation constants of the anions increase with an increase in the number of the imino groups which constitute the ligand molecules. The increase in the basicity of the ligands can primarily be interpreted by the difference in the electronegativity of the bridging oxygen and nitrogen atoms, however, tautomerism of the imidophosphate bonding is also considered to be responsible to the enhancement of the H^+ ion binding ability of the imidopolyphosphate anions. ^{31}P NMR chemical shift changes upon protonation and deprotonation of respective anions have been measured in order to obtain microscopic information on the proton bindings. It has been revealed that hydrogen bonding is formed among the phosphate groups belonging to the cyclic trimers, probably due to proximity of the neighboring phosphate units fixed to rigid rings.

INTRODUCTION

Among inorganic polyphosphate anions, imidopolyphosphate anions, whose phosphate units are linked by P-NH-P linkage, have been paid special attentions from the view points of metal complexation in aqueous solutions, because these anions contain nitrogen atoms as well as oxygen atoms as coordinating atoms[1]. The group of imidopolyphosphate anions has linear structures such as mono-μ-imidodiphosphate and di-μ-imidotriphosphate, and has cyclic structures such as *cyclo*-mono-μ-imidotriphosphate(cP3(NH)), *cyclo*-di-μ-imidotriphosphate(cP3(NH)2), and *cyclo*-tri-μ-imidotriphosphate(cP3(NH)3). The structures of the trimeric cyclic anions have been reported in the literature[1]. Sparse works have been reported on the acid dissociation constants of the anions of mono-μ-imidodiphosphate and di-μ-imidotriphosphate[2] and the stability constants of the complexes with mono-μ-

imidodiphosphate, di-μ-imidotriphosphate[3], and *cyclo*-tri-μ-imidotriphosphate anions[4]. However, no systematic work has been carried out on the protonation and complexation equilibria of the series of these multidentate ligand molecules.

Recently, we have reported preliminary experimental results[1, 5, 6] on the ion-binding equilibria of the cyclic imidopolyphosphate anions: the protonation constants estimated by ^{31}P NMR chemical shift measurements and the stability constants of the complexes with divalent metal ions evaluated by electrochemical methods increase with the number of the P-NH-P linkages in the ligand molecules. Also, it was found that the stability constants of the one-to-one complexes with divalent metal ions are greatly dependent on the nature of the metal ions, though such a substantial difference in the constants has never been observed in the complexation systems with *cyclo*-triphosphate anions (cP$_3$$^{3-}$)[7] which are composed of only P-O-P linkages.

In the present work, the protonation equilibria of the trimeric molecules, *i.e.*, cP$_3$, cP$_3$(NH), cP$_3$(NH)$_2$, and cP$_3$(NH)$_3$, have been re-investigated precisely by use of a potentiometric titration technique together with a ^{31}P NMR method.

EXPERIMENTAL

Synthesis of Na$_3$P$_3$O$_8$(NH) • H$_2$O

Trisodium *cyclo*-mono-μ-imidotriphosphate monohydrate, Na$_3$P$_3$O$_8$(NH) • H$_2$O, was prepared by a modification of the previously reported method[8]. Na$_3$P$_3$O$_6$(NH)$_3$ • 4H$_2$O (10 g) was dissolved in a 5 mol dm^{-3} aqueous solution of acetic acid (140 cm^3) in a three-necked round-bottom flask and the solution was reacted at 80°C for 8 h. After filtration of the reaction mixture, ethanol (200 cm^3) was added in the filtrate. After standing overnight in a refrigerator, a white precipitate which was a mixture of Na$_3$P$_3$O$_7$(NH)$_2$ • H$_2$O, Na$_3$P$_3$O$_8$(NH) • H$_2$O, and trisodium *cyclo*-triphosphate hexahydrate, Na$_3$P$_3$O$_9$ • 6H$_2$O, formed in the solution. After filtration of the solution, the mixture (4 g) was dissolved in 100 cm^3 water, and it was loaded on a Dowex 1-x8 (100-200 mesh) column(9.5×2.2 cm ϕ) which was pre-treated with 1 mol dm^{-3} HCl to convert it to the Cl$^-$ form. A 170 cm^3 solution of Na$_3$P$_3$O$_8$(NH) • H$_2$O as an effluent of 60-230 cm^3 was fractionated which was 2 cm^3/min of the flow rate by using a 0.4

mol dm^{-3} NaCl aqueous solution as an eluent. Ethanol (220 cm^3) was put into the effluent. Na$_3$P$_3$O$_8$(NH) • H$_2$O as a white precipitate was filtered off and washed with 50 vol% aqueous ethanol and then 100 vol% aceton, and dried in air. Yield was 1.2 g.

Synthesis of Na$_3$P$_3$O$_7$(NH)$_2$ • H$_2$O

Trisodium *cyclo*-di-μ-imidotriphosphate monohydrate, Na$_3$P$_3$O$_7$(NH)$_2$ • H$_2$O, was prepared by a modification of the previously reported method[9]. Na$_3$P$_3$O$_6$(NH)$_3$ • 4H$_2$O (10 g) was dissolved in a 1.6 mol dm^{-3} aqueous solution of acetic acid (110 cm^3) in a three-necked round-bottom flask and the solution was reacted at 65°C for 4.5 h. After filtration of the reaction mixture, ethanol (140 cm^3) was added in the filtrate. After standing overnight in a refrigerator, a white precipitate which was a mixture of Na$_3$P$_3$O$_6$(NH)$_3$ • 4H$_2$O, Na$_3$P$_3$O$_7$(NH)$_2$ • H$_2$O, and trisodium *cyclo*-mono-μ-imidotriphosphate monohydrate, Na$_3$P$_3$O$_8$(NH) • H$_2$O, formed in the solution. After filtration of the solution, the mixture (2 g) was dissolved in 50 cm^3 water, and it was loaded on a Dowex 1-x8 (100-200 mesh) column(9.5 × 1.5 cm φ) which was pre-treated with 1 mol dm^{-3} HCl to convert it to the Cl$^-$ form. A 40 cm^3 aqueous solution of Na$_3$P$_3$O$_7$(NH)$_2$ • H$_2$O as an effluent of 40-80 cm^3 was fractionated which was 1.5 cm^3/min of the flow rate by using a 0.25 M NaCl aqueous solution as an eluent. Ethanol (70 cm^3) was put into the effluent. Na$_3$P$_3$O$_7$(NH)$_2$ • H$_2$O as a white precipitate was filtered off and washed with 50 vol% aqueous ethanol and then 100 vol% aceton, and dried in air. Yield was 1.4 g.

Synthesis of Na$_3$P$_3$O$_6$(NH)$_3$ • 4H$_2$O

Trisodium *cyclo*-tri-μ-imidotriphosphate tetrahydrate, Na$_3$P$_3$O$_6$(NH)$_3$ • 4H$_2$O, was prepared according to the previously reported method[10]. Hexachlorocyclotriphosphazene (phosphonitrilic chloride trimer) as an intermediate product was obtained from Aldrich Chemical Co. and was used without further purification.

Purities of chemicals

The purity was determined by HPLC and ^{31}P NMR measurements to be over 97%. The phosphorus concentration in the ligand stock solution was determined colorimetrically with

a Mo(V)-Mo(VI) reagent[11].

Other chemicals

Trisodium *cyclo*-triphosphate hexahydrate, $Na_3P_3O_9 \cdot 6H_2O$, was purified by recrystallization of commercial products.

As supporting electrolyte, anhydrous sodium perchlorate, $NaClO_4$, was synthesized by neutralization of analytical grade of sodium carbonate by an analytical grade of perchloric acid, and was purified by recrystallization and dried perfectly under vacuum, so do not contain the hydroxides of metal ions.

The standard acid, $HClO_4$, was obtained from Kishida Chemical Co. Ltd. (Osaka, Japan). The $HClO_4$ stock solution was prepared at about 0.25 mol dm^{-3} from a 70% perchloric acid with distilled water and was standardized by strong acid-weak acid titration with $KHCO_3$. Carbonate-free NaOH stock solution of the titrant for the checking of the electrode system "Gran's procedure[12]", were prepared at about 1.0 mol dm^{-3} by dilution of a commercial plastic ampoule of sodium hydroxide obtained from Merck Co. Ltd. (Darmstadt, Germany) with Carbonate-free water which had been boiled at least 15 min to remove CO_2 under a stream of purified N_2 purge gas. The solutions were checked periodically by Gran's procedure and discarded when the percentage of carbonate reached about 1% of the NaOH present. Other reagents used in this work were of analytical grade.

Potentiometric titration with a glass electrode

Prior to the quantitative discussions on the metal-complexation behaviors of *cyclo*-imido polyphosphate anions, the protonation constants of the ligands should be evaluated. For this purpose, a potentiometric titration method which uses a potentiometer equipped with a glass electrode and a reference electrode(Ag/AgCl/sat. KCl) is generally utilized. A saturated KCl aqueous solution is used as the filling solution of the reference electrode, whose composition is usually much different from the sample solutions. Hence, the ionic composition of the sample solutions is sometimes influenced by the leakage of the filling solution. In order to avoid this disadvantage inherent in the usual reference electrode, the protonation constants of *cyclo*-imidopolyphosphate anions have been determined by using

Gran's plot method with a Kawai bridge [13] in the present study. As a glass electrode, an Orion 91-01 electrode was used and the Kawai bridge was constituted with an Ag/AgCl electrode. These electrodes were connected with an Orion research Ionalyzer 701A, and the emf values of the electrochemical cell were measured at $25\pm0.5°C$ under N_2 atmosphere.

The glass electrode which reacts reversibly with hydronium ions gives the electromotive force, emf(E). E can be expressed by the following equation:

$$E = E_0 + 59.154 \log[H^+] - j\,[H^+] \qquad (2\text{-}1)$$

where E_0 and j (liquid junction potential) values are constant, respectively. It is necessary to consider the influence of liquid junction potential at lower pH range (pH<2)[14]. Even though the j value is almost unvaried at -62mV when the ionic strength is 1.0 at 25°C, the E_0 value is changeable because of the contact of the glass electrode with air whenever it was taken in and out from the electrochemical cell. In order to avoid the change in the E_0 value, the following procedure is recommended, by which the calibration and measurement procedures are carried out continuously. A 20cm^3 portion of the solution of 0.03 mol dm^{-3} HClO$_4$ + 0.97 mol dm^{-3} NaClO$_4$ was neutralized stepwise by adding the solution of 0.02 mol dm^{-3} NaOH + 0.98 mol dm^{-3} NaClO$_4$. This is the calibration procedure. After neutralization, a 10cm^3 sample solution of 0.01 mol dm^{-3} cP$_3$(NH)$_n$ (n = 0-3) + 0.06 mol dm^{-3} HClO$_4$ + 0.91 mol dm^{-3} NaClO$_4$ was added to the neutralized solution, and the solution of 0.02 mol dm^{-3} NaOH + 0.98 mol dm^{-3} NaClO$_4$ was added dropwisely. All the titration procedures were carried out with a personal computer automatically and continuously at $25\pm0.5°C$ under N_2 atmosphere.

pH titration by a ^{31}P NMR method

A JEOL JNM-GX 400 NMR spectrometer was operated at 161.9 MHz for ^{31}P nuclei. As an external reference, 85% orthophosphoric acid in 10% D$_2$O was used. All the NMR spectra were obtained at $22\pm2°C$. Since it has not added D$_2$O to all sample solutions in order to retain the solvent purity, the spectrometer were not field-frequency locked during the measurement of all sample solutions. All spectra were recorded in the absence of ^1H decoupling. In order to measure the pH of sample solutions in 10 mm ϕ NMR tubes, a combination electrode (Horiba

6069-10C) connected with a Horiba pH meter(model F-14) was used. The initial compositions of the sample solutions were 0.01 mol dm^{-3} cP$_3$(NH)$_n$ (n = 0-3) of sodium salts + 0.100 mol dm^{-3} sodium chloride. To 4.00 cm^3 portions of the sample solutions contained in the NMR tubes, small aliquots of hydrochloric acid or sodium hydroxide of appropriate concentrations were added by a micro syringe stepwisely in order to define the pH of the solutions.

RESULTS AND DISCUSSION

Protonation constants determined by a potentiometric titration method.

A protonation equilibrium reaction for trivalent imidopolyphosphate anions, cP$_3$(NH)$_n$$^{3-}$ (n=0-3), can be expressed as,

$$H^+ + L^{3-} \rightleftarrows HL^{2-}$$
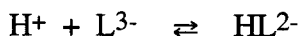
The protonation constant for this equilibrium reaction, K_H, can be written as,

$$K_H = \frac{[HL]}{[H][L]} \qquad (2\text{-}2)$$

The average number of bound hydrogen ions per a ligand ion, $\bar{n}$, can be determined by dividing the concentration of bound hydrogen ions, [H]$_b$, by the total concentration of ligand ions, C_L.

$$\bar{n} = \frac{[H]_B}{C_L} = \frac{C_H - [H]}{C_L} \qquad (2\text{-}3)$$

where C_H indicates the total concentration of hydrogen ions in the equilibrium solution. By use of eqn. 2-2, $\bar{n}$ can be written as a function of [H] as,

$$\bar{n} = \frac{K_H[H]}{1 + K_H[H]} \qquad (2\text{-}4)$$

The $\bar{n}$ vs. log[H] plots for the single protonation equilibrium give a sigmoidal curve whose inflection point corresponds to $\bar{n}$ = 0.5, and the log[H] value at $\bar{n}$ = 0.5 is equal to -log K_H. The plots obtained for all the samples are shown in Fig. 2-1. The log K_H values determined by

the non-linear least squares curve-fitting method are listed in Table 2-1. The solid lines in Fig. 2-1 refer to the formation curves calculated by use of the respective log K_H values. The experimental points for the $cP_3(NH)_n{}^{3-}$ anions exactly locate on the respective calculated curves, indicating that one-to-one protonation reactions are predominant under the present experimental conditions.

The log K_H values are plotted against n, the number of imino groups which constitute the trivalent anion molecules (Fig. 2-2). It is obvious that the log K_H value increases approximately linearly with an increase in n, showing that the basicity of the phosphate groups in the cyclic trimers increases with replacement of P-O-P linkages by P-NH-P linkages of the ligand molecules. Since the electronegativity of nitrogen atom is smaller than that of oxygen atom and the electron density around the center phosphorus atom of the phosphate unit containing imino group(s) is expected to be higher than that of the PO_4 tetrahedral units, it is anticipated that H^+ ions bind more preferentially to the phosphate groups in the order of O-P-O < NH-P-O < NH-P-NH.

In order to examine this possibility, the protonation constants of the anions of dihydrogen-orthophosphate, monohydrogen-monoamidophosphate, and diamidophosphate are compared. The equilibria for the first protonation of the monovalent anions

(L-; $[H_{(2-n)}(NH_2)_n PO_{(4-n)}]-$ (n = 0-2)), can be written as,

$$H^+ + L^- \rightleftarrows HL$$

The protonation constants[15] reported for the respective equilibrium reactions are plotted in Fig. 2-3 against n, the number of amino groups attached to the center phosphorus atoms. It is apparent from these plots that the basicity of the monovalent anions is greatly enhanced by substitution of oxygen atoms by nitrogen atoms bonded to the center phosphorus atoms, which is a proof for the higher basicity of the $cP_3(NH)_n{}^{3-}$ anions with higher n values.

In order to understand more precisely the increment of the macroscopic protonation constant with the number of imino groups of the $cP_3(NH)_n{}^{3-}$ anions, it is assumed that the macroscopic equilibrium reactions can be divided into three microscopic protonation processes at the non-bridging oxygen atoms of the phosphate groups, i.e., K_H can be expressed in the following

additive form of independent protonation constants at three phosphate sites,

$$K_H = i \, k_H(O, O) + j \, k_H(O, N) + k \, k_H(N, N) \qquad (2\text{-}5)$$

where $k_H(O, O)$, $k_H(O, N)$, and $k_H(N, N)$ indicate the microscopic protonation constants for O-P-O, O-P-NH, and NH-P-NH groups, respectively. i, j, and k stand for the numbers of the respective phosphate units in the ligand molecules where $i + j + k = 3$.

The additive expression of the macroscopic protonation constants, however, was not successful for the interpretation of the stepwise increase of the log K_H value with the n value as shown in Fig. 2-2; no consistent values of $k_H(O,O)$, $k_H(O,N)$, and $k_H(N,N)$ can be calculated by use of the four K_H values. This failure of the independent site model leads us to consider an important aspect in the protonation of imidopolyphosphate anions, *i.e.*, tautomerism of the molecules as shown in Fig. 2-4. The neighboring phosphate units linked by the P-NH-P bonding should be affected each other through this tautomerism. Delocalization of H$^+$ ions, through tautomerism, on the whole ring molecule of cP$_3$(NH)$_3$, for example, is expected to enhance the protonation.

In conclusion, the pronounced increase in the macroscopic protonation constant with an increase in the n value is not only due to the difference in the electronegativity of nitrogen and oxygen atoms, but also due to the tautomerism reaction between the phosphate units linked by the P-NH-P bonding. The nature of the protonation of the cyclic anions will be discussed at a molecular level based on a ^{31}P NMR measurement in detail in the following part of this work.

pH titration by a ^{31}P NMR method

The characteristics of the ^{31}P NMR spectra of respective phosphate molecules of cP$_3$(NH)$_n$ (n=0-3) are as follows; cP$_3$ and cP$_3$(NH)$_3$ give singlet peak, respectively, because of the equivalency of the magnetic environment around the ^{31}P nuclei belonging to these molecules, whereas cP$_3$(NH) and cP$_3$(NH)$_2$ having respective two different types of phosphorus atoms give one doublet and one triplet peaks, respectively. Under a neutral condition, *i.e.*, pH = ca. 7, the spin-spin coupling constants (J_{PP}) observed in the cP$_3$(NH)

and $cP_3(NH)_2$ molecules were 16.6 Hz and 7.4 Hz, respectively.

pH titration profiles of the ^{31}P NMR chemical shifts, δ_P, of the phosphorus atoms belonging to the anions of $cP_3(NH)_n{}^{3-}$ (n=0-3) are shown in Fig. 2-5, which suggest the following aspects on the direction and on the magnitude of the change of δ_P values.

(1)All the δ_P values show downfield-shift by deprotonation in the higher pH range (pH>11), whereas in the lower pH range (pH<4), the trends in the shift change by protonation are different from each other, depending on the types of the phosphorus atoms, *i.e.*, the phosphorus atoms of the O-P-O and O-P-N types show upfield shift change upon protonation, whereas the N-P-N type phosphorus atoms show downfield shift change.

(2)The phosphorus atoms of cP_3 and $cP_3(NH)_3$ molecules show little shift changes by protonation or deprotonation in comparison to the phosphorus atoms of $cP_3(NH)$ and $cP_3(NH)_2$ molecules.

The ^{31}P chemical shifts of a series of $cP_3(NH)_n{}^{3-}$ (n=0-3) anions varied with the degree of protonation. This change upon association with hydrogen ions has been interpreted on a quantum mechanical basis in terms of additive contributions to the chemical shift due to (1)variations in the effective electronegativity of the oxygen atoms bonded to the phosphorus atom, to (2)the O-P-O bond angles, and to (3)the occupation of phosphorus dp orbitals[16].

Approximate quantum mechanical treatment of ^{31}P chemical shifts[17,18] has pointed out that for molecules composed of the phosphorus atoms with a coordination number of 4, the ^{31}P chemical shift is comprised of a σ-bond contribution determined solely by the p orbital occupation and a π-bond contribution determined by the total occupation of the phosphorus d orbitals. It is assumed that σ-bonds use s and p orbitals, whereas the π bonds use d orbitals in addition to s and p orbitals. Hence, the measured chemical shift values, δ, is expressed by the linear conbinations of the contributions from σ and π bonds, as follows.

$$\delta = \delta_0 + \delta_\sigma + \delta_\pi \qquad (2\text{-}6)$$

where δ_0 is the absolute chemical shift values due to electrons in the inner shell, and δ_σ and δ_π are the changes of the chemical shift values by the contributions from σ and π bonds, respectively. Usually 85% H_3PO_4 is used as a reference standard. Further quantum chemical

calculations [19] have shown that the change in the chemical shift upon protonation or deprotonation, $\Delta\delta$, for ^{31}P atoms of phosphorus compounds such as orthophosphoric acid, originates from the δ_σ and δ_π terms in eqn. 2-6 and may be treated by the relationship

$$\Delta\delta = C\Delta\chi_0 - 147\Delta n_\pi - A\Delta\theta \qquad (2\text{-}7)$$

where $\Delta\chi_0$ is the change in the effective electronegativity of the non-bridging the PO_4 oxygens of the PO_4 units by the binding of counter ions to those oxygens, Δn_π is the change of the phosphorus d_π-orbital occupation by the change of the π character of the P-O bonds, and $\Delta\theta$ is any change in the O-$\underline{P}$-O bond angle caused by the addition of a salt to the solution. C and A are the coefficients which vary from one acid to another. Among these terms, Δn_π term is considered unvaried upon protonation or deprotonation, and the effect has not been taken into consideration hereafter. The phenomena of (1) and (2) observed in the present work can be interpreted as follows.

(1)The downfield shift upon deprotonation observed for all the phosphorus atoms involved in this deprotonation process at the imino groups should be explained by the difference in the electronegativities of the nitrogen atoms, because negative charge produced at the nitrogen atom upon deprotonation directly influence the atomic orbitals of the phosphorus atoms bonded to the nitrogen atoms. Due to the tautomerism equilibrium between the phosphate groups and the imino groups, the bound protons are delocalized among the non-bridging oxygen atoms and the bridging nitrogen atoms, and hence, it is impossible to determine the exact position of the bound proton on the $cP_3(NH)_n$ ($n = 1$-3) molecules even by this ^{31}P NMR technique. The similar pH profiles of the O-$\underline{P}$-N and N-$\underline{P}$-N types phosphorus atoms belonging to $cP_3(NH)_2$ ligand can be explained by this tautomerism. However, in the case of $cP_3(NH)$ ligand, where the similar pH profiles of the two different kinds of phosphorus atoms(O-$\underline{P}$-O and O-$\underline{P}$-N) is observed, the simultaneous δ_P changes cannot be explained solely by this tautomerism, because the O-$\underline{P}$-O type phosphorus atoms are not involved in this tautomerism equilibrium at all. Another explanation is needed to interpret the pH profile of the O-$\underline{P}$-O type δ_P change upon protonation.

(2)There is only one kind of bridging atoms in cP_3 and $cP_3(NH)_3$ ligands, whereas in

case of cP3(NH) and cP3(NH)2 ligands, there are two kinds of bridging atoms. The molecular structures in the formers are almost symmetrical, and the O-$\underline{P}$-O and the N-$\underline{P}$-N bond angles may be unchangeable upon protonation. In the case of asymmetrical ligands such as cP3(NH) and cP3(NH)2, however, the changes of (1)the O-$\underline{P}$-O, O-$\underline{P}$-N, and N-$\underline{P}$-N bond angles, and of (2)the polarity of the σ bonds may be relatively large upon protonation, which will lead to the large degree of the chemical shift change. It is worthwhile noting that it has already been reported that the C and A values in eqn. 2-7 are 180 and 0, respectively, for PO_4^{3-} anions of the T_d symmetry [19]. In contrast, for the anions with lower symmetry, the contribution of the $A\Delta\theta$ term cannot be neglected, i.e., C=115 and A=4.9 for phosphonate ion(PHO_3^{2-}) of C_{3v} symmetry [20,21], and C=ca.20 and A=0.4 for hypophosphate ion (PH_2O^{2-}) of C_{2v}[22].

It is well-known that most of the δ_P values of the O-$\underline{P}$-O type phosphorus atoms belonging to inorganic polyphosphate anions show upfield shift change upon protonation[23]. This change can be explained by the reduction of the effective electronegativity of the non-bridging oxygen atoms upon protonation[24]. It is also well-known that the δ_P values of the two phosphorus atoms belonging to the neighboring phosphate groups, i.e., both middle and end phosphate groups in triphosphate anions change upfield upon protonation, even though it has been expected that only the end groups of the triphosphate molecule are considered involved in the protonation process[25]. By this ^{31}P chemical shift profile, it is presumed that protons are bound to two different types of the phosphate groups simultaneously[26]. The trend observed in the present cP3(NH) protonation study may be consistent with this phenomenon; i.e., a hydrogen bond is formed

$$
\begin{array}{cc}
\overset{\displaystyle O}{\underset{\displaystyle |}{\overset{\displaystyle \|}{}}} & \overset{\displaystyle O}{\underset{\displaystyle |}{\overset{\displaystyle \|}{}}} \\
O\!-\!\underline{P}\!-\!O & O\!-\!\underline{P}\!-\!NH \\
\overset{\displaystyle |}{O^{\ominus}} & \overset{\displaystyle |}{O^{\ominus}}
\end{array}
$$

between the $\qquad$ and $\qquad$ the groups of cP3(NH) molecules. It is also notable that the δ_P values of the N-P-N type phosphorus atoms always show downfield shift upon protonation, even though the δ_P values of the O-P-N and O-P-O type phosphorus atoms always show upfield shift upon protonation.

The protonation(K_H) and deprotonation constants(K_{-H}) of the cyclo-imidopolyphosphate anions can be determined by these ^{31}P chemical shift profiles. The

intrinsic chemical shift values of each chemical species, δ_0, δ_{-1}, and δ_1 shown in the following schemes have been determined as well. Taking into consideration the following protonation equilibria, the averaged δ_P value can be expressed by eqn. 2-8.
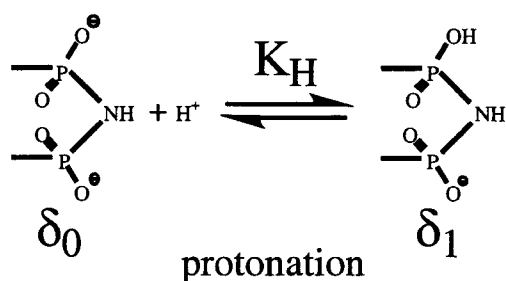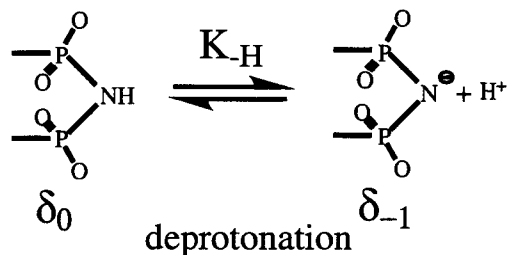

$$\delta_P = (\delta_{-H} + K_{-H}[H]\delta_0 + K_{-H}K_H[H]^2\delta_H)/(1 + K_{-H}[H] + K_{-H}K_H[H]^2)\ (2\text{-}8)$$

where K_H and K_{-H} indicate protonation and deprotonation constants, respectively; δ_0, δ_H, and δ_{-H} stand for the intrinsic shift values of trivalent anions(L^{3-}), monoprotonated species(HL^{2-}), and deprotonated species(L^{4-}), respectively. The equilibrium constants and the intrinsic shift values calculated with the non-linear least squares curve fitting method are listed in Table 2-2. Due to the quite small changes observed for symmetrical cP_3^{3-} and $cP_3(NH)_3^{3-}$ anions, these parameters are inaccessible; the values of δ_0 and δ_H have been determined by use of the K_H values determined potentiometrically. It is notable that the equilibrium constants for the asymmetrical anions evaluated by the δ_P-pH profiles of O-P-O and O-P-N phosphorus atoms belonging to $cP_3(NH)$ and the constants evaluated by those of O-P-N and N-P-N phosphorus atoms belonging to $cP_3(NH)_2$ are consistent with each other, within the experimental error.

2-12

This indicates protonation and deprotonation are not independent of the respective phosphate groups. The concurrent change observed in the shift values of O-P-N and N-P-N phosphorus nuclei of $cP_3(NH)_2$ can reasonably be explained by tautomerism of the imidopolyphosphate molecules, *i.e.*, protonation of imino groups can be represented as,
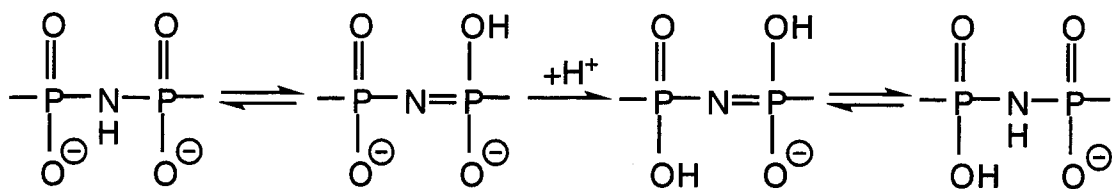
and deprotonation of imino groups can be expressed as
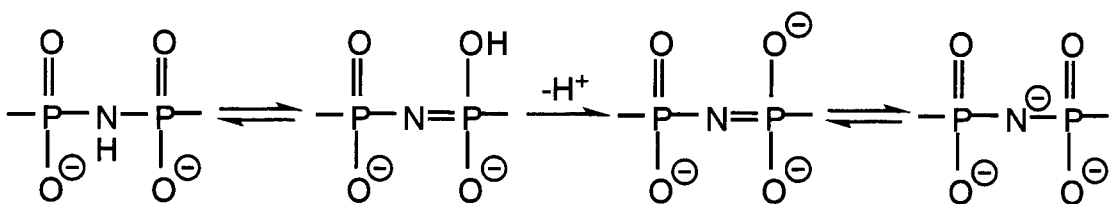
However, the concurrent shift change in $cP_3(NH)$ cannot be explained by tautomerism, because the O-P-O phosphorus atom is apparently free from tautomerism. Possible explanations for the shift changes are 1) bond angle variation of the O-P-O phosphate units, 2) change in the hydration structure around the phosphate units, and 3) hydrogen bonding among the phosphate units in $cP_3(NH)$ molecules. Taking into consideration the same shift values of the O-P-O phosphorus atoms belonging to cP_3 and $cP_3(NH)$ molecules, the most reasonable explanation is hydrogen bonding among the phosphate units in the ligand molecules.

Since the intrinsic shift values of respective phosphorus nuclei have been determined, it is of interest to relate the shift values(δ_0) of phosphorus nuclei for O-P-O, O-P-N, and N-P-N nuclei determined by the present study with the numbers of oxygen and/or nitrogen atoms bonded to the central phosphorus atoms, because an additivity rule has already been reported on phosphorus-nitrogen compounds. δ_0 of phosphorus nuclei of $cP_3(NH)_n$ (n = 0-3) molecules can emprically be expressed as in an additive form as,

$$\delta_{0,cald} = n_O \delta_{0,O} + n_N \delta_{0,N} \qquad (2-9)$$

where $\delta_{0,cald}$ indicates the calculated shift value; n_O and n_N stand for the numbers of the bridging oxygen and nitrogen atoms in the phosphate unit, and $\delta_{0,O}$ and $\delta_{0,N}$ represent the intrinsic shift values affected by each bridging atoms, respectively. The $\delta_{0,O}$ and $\delta_{0,N}$ values can be estimated as the half δ_0 values of cP_3 and $cP_3(NH)_3$ molecules, respectively, *i.e.*, $\delta_{0,O}$ = -21.0/2 = -10.5 (ppm) and $\delta_{0,N}$ = -1.34/2 = -0.67 (ppm). The observed shift values (δ_0) are plotted in Fig. 2-6 against the $\delta_{0,cald}$ values. Even though small deviations due to the effect of the third bridging atoms in the cyclic molecules cannot be ignored, it is obvious that the δ_0 value can roughly be expressed by eqn. 2-9.

This additivity rule can also be applicable to the interpretation of the shift values of respective nuclei belonging to monoprotonated phosphate species. In this case, the calculated shift values, $\delta_{H,cald}$, can be expressed as,

$$\delta_{H,cald} = n_O\delta_{OH} + n_N\delta_{NH} \qquad (2\text{-}10)$$

In Fig. 2-7 are plotted the δ_H values against the $\delta_{H,cald}$ values calculated by use of δ_{OH}=-10.5 ppm and δ_{NH}= -0.61 ppm, respectively. A comparison of Fig. 2-7 with Fig. 2-6 indicates a better linearity between δ_H and $\delta_{H,cald}$. Consistency in the respective magnetic environments of O-P-O, O-P-N, and N-P-N phosphorus nuclei belonging to different monoprotonated species indicate that the effect of proton binding on the three phosphorus atoms of mono-protonated molecules is equivalent. It can be estimated that a simultaneous hydrogen bonding is formed among the three phosphate units. This protonation scheme can reasonably explain the relationship between the log K_H value and the number of imino groups in $cP_3(NH)_n$ molecules obtained by the preceding potentiometric study.

One of the most interesting features in shift change at higher pH region is the downfield shift of O-P-O phosphorus nuclei of $cP_3(NH)$ upon deprotonation, though the O-P-O phosphorus atom is expected to be independent of deprotonation at imino group. This phenomenon can be explained by proximity of the O-P-O phosphorus atom to the nitrogen atoms which constitute the rigid ring structure. It is anticipated therefore, that hydrogen atom fixed on the imino group of the P-NH-P linkage interact with the O-P-O phosphate units.

Compared with the additivity rule found in the δ_0 and δ_H values, no simple correlation is found between the δ_H value and the number of oxygen and/or nitrogen atoms attached to the central phosphorus atoms.

Finally, it should be noted that the protonation constants determined by the ^{31}P NMR method and potentiometry are in good agreement with each other within the experimental error, despite the difference in principles of the two methods. This indicates the validity of the protonation constants as well as the intrinsic shift values evaluated by the present study. One advantageous aspect of the ^{31}P NMR method over the potentiometric method is the capability of determining the deprotonation constants of $cP_3(NH)_n^{3-}$ anions.

REFERENCES

1. T. Miyajima, H. Maki, M. Sakurai, S. Sato, M. Watanabe, *Phosphorus Res. Bull.*, **3**, 31(1993).

2. R. R. Irani, C. F. Callis, *J. Phys. Chem.*, **65**, 934(1961).

3. R. R. Irani, C. F. Callis, *J. Phys. Chem.*, **65**, 296(1961).

4. A. E. Martell, R. M. Smith (Eds.), "*Critical Stability Constants*", vol. 4, Plenum Press, New York (1976).

5. M. Komiya, T. Miyajima, S. Sato, M. Watanabe, *Phosphorus Res. Bull.*, **1**, 137(1991).

6. M. Komiya, T. Miyajima, S. Sato, M. Sakurai, S. Sato, M. Watanabe, *Phosphorus Res. Bull.*, **2**, 33(1992).

7. G. Kura, S. Ohashi, S. Kura, *J. Inorg. Nucl. Chem.*, **36**, 1605(1974).

8. M. Sakurai, M. Watanabe, *J. Mater. Sci.*, **29**, 4897(1994).

9. M. Watanabe, M. Sakurai, S. Sato, H. Mori, *Gypsum and Lime*, **239**, 245(1992).

10. M. Watanabe, M. Sakurai, M. Hinatase, S. Sato, *J. Mater. Sci.*, **27**, 743(1992).

11. F. L. Conde, L. Prat, *Anal. Chim, Acta.*, **16**, 473(1957).

12. G. Gran, *Analyst*, **77**, 661(1951).

13. H. Tsukuda, T. Kawai, M. Maeda, H. Ohtaki, *Bull. Chem. Soc. Japan.*, **48**, 691(1975).

14. G. Biedermann, L. G. Sillen, *Arkiv. Kem.*, **5**, 425(1953).

15. "*Stability Constants of Metal Complexes, Part A. Inorganic Ligands*", compiled by E. Hogfeldt, Pergamon Press, 1982.

16. D.G.Gorenstein, *Chem. Rev.*, **94**, 1315(1994).

17. J.H.Letcher, J.R.Van Wazer, *J. Chem. Phys.*, **44**, 815(1966).

18. J.H.Letcher, J.R.Van Wazer, *J. Chem. Phys.*, **45**, 2916(1966).

19. K.Moedrizer, *Inorg. Chem.*, **5**, 936(1967).

20. S.Furberg, P.Landmark, *Acta Chem.Scand.*, **11**, 1505(1957).

21. D.E.C.Corbridge, *Acta Cryst.*, **9**, 991(1956).

22. W.H.Zachariasen, R.C.L.Mooney, *J. Chem. Phys.*, **2**, 34(1934).

23. K.B.Dillon, T.C.Waddington, *J. Chem. Soc.(A).*, 1146(1970).

24. A.J.R.Costello, T.Glonek, J.R.Van Waser, *Inorg. Chem.*, **15**, 972(1976).

25. H.Waki, M.Hatano, *Polyhedron*, **1**, 69(1982).

26. S.Tran-Dinh, M.Roux, *J. Biochem.*, **76**, 245(1977).
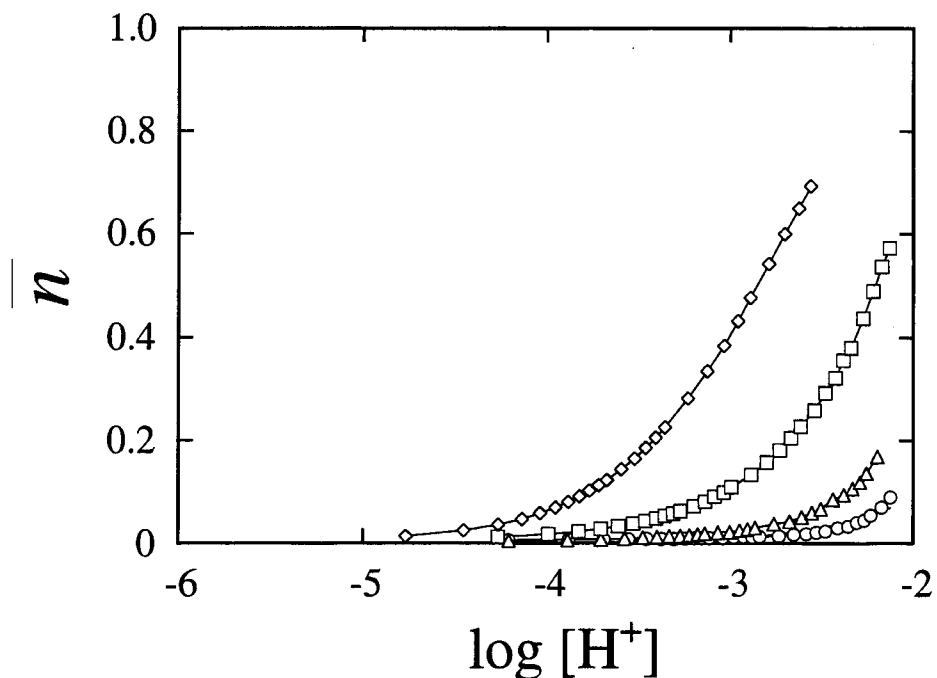
Fig.2-1 Formation curves of H^+-$cP_3(NH)_n^{3-}$ (n=0-3) systems (25±0.5°C).
(○) cP_3; (△) $cP_3(NH)$; (□) $cP_3(NH)_2$; (◇) $cP_3(NH)_3$;
C_{NaClO4}=1.0 mol dm^{-3}, Cp=0.01 mol dm^{-3};
solid lines refer to the calculated curves.
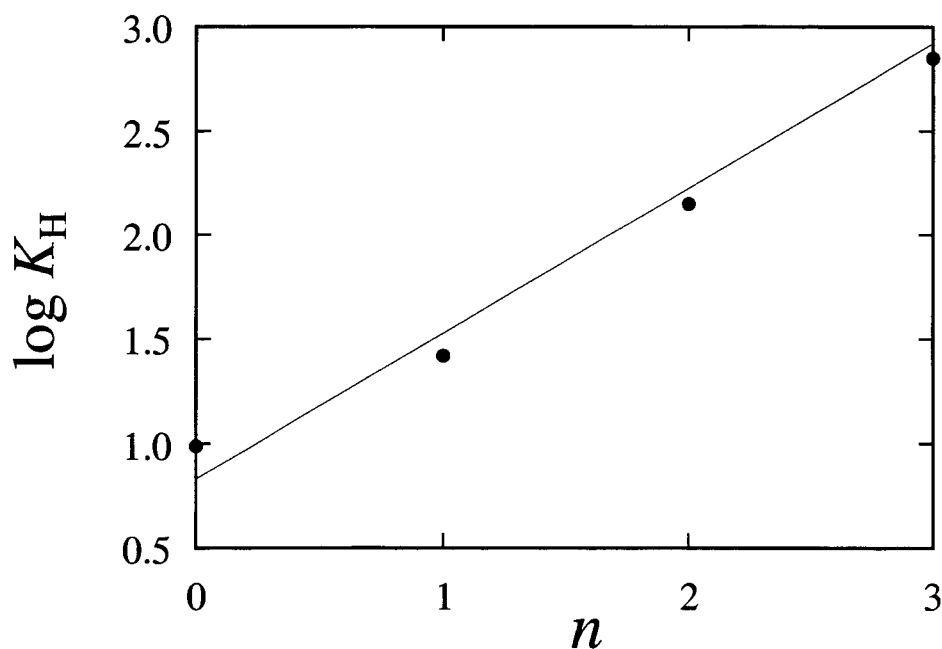
Fig.2-2 Relationship between log K_H and the number of imino groups in the ligand molecule.

(The log K_H value at n=0 is not as precise as other values due to the difficulty in the pH determination at low pH region.)
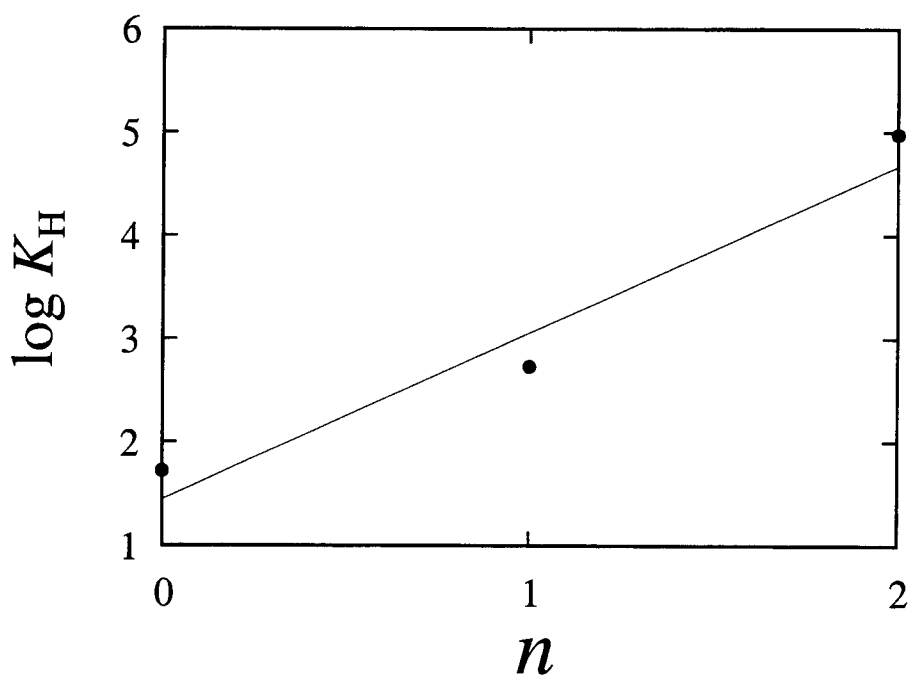
Fig.2-3 Relationship between log K_H and the number of amido groups in the amidophosphate anions.
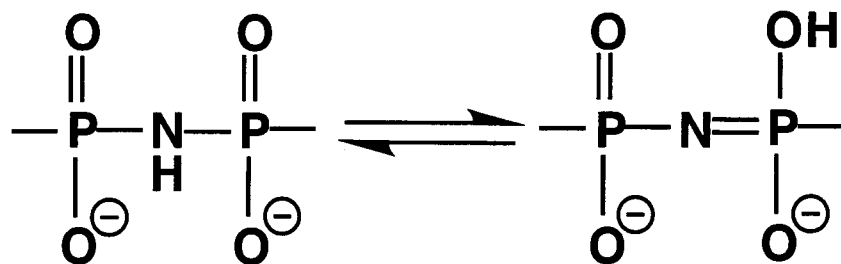
Fig. 2-4 Tautomerism of imidopolyphosphates.
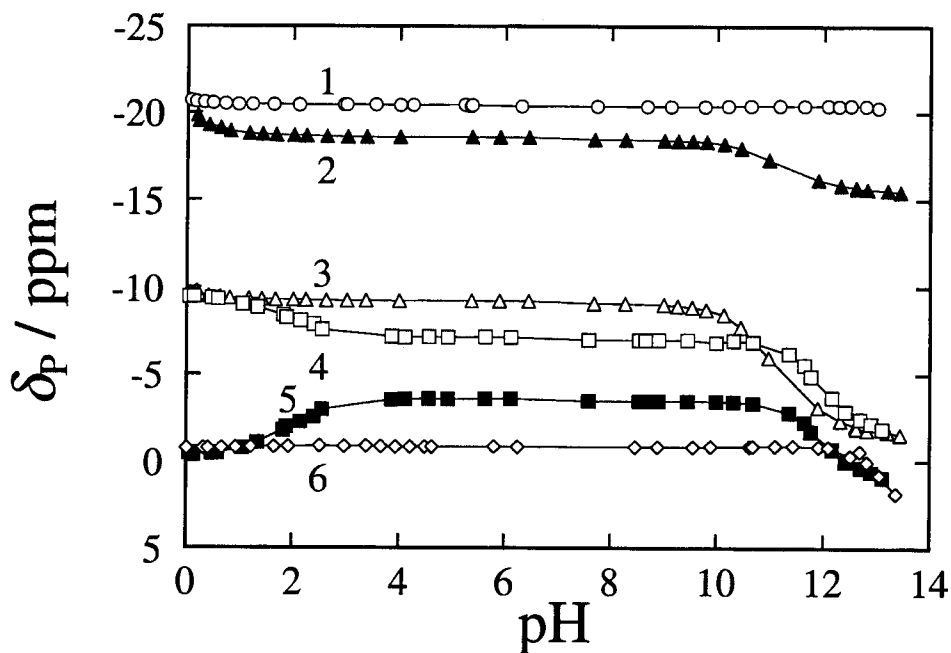
Fig.2-5 pH titration profiles of ^{31}P chemical shifts (I=1.0, $NaClO_4$).

1; cP_3 (O-P-O), 2; $cP_3(NH)$ (O-P-O), 3; $cP_3(NH)$ (O-P-N),

4; $cP_3(NH)_2$ (O-P-N), 5; $cP_3(NH)_2$ (N-P-N), 6; $cP_3(NH)_3$ (N-P-N),

Cp = 0.01 mol dm^{-3}, 25°C;

solid lines refer to the calculated curves.
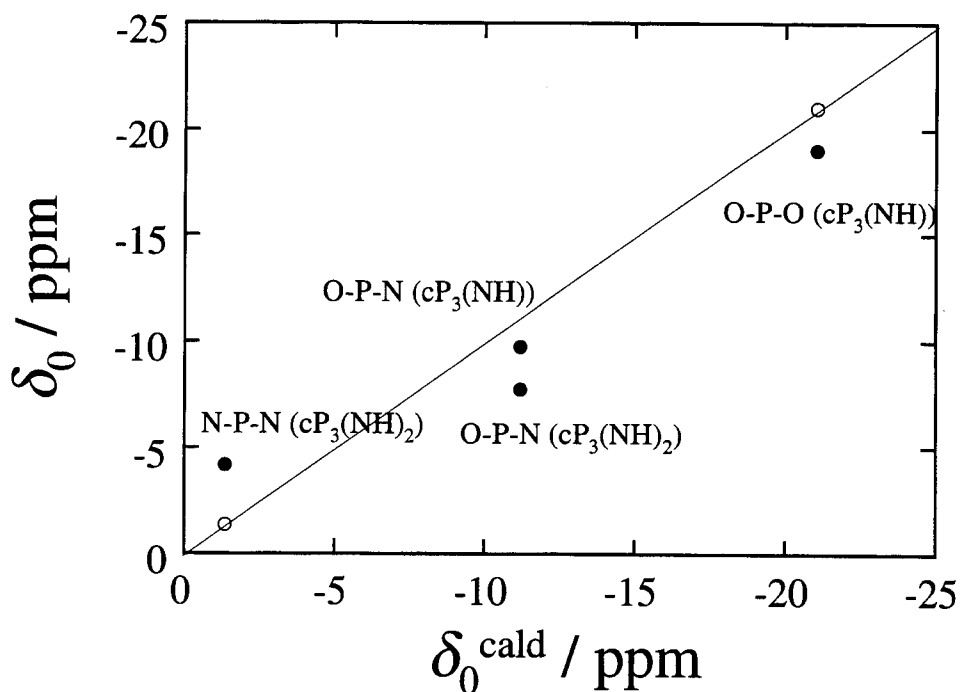
Fig.2-6 Additivity law for intrinsic chemical shift values.

open; the δ_0 values of cP_3 and $cP_3(NH)_3$ molecules, respectively.

2-19
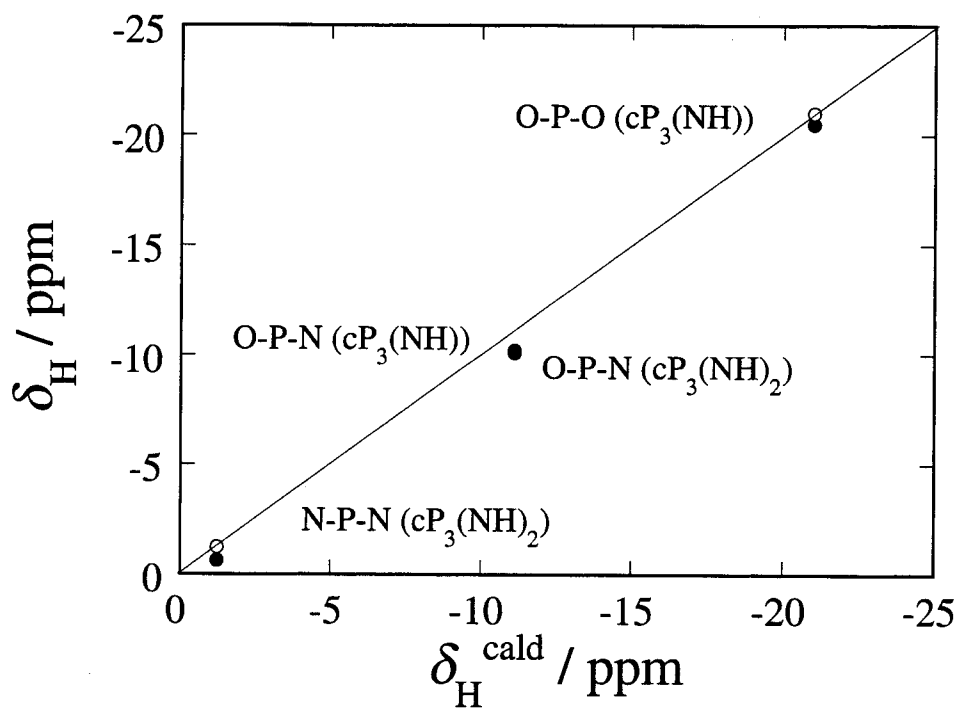
Fig.2-7 Additivity law for intrinsic chemical shift values "δ_H".

open; the δ_N values of cP$_3$ and cP$_3$(NH)$_3$ molecules, respectively.

Table 2-1 Log K_H values measured with the potentiometric titration method
($I = 1.0$, 25°C).

$cP_3(NH)_n$	log K_H
$n = 0$	$0.99 \pm 0.05*$
$= 1$	1.42 ± 0.01
$= 2$	2.15 ± 0.02
$= 3$	2.85 ± 0.01

*In spite of the effort of correcting for the liquid junction potential of the electrochemical cell, the formation curve obtained for cP_3 anion did not fit the calculated curve.

No hydrolysis during the titration process has been observed and the reason for the incorrect K_H value determined still remains unclear at the present stage.

Table 2-2 Log K_H, K_{-H} and intrinsic δ_i (i=-H, 0, H) values of $cP_3(NH)_n$ (n=0-3) determined by the pH profiles of δ_P values of respective phosphorus atom (I=1.0 (NaClO$_4$), 22±2°C).

Ligand	probe	δ_H	δ_0	δ_{-H}	log K_{-H}	log K_H
cP_3	O-P-O	-21.0±0.3	-20.4±0.0	—	—	1.06±0.95*
$cP_3(NH)$	O-P-O	-24.0±3.8**	-18.6±0.1	-15.02±0.05	11.21±0.04	0.39±0.34**
	O-P-N	-11.5±2.2**	-9.23±0.02	-1.4±0.1	11.16±0.03	0.42±0.50**
$cP_3(NH)_2$	O-P-N	-9.42±0.04	-7.16±0.03	-1.4±0.1	12.02±0.03	81.4±7.0
	N-P-N	-0.37±0.04	-3.58±0.03	1.28±0.08	12.03±0.03	92.7±5.2
$cP_3(NH)_3$	N-P-N	-0.70±0.03	-0.81±0.01	23±25*	_*	4.57±2.92*

* The error is expected to be quite large because of the small change in the δ_P value.

** Since the complete protonation could not be achieved in the present experimental conditions, incorrect values may be obtained.

CHAPTER 3

Polydentate coordination effect on the complex stabilities of *cyclo*-µ-imidotriphosphate anions.

ABSTRACT

Metal ion complexation behavior with cyclic triphosphate anions, which constitute P-O-P and / or P-NH-P linkages, were compared with each other in order to see the role of the imido groups on the complexation equilibria. The stability constants of various divalent metal ion complexes with the *cyclo*-triphosphate analogues increases proportionally to the number of the P-NH-P bondings in the phosphate anions, *i.e.*, in the order of *cyclo*-triphosphate, *cyclo*-mono-µ-imidotriphosphate, *cyclo*-di-µ-imidotriphosphate, and *cyclo*-tri-µ-imidotriphosphate anions. The enhancement of the stabilities with the addition of imino groups to the *cyclo*-triphosphate molecule is pronounced in a transverse metal ion binding.

INTRODUCTION

By our thermodynamic and NMR studies in chapter 2 in this thesis, it can be estimated that the stabilities of the metal complexes with cyclic polyphosphate anions which contain P-NH-P bondings are higher than those of the corresponding cyclic anions composed of just P-O-P linkages. Possible explanations for this enhancement in the stabilities of the complexes are 1) the higher basicity of the non-bridging oxygen atoms of the polyphosphate molecules and 2) the direct coordination of the metal ions to the bridging nitrogen atoms of the imino groups. Among imidopolyphosphate anions the N-coordination behavior of cyclic anions with metal ions is notable compared with anions of linear structure. In this chapter, a further information on the complexation behavior of cyclic imidopolyphosphate ligands has been obtained by use of a series of ligands, *i.e.*, *cyclo*-triphoshate (cP3), *cyclo*-mono-µ-imidotriphosphate (cP3(NH)), *cyclo*-di-µ-imidotriphosphate (cP3(NH)2), and *cyclo*-tri-µ-imidotriphosphate (cP3(NH)3)) as examples. Metal ion complexation equilibria have been studied by potentiometry and ^{31}P NMR chemical shift. All the experimental results obtained up to present are summarized to gain a systematic understanding of the complexation scheme of the *cyclo*-imidopolyphoshate ligands.

EXPERIMENTAL

Synthesis of Na₃P₃O₈(NH) • H₂O, Na₃P₃O₇(NH)₂ • H₂O, and Na₃P₃O₆(NH)₃ • 4H₂O

Trisodium *cyclo*-mono-μ-imidotriphosphate monohydrate, $Na_3P_3O_8(NH) \cdot H_2O$,

trisodium *cyclo*-di-μ-imidotriphosphate monohydrate, $Na_3P_3O_7(NH)_2 \cdot H_2O$, and trisodium

cyclo-tri-μ-imidotriphosphate tetrahydrate, $Na_3P_3O_6(NH)_3 \cdot 4H_2O$, was prepared according to

the method in chapter 2 in this thesis.

The purity was determined by HPLC and ^{31}P NMR measurements to be over 97%. The

phosphorus concentration in the ligand stock solution was determined colorimetrically with a

Mo(V)-Mo(VI) reagent[1].

Other chemicals

As supporting electrolyte, analytical grade of anhydrous sodium nitrate, $NaNO_3$ and

anhydrous sodium chloride, NaCl, were obtained from Merck Co. Ltd. (Darmstadt, Germany)

were used without further purification. The standard $NaNO_3$ and NaCl stock solutions were

prepared at about 2.0 mol dm⁻³ from respective reagents with distilled water. About 10 cm³

portions of respective stock solutions were weighed precisely, and dried perfectly at 110°C at

least 5 days and were weighed residues, so the concentrations of these stock solutions were

determined accurately.

Anhydrous calcium chloride, $CaCl_2$, copper nitrate trihydrate, $Cu(NO_3)_2 \cdot 3H_2O$,

cadmium nitrate tetrahydrate, $Cd(NO_3)_2 \cdot 4H_2O$, and anhydrous silver nitrate, $AgNO_3$, were

obtained from Kishida Chemical Co. Ltd. (Osaka, Japan) were used without further purification.

$AgNO_3$ was ground to a powder, and dried perfectly under vacuum at least 1 day. The reagent

was preserved in a light resistant bottle in order to prevent decomposition. The standard $CaCl_2$,

$Cu(NO_3)_2$, and $Cd(NO_3)_2$ stock solutions were prepared at about 0.2 mol

dm⁻³ from respective reagents with distilled water. Stock solutions of $Cu(NO_3)_2$ and

$Cd(NO_3)_2$ were standardized complexometric titration with EDTA. Stock solution of $CaCl_2$

was determined from the concentration of chloride ion which standardized by Mohr's

procedure. Other reagents used in this work were of analytical grade.

Potentiometric titration with metal ion selective electrodes.

The free concentrations of Ag^+, Ca^{2+}, Cu^{2+}, and Cd^{2+} ions of the sample solutions at equilibrium were measured with a Horiba 8011-10C, Orion 93-20, Horiba 80-06, and Horiba 80-07 membrane electrode, respectively. Each metal ion selective electrode was connected with an Orion research ionalyzer 720A. The reference electrodes used were single junction type(Orion 90-01) for Ca^{2+} ion and double junction type(Orion 90-02) for Ag^+, Cu^{2+}, and Cd^{2+} ion measurements, respectively. The measurements were carried out at $25 \pm 0.5°C$, keeping the ionic strength constant at 0.1 by use of NaCl for Ca^{2+} ion and $NaNO_3$ for Ag^+, Cu^{2+}, and Cd^{2+} ion measurements, respectively. In the case of Ca^{2+} ion complexation system, $10cm^3$ portions of the solutions of 0.1 mol dm^{-3} NaCl + 0.01 mol dm^{-3} $cP_3(NH)_n$ (n=0-3) were titrated by the solutions of 0.01 mol dm^{-3} $CaCl_2$ + 0.1 mol dm^{-3} NaCl. In the case of Ag^+, Cu^{2+}, and Cd^{2+} ion complexation systems, $10cm^3$ portions of the solutions of 0.1 mol dm^{-3} $NaNO_3$ + 0.01 mol dm^{-3} $cP_3(NH)_n$ were titrated by the solutions of 0.01 mol dm^{-3} $M(NO_3)_n$ (M; Ag^+(n=1), Cu^{2+}(n=2), and Cd^{2+}(n=2)) + 0.1 mol dm^{-3} $NaNO_3$, and the e.m.f. values were measured. Before and after the titration procedures the electrochemical cells were calibrated. The emf values can be expressed by eqn. 3-1.

$$E = E_0{}' + s \log[M^{2+}] \qquad (3\text{-}1)$$

where "s" is the Nernstian slope. In the present study, the "s" values were consistent with the theoretical value (ca. 27-28 mV for Ca^{2+}, Cu^{2+}, Cd^{2+}; 53-55 mV for Ag^+). Before and after the titration procedures, the pH values of the sample solutions were measured to be between 4 and 5, which ensures that all the phosphate groups of $cP_3(NH)_n$ (n=0-3) anions were deprotonated completely.

Both the values of enthalpies, ΔH^o, and entropies, ΔS^o, of the complexation equilibria were calculated from the temperature dependence of the stability constants. The measurements were carried out for Ca^{2+}-, Cu^{2+}-, and Cd^{2+}-$cP_3(NH)_n$ (n=0-3) systems between $5 \pm 0.5°C$ and $45 \pm 0.5°C$.

Complexation studies by a ^{31}P NMR method.

NMR spectra for ^{31}P ($I=1/2$) were obtained with a JEOL JNM-GX 400 NMR spectrometer at 161.9 MHz. As an external reference, 75 % orthophosphoric acid in 10% D_2O was used. Since it has not added D_2O to all sample solutions in order to retain the solvent purity, the spectrometer were not field-frequency locked during the measurement of all sample solutions. All spectra were recorded in the absence of ^1H decoupling. All the NMR spectra were obtained at $22\pm2°C$. The measurements were carried out with keeping the ionic strength constant at 0.1 by use of NaCl for Ca^{2+} ion and $NaNO_3$ for Mg^{2+}, Sr^{2+}, Zn^{2+}, Cd^{2+}, Pb^{2+}, and Ag^+ ion measurements, respectively. In the case of the Ca^{2+} ion complexation system, 3 cm^3 portions of the solutions of 0.10 mol dm^{-3} NaCl + 0.01 mol dm^{-3} $cP_3(NH)_n$ ($n=0$-3) were titrated stepwisely by the solutions of 0.10 mol dm^{-3} NaCl + 0.015 mol dm^{-3} $CaCl_2$. In the case of other metal ion complexation systems, 3 cm^3 portions of the solutions of 0.10 mol dm^{-3} $NaNO_3$ + 0.01 mol dm^{-3} $cP_3(NH)_n$ ($n=0$-3) were titrated stepwisely by the solutions of 0.10 mol dm^{-3} $NaNO_3$ + 0.015 mol dm^{-3} $M(NO_3)_n$ (M; Mg, Sr, Zn, Cd, Pb($n=2$), and Ag($n=1$)). All the titration operations were performed in 10 mm ϕ NMR sample tubes by use of a micro syringe.

RESULTS AND DISCUSSION

Stability constants determined by a potentiometric titration method.

A one-to-one complexation formation reaction of trivalent $cP_3(NH)_n^{3-}$ ($n=0$-3) anions with divalent metal ions can be written as,

$$M^{2+} + L^{3-} \rightleftarrows ML^-$$
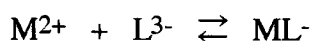
The stability constant, β_1, can be written as,

$$\beta_1 = \frac{[ML]}{[M][L]} \qquad (3\text{-}2)$$

In the similar manner with the protonation equilibria, the average number of bound metal ions per a ligand ion, $\bar{n}$, can be defined as follows,

$$\bar{n} = \frac{C_M - [M]}{C_L} \qquad (3\text{-}3)$$

where C_M and C_L are the total concentrations of metal ions and ligand ions, respectively. By use of eqn. 3-2, $\bar{n}$ can also be expressed as a function of [M].

$$\bar{n} = \frac{\beta_1[M]}{1 + \beta_1[M]} \qquad (3\text{-}4)$$

The $\bar{n}$ values calculated by eqn. 3-3 are plotted against log[M]. The formation curves, thus obtained for the Ca^{2+}, Cu^{2+}, Cd^{2+}, and Ag^+ ion systems are shown in Figs. 3-1 - 3-4, respectively. In these potentiometric titration experiments, the initial concentrations of the ligands were fixed at 0.01 mol dm^{-3} or 0.02 mol dm^{-3} for the Ag^+ ion system. It was confirmed that the formation curves for respective systems are consistent with each other, i.e., no ligand concentration effect has been observed. This excludes the possibility of the formation of ML_2 or ML_3 type complexes under the present experimental conditions. The log β_1 values have been determined by the non-linear least squares curve fitting method, and are listed in Table 3-1. The log β_1 values for all the metal ions investigated increase linearly with the number of the imino groups in the $cP_3(NH)_n$ (n=0-3) molecules. The log β_1 values as shown in Fig. 3-5 are plotted against n. In the case of cP_3 ligand complex formation, no significant difference is observed among the log β_1 values for the divalent metal ions, whereas in the case of $cP_3(NH)_3$ ligand, Cu^{2+} and Cd^{2+} complexes have much higher log β_1 values than Ca^{2+} complex. Also, it should be noted that the log β_1 values increase with an increase in "n", and the slopes of the linearities in the Cu^{2+} and Cd^{2+} systems are much larger than that in the Ca^{2+} system. Such a difference in the formation constants among the divalent metal ions investigated has not been found in the complexation formation systems of other inorganic cyclo-polyphosphate ligands such as cP_4, cP_6 and $cP_8[2]$, and this metal ion specificity observed in the cyclo-imidopolyphosphate is considered of significance.

It is of special interest to plot the formation constants of these imidopolyphosphate complexes against the corresponding protonation constants in order to see the relationship between the basicities of the ligands and the complex formation constants, i.e., the linear free

energy relationship(LFER). One can discover many relationships between the free energies or rates of complex formation of sets of complexes, and a variety of properties of the metal ions, ligands, or complexes[1-3]. Such regularities are not derivable in any strict thermodynamic way, and are hence called extra-thermodynamic relationships. The correlations do, however, provide insights into the factors governing complex formation, and in addition may allow for prediction of unknown formation or rate constants. The LFER has been known for a long time in organic chemistry with correlations involving rates and proton basicity of series of organic bases[4]. In coordination chemistry the first observations of LFER[5] were correlations between the protonation constant of the ligand and log K_{ML} with a variety of metal ions. This is still the most common type of correlation. The LFER is a common phenomenon in coordination chemistry, and is used throughout this work to analyze metal to ligand bonding[6-19].

Even though the formation constants have been evaluated at $I=0.1$, being different from the ionic strength, at which the protonation constants have been determined, the log β_1 values have been plotted in Fig. 3-6 against the respective log K_H values in order to see this relationship. It can be seen that linearities are observed for all the systems, and the slopes of this linear free energy relationship for Cu^{2+} and Cd^{2+} complexes are much larger than that for Ca^{2+} complexes. This result again suggests that the coordination behavior of cyclo-imidopolyphosphate anions with the Cu^{2+} and Cd^{2+} ion systems may be different from that is the Ca^{2+} ion system.

In order to clarify the effect of the imino groups in the ligand molecules on the complex formation equilibrium, thermodynamic parameters, ΔH^o and ΔS^o, of the complex formation reactions have been determined by examining the temperature dependence of the formation constants. The following equation was applied to evaluate the respective values,

$$\ln \beta_1 = -\frac{\Delta H^{\circ}}{RT} + \frac{\Delta S^{\circ}}{R}$$

(3-5)

where R and T indicate the gas constant, and absolute temperature, respectively. Good linearities are obtained for all the series of the complexation systems investigated, and the respective ΔH^o

and ΔS^o values calculated from the slopes and the intercepts of the straight lines, respectively, are listed in Table 3-2.

In the cP_3 system where only non-bridging oxygen atoms are expected to participate in the complexation, the ΔH^o and ΔS^o values of the Cu^{2+} and Cd^{2+} complexation systems are of the same magnitude. However, in the $cP_3(NH)_3$ system, the ΔH^o and ΔS^o values in the Cu^{2+} and Cd^{2+} complexation system are greatly different from those in Ca^{2+} complexation. The large positive ΔS^o value of the Cu^{2+}-, and Cd^{2+}-$cP_3(NH)_3{}^{3-}$ systems compared with other complexation systems is enlightening. Release of water molecules bound to free Cu^{2+} ion upon complexation with $cP_3(NH)_3$ molecule is a possible explanation for this phenomenon. It is anticipated that monodentate ligand complexation is predominant in the Ca^{2+}-$cP_3{}^{3-}$, Cu^{2+}-$cP_3{}^{3-}$, Cd^{2+}-$cP_3{}^{3-}$, and Ca^{2+}-$cP_3(NH)_3{}^{3-}$ systems, whereas multidentate ligand complexation is predominant in the Cu^{2+}-, and Cd^{2+}-$cP_3(NH)_3{}^{3-}$ systems. These thermodynamic experimental results cannot give a straightforward evidence for the coordination structures on these multidentate ligand complexes. This result again suggests that the coordination behavior of Cu^{2+} and Cd^{2+} ion is different from the Ca^{2+} ion coordination in the $cP_3(NH)_3$ system.

A complexation study by a ^{31}P NMR method.

The ^{31}P chemical shifts of imidopolyphosphate anions are sensitive to their complexation with multivalent metal ions in a similar manner with protonation. The shift changes($\Delta\delta_P$) with Mg^{2+}, Ca^{2+}, Sr^{2+}, Zn^{2+}, Cd^{2+}, and Ag^+ ions upon complexation are shown in Figs. 3-7 - 3-12, respectively. Compared with the shift change upon protonation or deprotonation, the change observed in metal complexation is relatively small. The direction and the magnitude of the shift change are quite dependent on the nature and the concentrations of the metal ions. In order to interpret these shift changes, the $\Delta\delta_P$ values for Ca^{2+}, Cd^{2+}, and Ag^+ ion binding systems are plotted against $\bar{n}$ in Figs. 3-13 - 3-18, respectively. The $\bar{n}$ values, the average numbers of bound metal ions per a ligand molecule, have been calculated by use of the formation constants of respective complexes evaluated by the potentiometric study(Table 2-2). The δ_1 values can be expressed by eqn. 3-6.

$$\delta_1 = \frac{\Delta\delta_P}{\bar{n}} + \delta_0 \qquad (3\text{-}6)$$

The plots of $\Delta\delta_P$ against $\bar{n}$ give straight lines, by which the intrinsic chemical shift values of the 1:1 complexes, δ_1, can be evaluated by the least squares method(see Figs. 3-13 - 3-18). In order to clarify the direction and the magnitude of the shift change, the $\Delta\delta(=\delta_1 - \delta_0)$ values for Ca^{2+}, Cd^{2+}, and Ag^+ ion systems are presented in Figs. 3-19 - 3-21, respectively. Also, in order to examine the influence of the complexation on the shift changes of cP_3 and $cP_3(NH)_3$ molecules, the $\Delta\delta$ values for O-$\underline{P}$-O and N-$\underline{P}$-N nuclei are plotted for respective metal ion complexation systems in Fig.3-22. It is apparent from these observations that complexation of $cP_3(NH)_3$ ligand with divalent transition metal ions induces large downfield shift change, whereas no or little shift change has been observed for the complexation with cP_3 ligand. It is clear that complexation of cP_3 with divalent alkaline earth metal ions leads to a large upfield shift change, whereas no or little shift change has been observed for the complexation with $cP_3(NH)_3$ ligand. These two extreme examples tell us that hard metal ions induces large shift change of O-$\underline{P}$-O nucleus, whereas soft metal ions induces large shift change of N-$\underline{P}$-N nucleus. It is also important to point out that no shift change does not always indicate the absence of complexation, however. Another important aspect observed in these shift changes is that the ^{31}P nuclei belonging to the asymmetrical ligand molecules, i.e., $cP_3(NH)$ and $cP_3(NH)_2$, give larger changes compared with the symmetrical ligand molecules such as cP_3 and $cP_3(NH)_3$, which is consistent with the tendency observed in the protonated species. It is obvious that the O-$\underline{P}$-O nucleus in a $cP_3(NH)$ molecule and the O-$\underline{P}$-N nucleus in a $cP_3(NH)_2$ molecule give upfield shift whereas the O-$\underline{P}$-N nucleus in a $cP_3(NH)$ molecule and N-$\underline{P}$-N nucleus in a $cP_3(NH)_2$ molecule give down field shift upon complexation, which is consistent with the observation in the protonation process.

REFERENCES

1. N. B. Chapman, J. Shorter, "*Advances in Lineer Free Energy Relationships*", Plenum Press, London (1972)

2. J. Shorter, *Q. Rev. Chem. Soc.*, **24**, 433(1970)

3. R. D. Hancock, *J. Chem. Soc., Dalton Trans.*, 416(1980)

4. L. P. Hammett, "*Physical Organic Chemistry*", McGraw-Hill, New York (1940)

5. E. Larsson, *Z. Phys. Chem., A*, **169**, 215(1934)

6. J. S. Uppal, R. H. Staley, *J. Am. Chem. Soc.*, **104**, 1238(1982)

7. M. M. Kappes, R. H. Staley, *J. Am. Chem. Soc.*, **104**, 1813(1982)

8. R. W. Jones, R. H. Staley, *J. Phys. Chem.*, **86**, 1387(1982)

9. R. R. Corderman, J. L. Beauchamp, *J. Am. Chem. Soc.*, **98**, 3998(1976)

10. M. M. Kappes, R. H. Staley, *J. Am. Chem. Soc.*, **104**, 1819(1982)

11. F. J. C. Rossotti, in *"Modern Coordination Chemistry"*, J. Lewis, R. G. Wilkins, Eds., Interscience, New York (1960)

12. G. Hefter, *Coord. Chem. Rev.*, **12**, 221(1974)

13. R. G. Pearson, *J. Am. Chem. Soc.*, **85**, 3533(1963)

14. R. D. Hancock, F. Marsicano, *Inorg. Chem.*, **17**, 560(1978)

15. R. D. Hancock, F. Marsicano, *Inorg. Chem.*, **19**, 2709(1980)

16. J. O. Edwards, *J. Am. Chem. Soc.*, **76**, 1540(1954)

17. S. Yamada, M. Tanaka, *J. Inorg. Nucl. Chem.*, **37**, 587(1975)

18. A. Yingst, D. H. McDaniel, *J. Am. Chem. Soc.*, **89**, 1067(1967)

19. R. S. Drago, G. C. Vogel, T. E. Needham, *J. Am. Chem. Soc.*, **93**, 6014(1971)
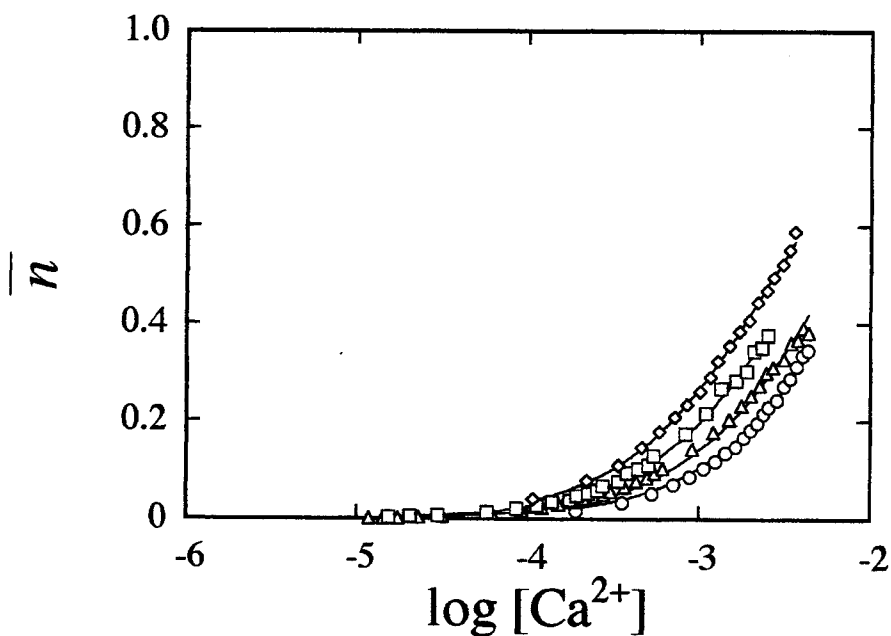
Fig.3-1 Formation curves of Ca^{2+}-$cP_3(NH)_n^{3-}$ (n=0-3) systems(25±0.5°C).
(○) cP_3; (△) $cP_3(NH)$; (□) $cP_3(NH)_2$; (◇) $cP_3(NH)_3$;
C_{Na}=0.1 mol dm^{-3}, Cp=0.01 mol dm^{-3};
solid lines refer to the calculated curves.
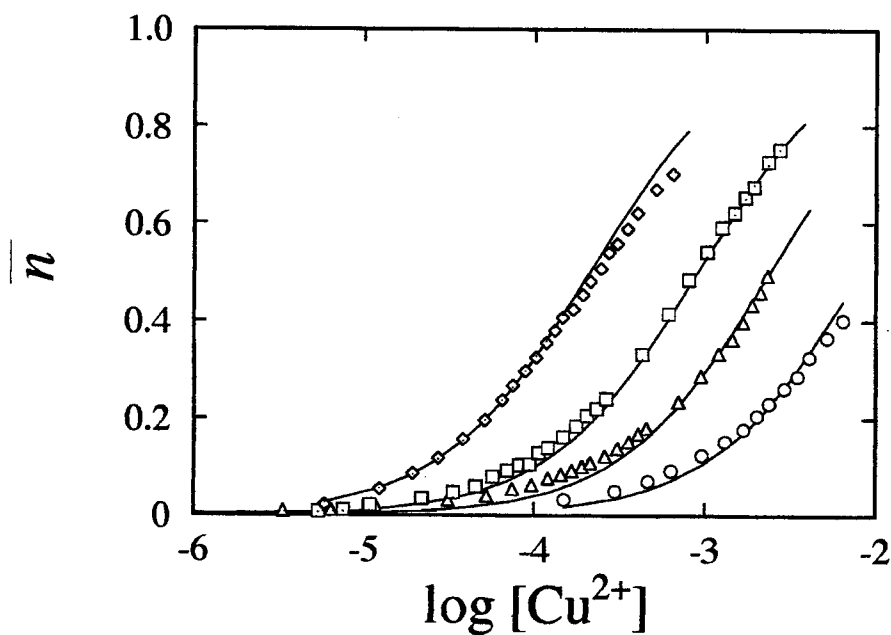
Fig.3-2 Formation curves of Cu^{2+}-$cP_3(NH)_n^{3-}$ (n=0-3) systems(25±0.5°C).
(○) cP_3; (△) $cP_3(NH)$; (□) $cP_3(NH)_2$; (◇) $cP_3(NH)_3$;
C_{Na}=0.1 mol dm^{-3}, Cp=0.01 mol dm^{-3};
solid lines refer to the calculated curves.
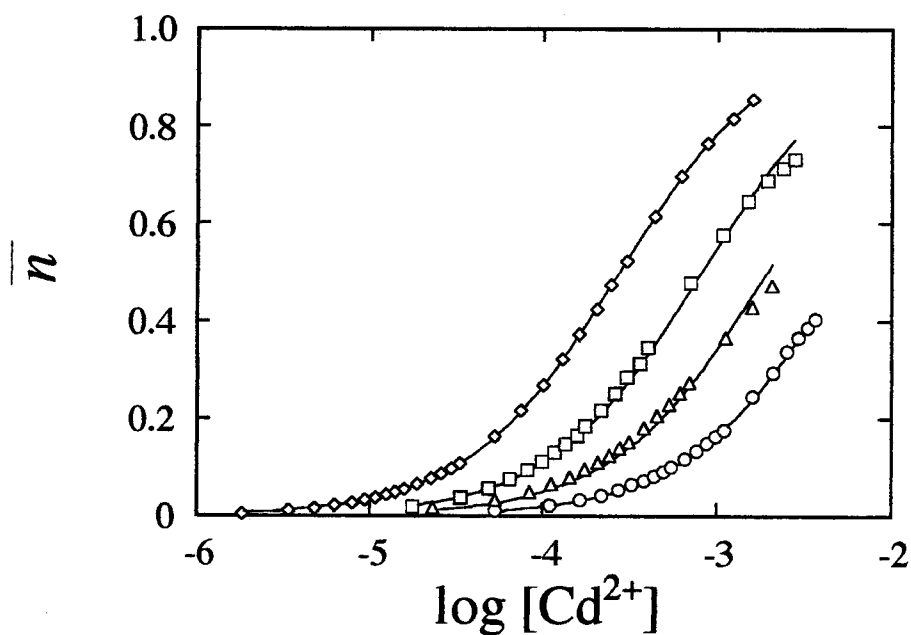
Fig.3-3 Formation curves of Cd^{2+}-$cP_3(NH)_n^{3-}$ (n=0-3) systems(25±0.5°C).
(○) cP_3; (△) $cP_3(NH)$; (□) $cP_3(NH)_2$; (◇) $cP_3(NH)_3$;
C_{Na}=0.1 mol dm^{-3}, Cp=0.01 mol dm^{-3};
solid lines refer to the calculated curves.
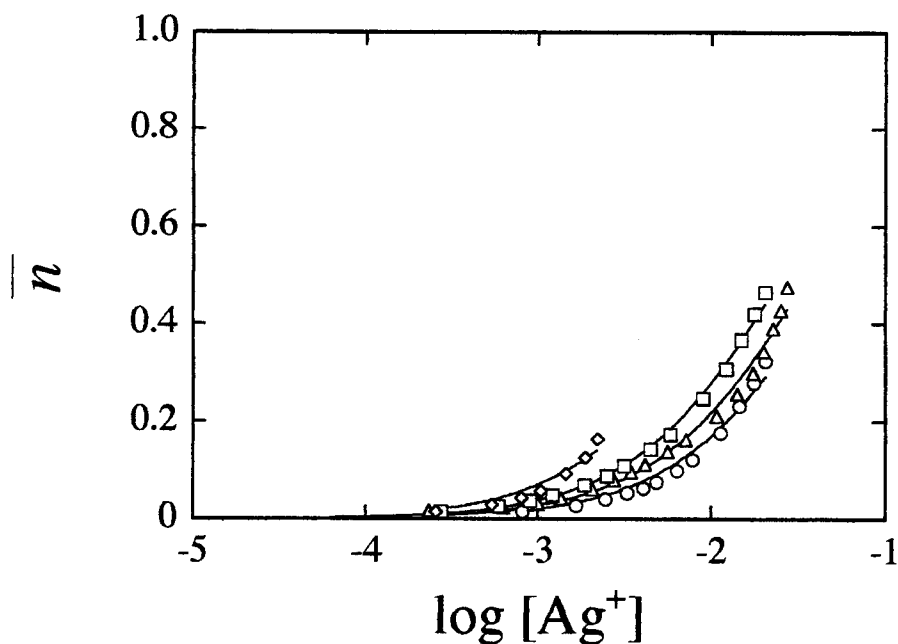
Fig.3-4 Formation curves of Ag^+-$cP_3(NH)_n^{3-}$ (n=0-3) systems(25±0.5°C).
(○) cP_3; (△) $cP_3(NH)$; (□) $cP_3(NH)_2$; (◇) $cP_3(NH)_3$;
C_{Na}=0.1 mol dm^{-3}, Cp=0.02 mol dm^{-3};
solid lines refer to the calculated curves.
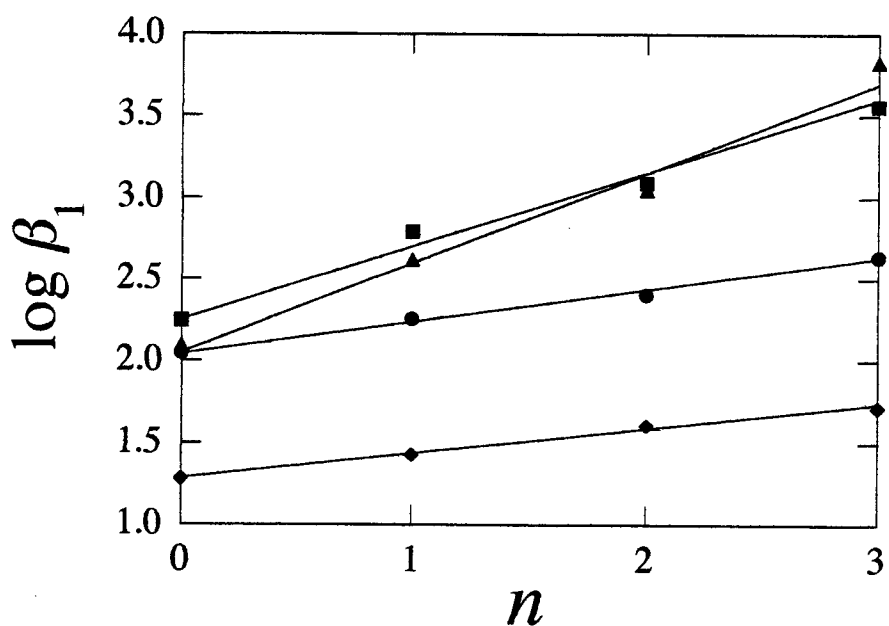
Fig.3-5 Relationships between log β_1 and the number of imino groups in the $cP_3(NH)_n^{3-}$ (n=0-3) anions.
M; (●) Ca^{2+}; (▲) Cu^{2+}; (■) Cd^{2+}; (◆) Ag^+.
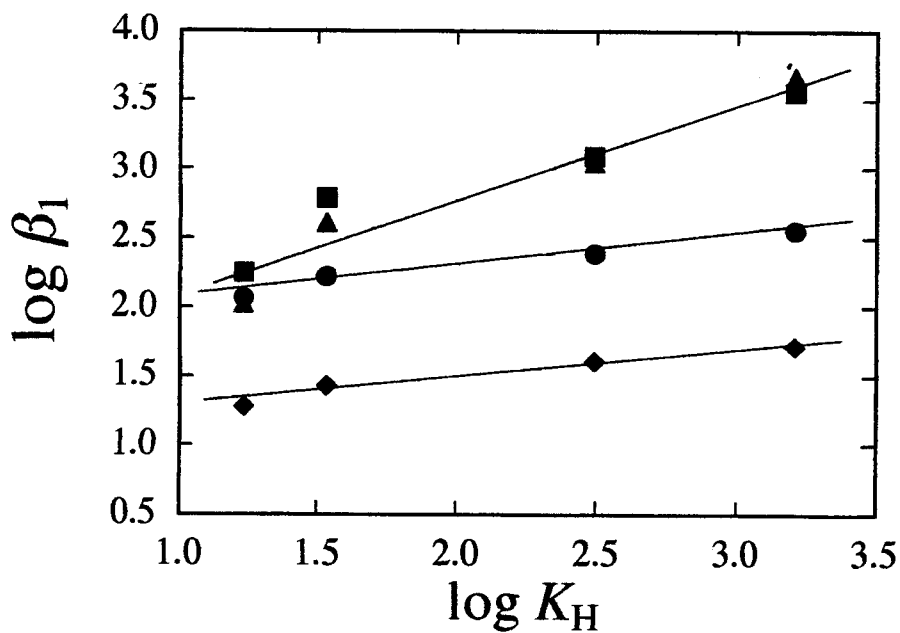
Fig.3-6 LFER between log β_1 and log K_H.
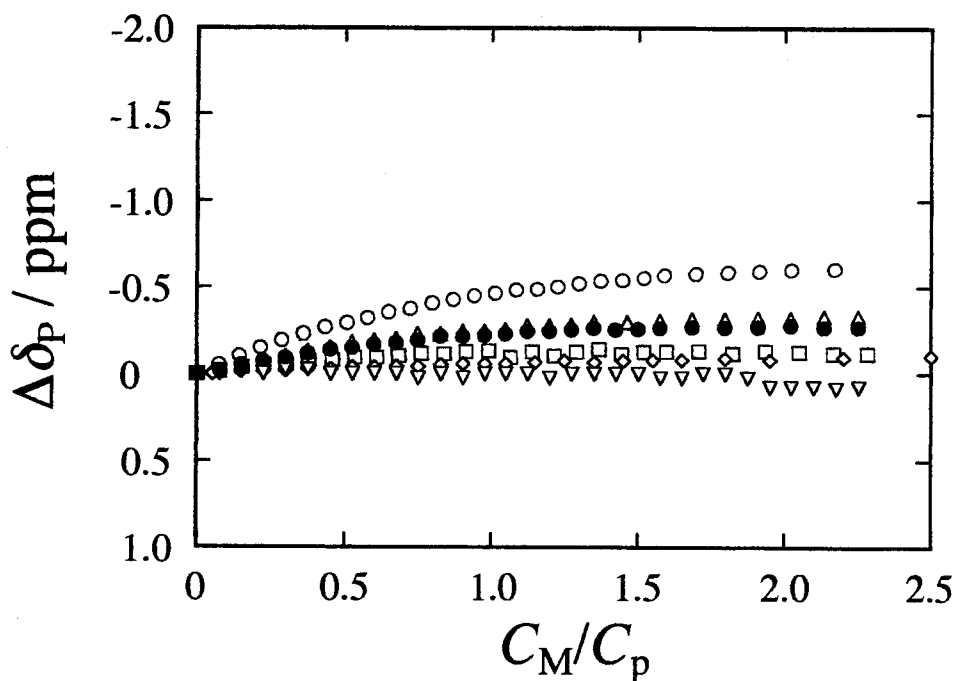M; (●) Ca^{2+}; (▲) Cu^{2+}; (■) Cd^{2+}; (◆) Ag^+.

Fig.3-7 Metal ion titration profiles of ^{31}P chemical shifts of O-P-O in cP_3.

(○) Mg^{2+}; (△) Ca^{2+}; (□) Sr^{2+}; (◇) Zn^{2+}; (▽) Cd^{2+}; (●) Ag^+; $Cp = 0.01$ mol dm^{-3}, $C_{Na}=0.1$ mol dm^{-3}, 22°C.
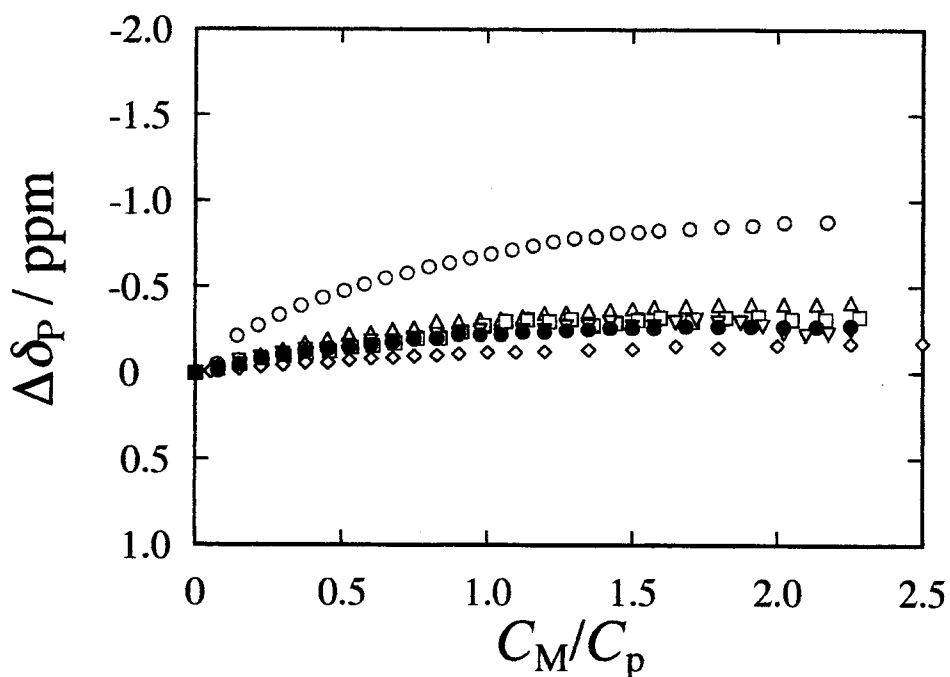
Fig.3-8 Metal ion titration profiles of ^{31}P chemical shifts of O-P-O in $cP_3(NH)$.

(○) Mg^{2+}; (△) Ca^{2+}; (□) Sr^{2+}; (◇) Zn^{2+}; (▽) Cd^{2+}; (●) Ag^+; $Cp = 0.01$ mol dm^{-3}, $C_{Na}=0.1$ mol dm^{-3}, 22°C.

3-13
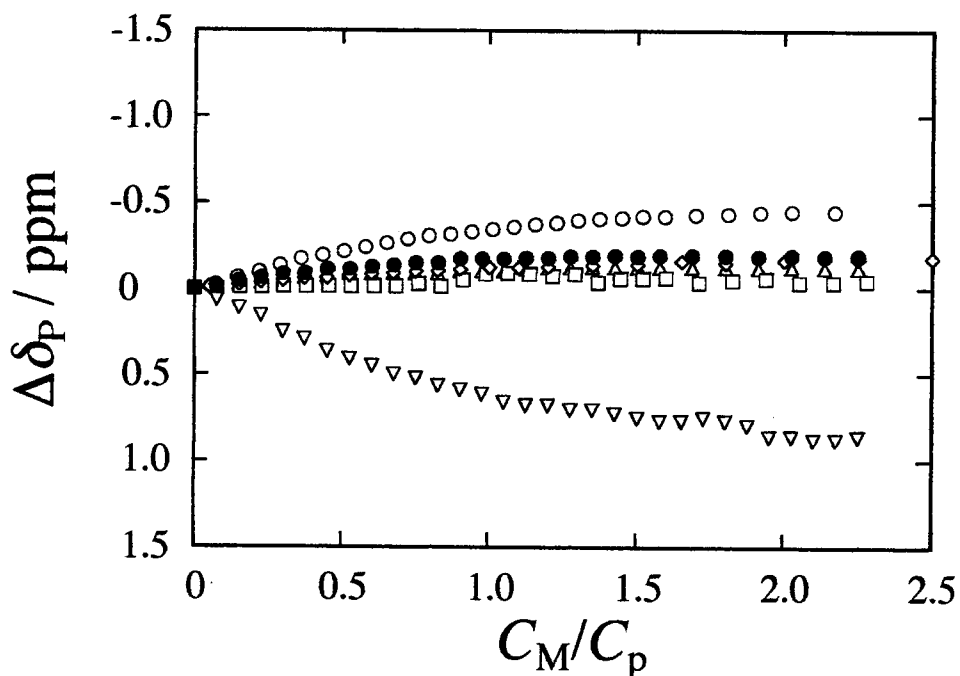
Fig.3-9 Metal ion titration profiles of ^{31}P chemical shifts of O-P-N in $cP_3(NH)$.

($\bigcirc$) Mg^{2+}; ($\triangle$) Ca^{2+}; ($\square$) Sr^{2+}; ($\diamond$) Zn^{2+}; ($\triangledown$) Cd^{2+}; ($\bullet$) Ag^+; $Cp = 0.01$ mol dm^{-3}, $C_{Na}=0.1$ mol dm^{-3}, 22°C.
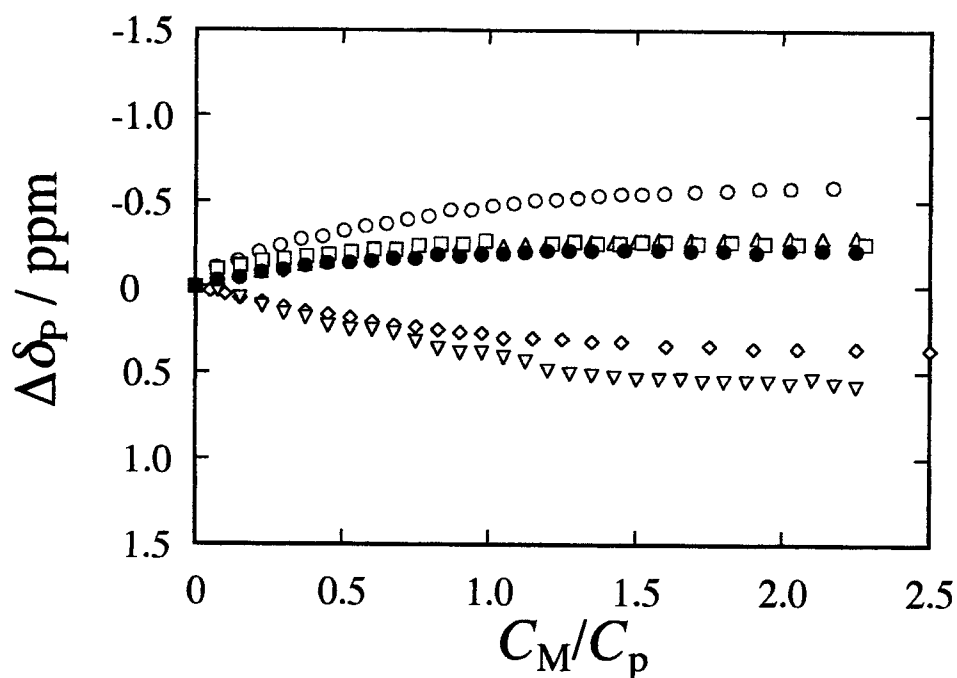
Fig.3-10 Metal ion titration profiles of ^{31}P chemical shifts of O-P-N in $cP_3(NH)_2$.

($\bigcirc$) Mg^{2+}; ($\triangle$) Ca^{2+}; ($\square$) Sr^{2+}; ($\diamond$) Zn^{2+}; ($\triangledown$) Cd^{2+}; ($\bullet$) Ag^+; $Cp = 0.01$ mol dm^{-3}, $C_{Na}=0.1$ mol dm^{-3}, 22°C.

3-14
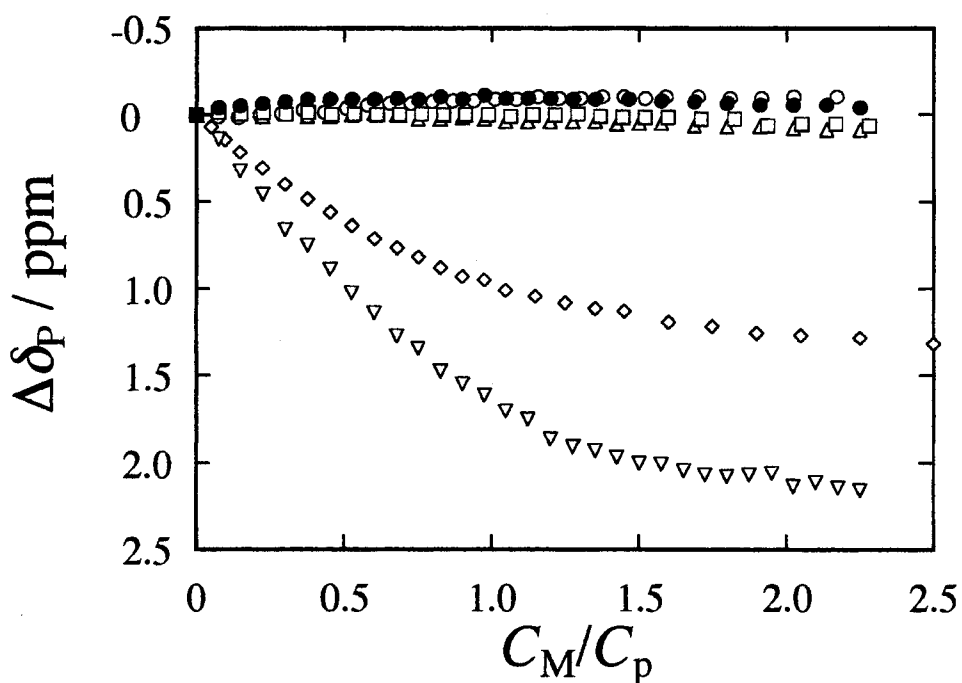
Fig.3-11 Metal ion titration profiles of ^{31}P chemical shifts of N-P-N in $cP_3(NH)_2$.

(○) Mg^{2+}; (△) Ca^{2+}; (□) Sr^{2+}; (◇) Zn^{2+}; (▽) Cd^{2+}; (●) Ag^+; $Cp = 0.01$ mol dm^{-3}, $C_{Na}=0.1$ mol dm^{-3}, 22°C.
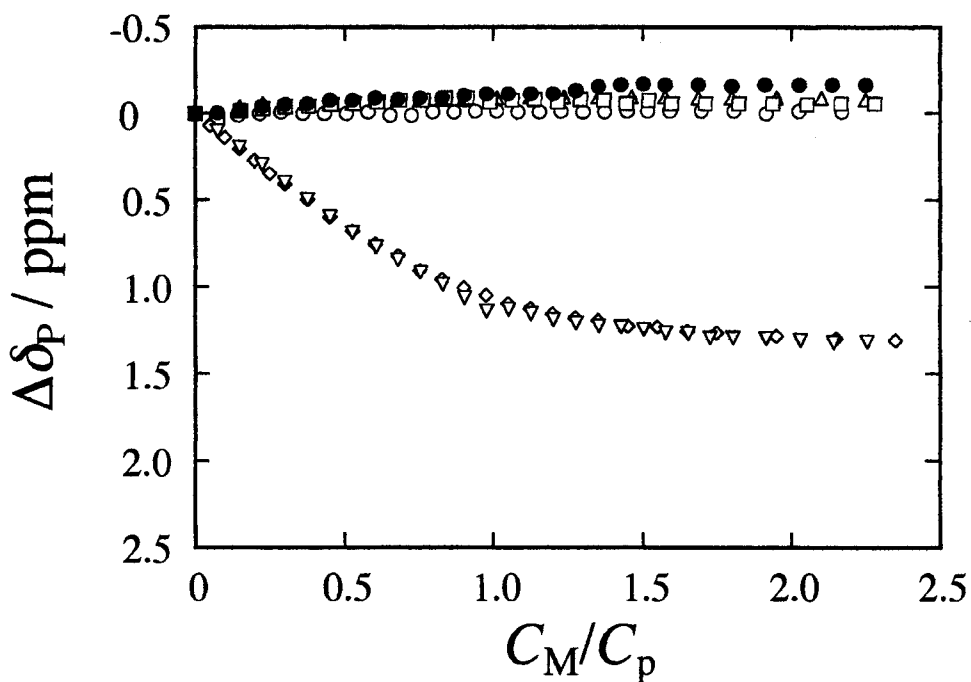
Fig.3-12 Metal ion titration profiles of ^{31}P chemical shifts of N-P-N in $cP_3(NH)_3$.

(○) Mg^{2+}; (△) Ca^{2+}; (□) Sr^{2+}; (◇) Zn^{2+}; (▽) Cd^{2+}; (●) Ag^+; $Cp = 0.01$ mol dm^{-3}, $C_{Na}=0.1$ mol dm^{-3}, 22°C.

Fig.3-13 The plots of $\Delta\delta_P$ vs. $\bar{n}$ (O-P-O in cP_3).
($\bigcirc$) Ca^{2+}; ($\triangle$) Cd^{2+}; ($\square$) Ag^+;
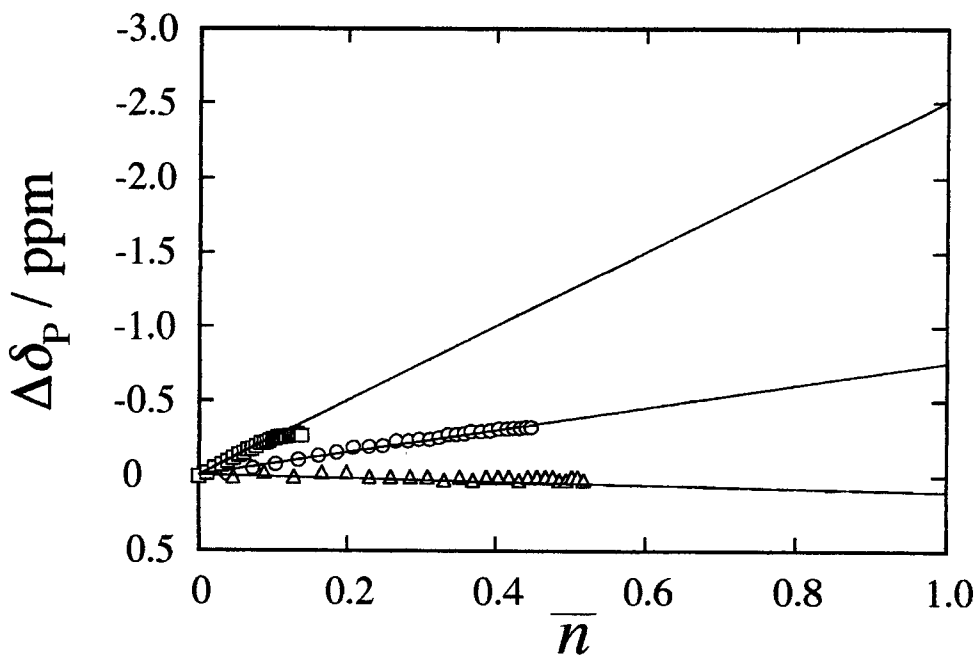$Cp = 0.01$ mol dm^{-3}, C_{Na}=0.1 mol dm^{-3}, 22°C.
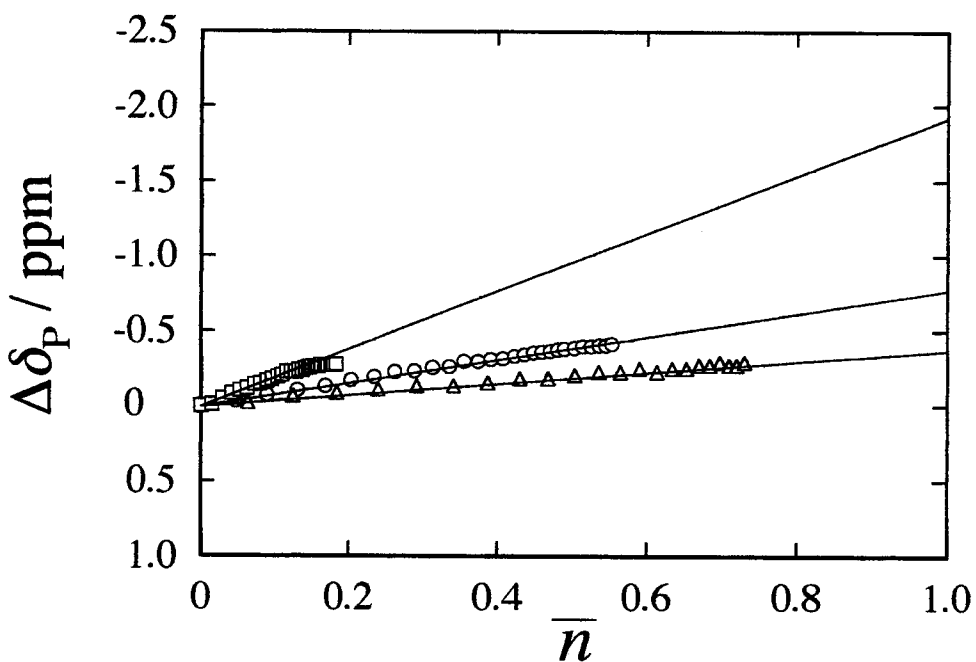
Fig.3-14 The plots of $\Delta\delta_P$ vs. $\bar{n}$ (O-P-O in $cP_3(NH)$).
($\bigcirc$) Ca^{2+}; ($\triangle$) Cd^{2+}; ($\square$) Ag^+;
$Cp = 0.01$ mol dm^{-3}, C_{Na}=0.1 mol dm^{-3}, 22°C.
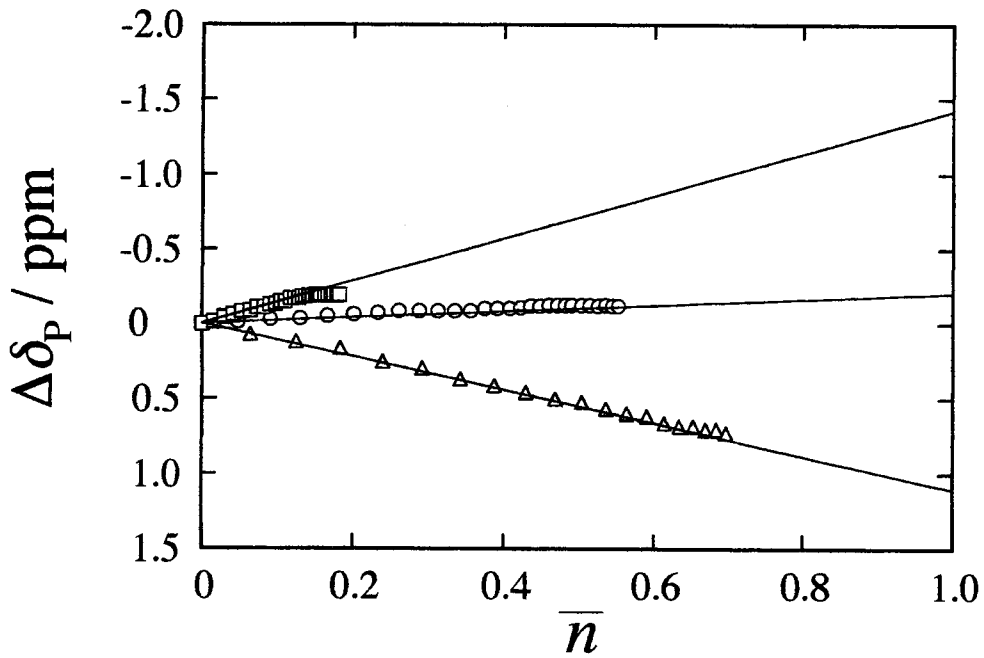
Fig.3-15 The plots of $\Delta\delta_P$ vs. $\bar{n}$ (O-P-N in $cP_3(NH)$).
(○) Ca^{2+}; (△) Cd^{2+}; (□) Ag^+;
$Cp = 0.01$ mol dm^{-3}, $C_{Na}=0.1$ mol dm^{-3}, 22°C.
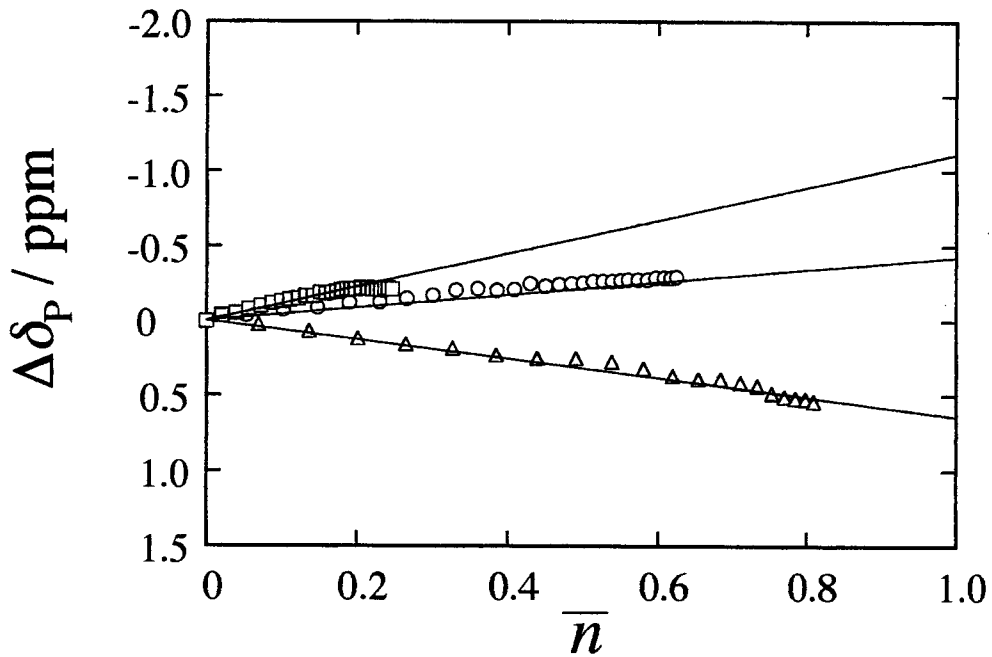
Fig.3-16 The plots of $\Delta\delta_P$ vs. $\bar{n}$ (O-P-N in $cP_3(NH)_2$).
(○) Ca^{2+}; (△) Cd^{2+}; (□) Ag^+;
$Cp = 0.01$ mol dm^{-3}, $C_{Na}=0.1$ mol dm^{-3}, 22°C.
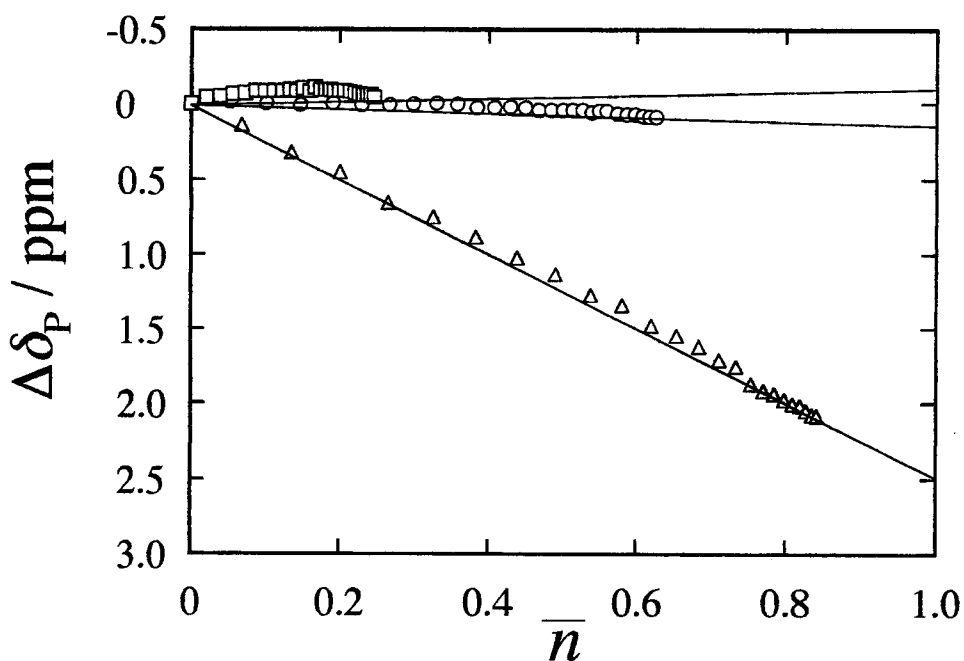
Fig.3-17 The plots of $\Delta\delta_P$ vs. $\bar{n}$ (N-P-N in $cP_3(NH)_2$).
(○) Ca^{2+}; (△) Cd^{2+}; (□) Ag^+;
$Cp = 0.01$ mol dm^{-3}, $C_{Na}=0.1$ mol dm^{-3}, 22°C.
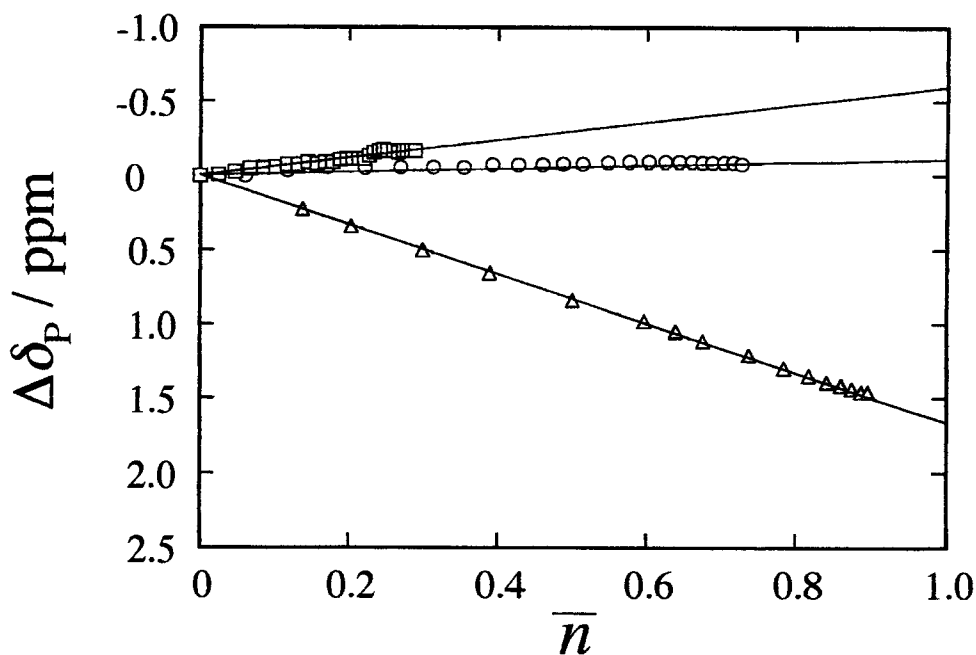
Fig.3-18 The plots of $\Delta\delta_P$ vs. $\bar{n}$ (N-P-N in $cP_3(NH)_3$).
(○) Ca^{2+}; (△) Cd^{2+}; (□) Ag^+;
$Cp = 0.01$ mol dm^{-3}, $C_{Na}=0.1$ mol dm^{-3}, 22°C.
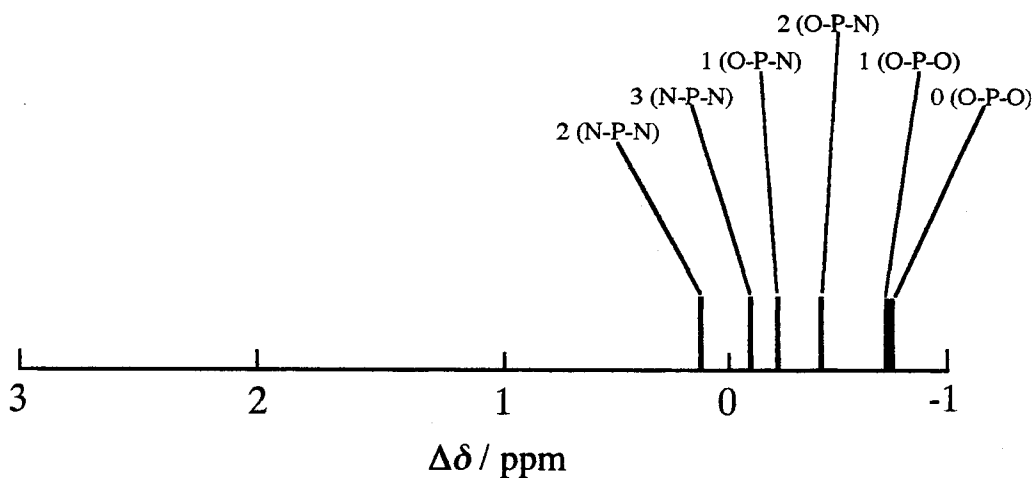
Fig. 3-19 The $\Delta\delta$ values of respective phosphorus atom of the $cP_3(NH)_n$ (n=0-3) ligand molecules complexed with Ca^{2+} ions.
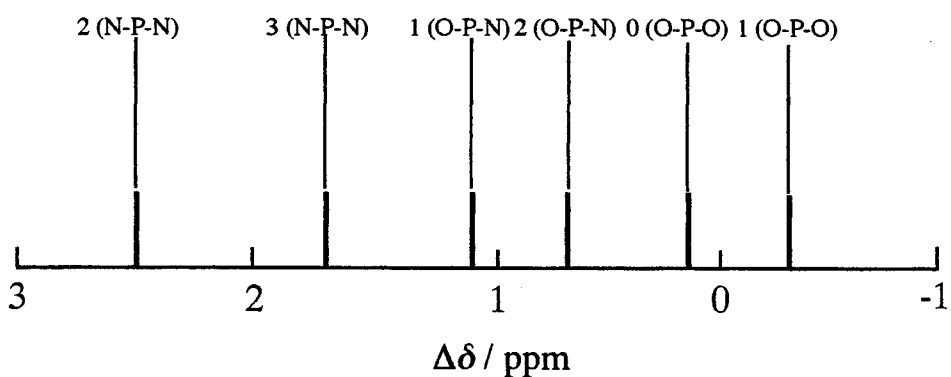
Fig. 3-20 The $\Delta\delta$ values of respective phosphorus atom of the $cP_3(NH)_n$ (n=0-3) ligand molecules complexed with Cd^{2+} ions.
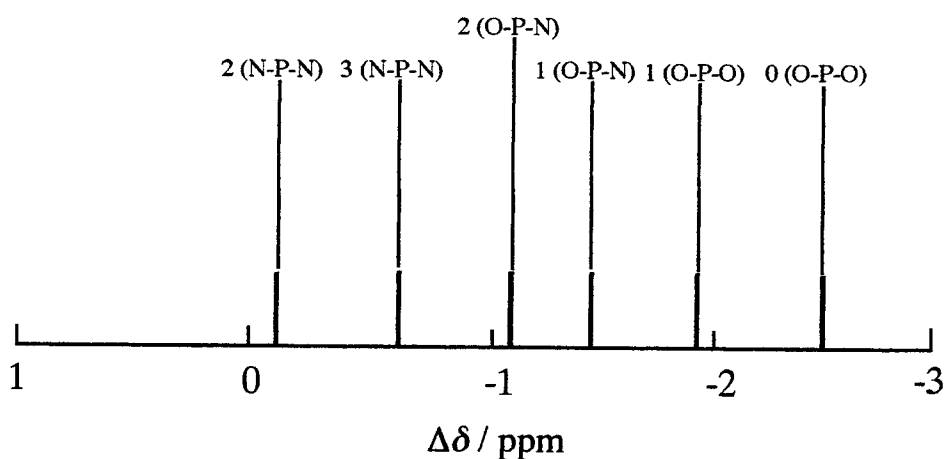
Fig. 3-21 The $\Delta\delta$ values of respective phosphorus atom of the cP$_3$(NH)$_n$ (n=0-3) ligand molecules complexed with Ag$^+$ ions.
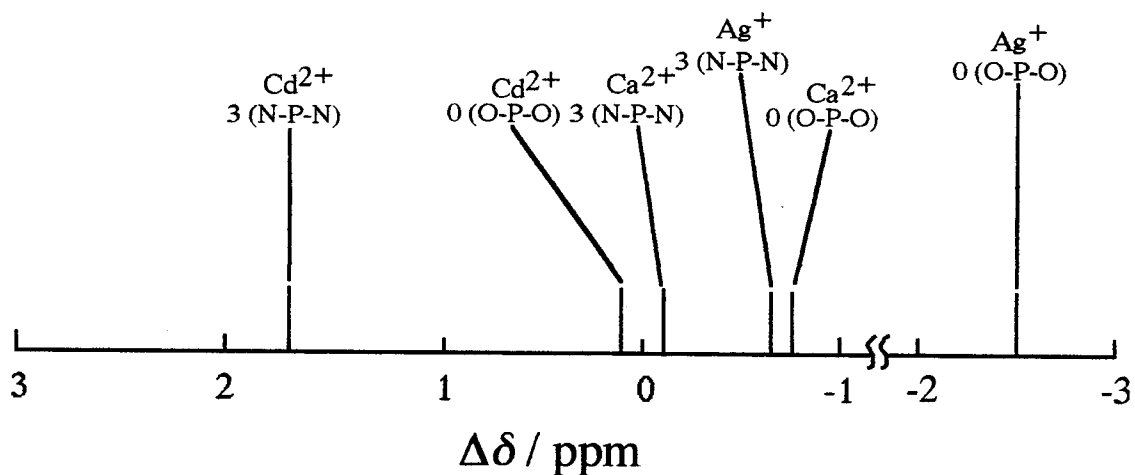
Fig. 3-22 The $\Delta\delta$ values of phosphorus atom of the cP$_3$(NH)$_n$ (n=0, 3) ligand molecules complexed with respective metal ions.

3-20

Table 3-1 Log β_1 values measured with the potentiometric titration method $(I=0.1, 25°C)$.

$cP_3(NH)_n$	Ag^+	Ca^{2+}	Cu^{2+}	Cd^{2+}
$n = 0$	1.28 ± 0.02	2.05 ± 0.02	2.09 ± 0.02	2.25 ± 0.01
$= 1$	1.43 ± 0.03	2.26 ± 0.02	2.62 ± 0.01	2.79 ± 0.02
$= 2$	1.61 ± 0.02	2.41 ± 0.01	3.05 ± 0.01	3.09 ± 0.01
$= 3$	1.72 ± 0.03	2.64 ± 0.01	3.83 ± 0.01	3.56 ± 0.02

Table 3-2 Thermodynamic quantities associated with the interaction of $cP_3(NH)_n{}^{3-}$ $(n=0-3)$ anions with metal ions in a 1:1 ratio (298.15 K, $I = 0.1$)

Ligand	Metal ion	$-\Delta G^o$ / kJ mol^{-1}	$-\Delta H^o$/ kJ mol^{-1}	$T\Delta S^o$ / kJ mol^{-1}
$cP_3{}^{3-}$	Ca^{2+}	11.7	-13.0	24.6
	Cu^{2+}	11.9	-6.0	17.9
	Cd^{2+}	12.9	95.7	-82.8
$cP_3(NH)^{3-}$	Ca^{2+}	12.9	1.0	11.9
	Cu^{2+}	14.9	-17.7	32.5
	Cd^{2+}	15.9	-9.0	24.9
$cP_3(NH)_2{}^{3-}$	Ca^{2+}	13.7	-14.0	27.7
	Cu^{2+}	17.4	7.0	10.4
	Cd^{2+}	17.7	33.6	-15.9
$cP_3(NH)_3{}^{3-}$	Ca^{2+}	15.0	-24.6	39.6
	Cu^{2+}	21.0	-14.3	35.3
	Cd^{2+}	20.3	5.3	15.0

CHAPTER 4

^{27}Al NMR study on multidentate complexation behavior of *cyclo*-μ-imidotriphosphate anions in aqueous solution.

ABSTRACT

^{27}Al NMR spectra of Al^{3+} ions complexed with *cyclo*-triphosphate anions, cP_3, and *cyclo*-μ-imidotriphosphate anions, $cP_3(NH)_n$ (n=1-3) have been measured. In the Al^{3+}-$cP_3(NH)_3{}^{3-}$ complexation system, successive complexations to form mono-, di-, and tridentate complexes have been confirmed by an additivity rule found in the relationship between the number of coordination atoms and the ^{27}Al chemical shift value of respective complex. The peak area ratio calculated for tridentate complexes to didentate complexes remains constant(= ca. 0.3) irrespective of the change in the concentrations of Al^{3+} and the ligand anions, indicating that the successive complexation is intramolecular reaction. A further deconvolution of the ^{27}Al spectra revealed direct coordination of Al^{3+} ions with nitrogen atoms as well as non-bridging oxygen atoms belonging to the ligand molecules.

INTRODUCTION

cyclo-μ-imidotriphosphate anions, $cP_3(NH)_n{}^{3-}$ (n=1-3) anions composed of P-O-P and P-NH-P linkages contain oxygen atoms and nitrogen atoms, which may participate in coordination with metal ions. Much attention has been drawn for the multidentate complexation property of the cyclic ligand molecule, because most of inorganic polyphosphate anions have only phosphate oxygen atoms as coordination atoms. The present authors have observed a preferential binding of divalent transition metal ions, such as Cu^{2+} and Cd^{2+} ions to $cP_3(NH)_3{}^{3-}$ anions[1]. Also, by comparison with the complexation behavior of anions of $cP_3(NH)_n{}^{3-}$ (n=0-2), participation of nitrogen atoms in the coordination of $cP_3(NH)_3$ anions has been indicated[2]. It has been claimed by the present authors that metal NMR technique is one of the promising approaches to investigate the microscopic structures of the complexes with the ligands composed of different coordinating atoms[3].

4-1

EXPERIMENTAL

Chemicals

Trisodium *cyclo*-mono-μ-imidotriphosphate monohydrate, $Na_3P_3O_8(NH) \cdot H_2O$, trisodium *cyclo*-di-μ-imidotriphosphate monohydrate, $Na_3P_3O_7(NH)_2 \cdot H_2O$, and trisodium *cyclo*-tri-μ-imidotriphosphate tetrahydrate, $Na_3P_3O_6(NH)_3 \cdot 4H_2O$, were prepared according to the method in chapter 2 in this thesis.

The purity was determined by HPLC and ^{31}P NMR measurements to be over 97%. The phosphorus concentration in the ligand stock solution was determined colorimetrically with a Mo(V)-Mo(VI) reagent[4]. The standard $Al(NO_3)_3$ stock solution was prepared at about 2.0 mol dm^{-3} from respective reagents with distilled water, and was standardized by the EDTA complexometry. Other reagents used in this work were of analytical grade.

NMR measurements

All NMR titrations were carried out by adding a portion of $cP_3(NH)_n{}^{3-}$ (*n*=0-3) sodium salt solution to a 3.00 cm[3] portion of $Al(NO_3)_3$ solution contained in an NMR sample tube with a micro-syringe. Since Al^{3+} is highly hydrolyzable, the pH of the sample solutions was kept between 4.2 and 4.7 throughout the NMR titration experiment by adding 0.1 mol dm^{-3} HNO_3 or NaOH solution. Supporting electrolyte was not added to the sample solutions. All NMR spectra were recorded on a JEOL JNM-GX-400 (9.39 T) Fourier-transform pulse NMR spectrometer with a tunable broad-band probe. ^{27}Al NMR spectra were recorded at an operating frequency of 104.2 MHz, and were applied a sweep width of 13000 Hz (124.76 ppm); the data acquisition time was 0.4 sec. The Lorentzian line-broadening factor of 1.0 Hz was applied to the total free induction decay prior to Fourier transformation. The relaxation delay between each scan of 0.1 sec was employed. Since it was confirmed that further extension of the relaxation delay did not change the intensity of ^{27}Al NMR spectra, it was concluded that the ^{27}Al NMR peak area was nearly proportional to the number of ^{27}Al nuclei producing the NMR resonance. ^{31}P NMR spectra were recorded at an operating frequency of 161.8 MHz; the data acquisition time was 2.0 sec, and the Lorentzian line-broadening factor

was 1.5 Hz. A relaxation delay between each scan was 0.5 sec. The NMR chemical shifts were recorded against external standards of 0.1 mol dm^{-3} Al(NO$_3$)$_3$ + 0.1 mol dm^{-3} HNO$_3$ in 10% D$_2$O for ^{27}Al measurements, and 75% H$_3$PO$_4$ in 10% D$_2$O for ^{31}P measurements, respectively. All sample solutions did not contain D$_2$O for a field-frequency locking, because it was suspected that D$_2$O would change the chemical atmosphere of the solvent. All the spectra were recorded with non-^{1}H decoupling. All of ^{31}P NMR spectra were measured at 22 ± 1°C, whereas ^{27}Al NMR spectra were measured at 0, 10, 22, 30, 40 ± 0.5°C.

RESULTS AND DISCUSSION

^{27}Al NMR spectra of Al^{3+}-ligand mixture solutions have been obtained in order to determine of the structures of the complexes. ^{27}Al NMR method has the advantage of both the high sensitivity (the isotopic abundance of ^{27}Al nuclei is 100%), and the well-resolved peaks due to the slow chemical exchange[5]. Futhermore, the chemical shift value corresponding to the complexes changes linearly with an increase in the ligand coordination number[3]. These enable us to determine the microscopic structures of the Al^{3+}-cP$_3$(NH)$_n$ (n=0-3) complexes. The concentrations of the monodentate, bidentate and tridentate ligand complexes can be calculated from the areas of the deconvoluted peaks.

It should be pointed out that, an additivity law has been reported on the ^{27}Al NMR measurement of successive complexation of Al^{3+} ion in aqueous solution; respective spectra corresponding to [AlX$_i$Y$_{6-i}$] (i=0-6) type complexes give ^{27}Al chemical shift values varying proportionally to i upon exchanging Y by X[3]. In an aqueous solution of inorganic polyphosphate molecules, such as cyclic polyphosphate, cP$_n$, where Y=H$_2$O and X=PO$_3^-$, the shift change is approximately 3 ppm upfield upon coordination with one phosphate moiety[6]. By applying this law to examine the microscopic coordination structures of the complexes with inorganic cyclic polyphosphate anions, it has been verified that the ligand molecules form not only monodentate ligand complexes, but also multidentate ligand complexes, depending on the number of the phosphate groups which constitute the cyclic molecules. It is also notable that the shift change upon substitution by phosphate group is not depending on the number of phosphate groups which constitute the cyclic molecules; the shift value is just influenced by the

number of phosphate moieties bound directly to Al^{3+} ions.

Based on above informations, the ^{27}Al NMR spectra of Al^{3+}-$cP_3(NH)_n$ (n=0-3) system can be analyzed. The representative ^{27}Al NMR spectra of the mixture solutions of 0.02 mol dm^{-3} Al^{3+} and 0.033 mol dm^{-3} $cP_3(NH)_n$ (n=0-3) are shown in Fig. 4-1. The peaks appearing at -4 ppm correspond to monodentate complexes, whereas the peaks appearing at -8 ppm and -12 ppm correspond to bidentate and tridentate complexes, respectively. The peak assignment is based on the fact that ^{27}Al NMR chemical shift, δ_{Al}, change stepwisely, due to the successive complexation. δ_{Al} is additive to the number of the coordinating ligand molecules displaced for the coordinated H_2O molecules in hexa-hydrated Al^{3+}-ion, $[Al(H_2O)_6]^{3+}$. In Fig. 4-1, a good linear relationship holds between the chemical shift values and the coordination numbers. In addition, since the half-width of the peaks due to monodentate and bidentate complexes increases with the number of P-NH-P linkages, it can be seen that nitrogen atoms of imino groups coordinate directly to Al^{3+} ions. And the peak due to tridentate complexes can only be observed in the Al^{3+}-$cP_3(NH)_3^{3-}$ system. It is obvious that three P-NH-P linkages in a $cP_3(NH)_3$ ligand are necessary for the formation of tridentate complexes. The protonation behavior of these $cP_3(NH)_n$ (n=0-3) ligands has been investigated by an electrochemical method as well as by measuring the change of the ^{31}P NMR chemical shifts upon protonation. The basicity of the phosphate groups in the cyclic trimers increases with replacement of P-O-P linkages by P-NH-P linkages of the ligand molecules[24,25]. Because of the increase in the ligand basicity, affinity between Al^{3+} ions and $cP_3(NH)_n$ (n=0-3) increases with the number of P-NH-P linkages of the ligands. ^{27}Al NMR spectra of Al^{3+}-$cP_3(NH)_3^{3-}$ ligand mixture solutions have been obtained at various ratio of the total concentrations $cP_3(NH)_3$ ligands to Al^{3+} ions, C_P/C_{Al}, in order to determine the structures of the complexes and the microscopic complexation behavior of the $cP_3(NH)_3$ ligands. In Fig. 4-2 are shown the representative ^{27}Al NMR spectra of the mixture solutions of Al^{3+} ions and $cP_3(NH)_3$ ligands at various C_P/C_{Al}. As mentioned above, the peaks appearing at -4, -8 and -12 ppm are considered to correspond to mono-, bi-, and tridentate complexes, respectively.

An interesting result obtained is that the peak area ratio of the tridentate complex to the bidentate complex seems to be always constant. In order to get acquainted with this phenomenon, these spectra have been separated into three peaks by the non-linear curve fitting

method for the Lorentzian curve. The intensities of the Lorentzian peaks, I_δ, at certain chemical shift values, δ, can be expressed by eqn. 4-1.

$$I_\delta = \frac{I_{max}}{1 + (\delta_0 - \delta)^2 / W_{1/2}{}^2} \qquad (4\text{-}1)$$

where I_{max}, δ_0, and $W_{1/2}$ indicate the maximum intensity, the center chemical shift, and the half-height width of the Lorentzian peak, respectively. The peak area of the Lorentzian signal, S, can be calculated by the definite integral as follows;

$$S = \int_{\delta_A}^{\delta_B} \frac{I_{max}}{1 + (\delta_0 - \delta)^2 / W_{1/2}{}^2} \, d\delta$$

$$= I_{max} \cdot W_{1/2} \arctan\left(\frac{\delta_A - \delta_0}{W_{1/2}}\right) - I_{max} \cdot W_{1/2} \arctan\left(\frac{\delta_B - \delta_0}{W_{1/2}}\right) \qquad (4\text{-}2)$$

The peak area ratios of the tridentate complexes to the bidentate complexes, S_3/S_2, are plotted against the C_P/C_{Al} values, as shown in Fig. 4-3. These ratio, S_3/S_2, are equal to the concentration ratios of the respective chemical species, i.e., the tridentate to bidentate complexes. The S_3/S_2 value remain constant (=0.27) irrespective of the C_P/C_{Al} values. Furthermore, the plots of the $S_1/(S_2+S_3)$ remain constant irrespective of the C_P/C_{Al} change, as shown in Fig. 4-4. The $S_1/(S_2+S_3)$ values also remain constant (=0.12) irrespective of the C_P/C_{Al} values in the high C_P/C_{Al} range, i.e., $C_P/C_{Al} \geqq 6.7$. These results are strong proofs for the intramolecular complexation reaction of Al^{3+} ion with $cP_3(NH)_3$ ligand.

In the lower temperature, since the exchange rate is slower, it can be obtained the information about more microscopic complex formation behavior. The ^{27}Al NMR spectrum of the mixture solution of 0.02 mol dm^{-3} Al^{3+} and 0.033 mol dm^{-3} $cP_3(NH)_3$ ligands at 0±2 °C is shown in Fig. 4-5. It is obvious that the peak of the monodentate complexes separates into two peaks, and that of the bidentate complexes separates into two peaks. It can be seen that the coordinating atoms in the cyclic trimers are not only oxygen atoms but also nitrogen atoms. Since there are two kinds of the coordination atoms, it seems that the peaks of the monodentate complexes consist of two peaks, i.e., O-coordination and N-coordination, essentially.

Similarly, the peaks of the bidentate complexes may consist of three peaks, *i.e.*, O,O-, O,\N- and N,N-coordination, and the peaks of the tridentate complexes may consist of four peaks, *i.e.*, O,O,O-, O,O,N-, O,N,N-, and N,N,N-coordination.

In order to get information about the microscopic complexation behavior, all ^{27}Al NMR spectra of the Al^{3+}-$cP_3(NH)_3^{3-}$ mixture solutions at 22 ± 2 °C have been separated into six Lorentzian curves by the non-linear curve fitting method. In this study, the peak of the tridentate complex has not been separated, because the number of the microscopic complexes is too large, *i.e.*, 4. The representative separated ^{27}Al NMR spectrum of Al^{3+}-$cP_3(NH)_3^{3-}$ mixture solution is shown in Fig. 4-6. All of the spectra can be expressed as the sums of the six peaks correspond to the respective microscopic complexes. The chemical shifts, δ_{Al}, which determined by the peak separation are plotted against the C_P/C_{Al} values in Fig. 4-7. The δ_{Al} values of each chemical species remain almost constant irrespective of the C_P/C_{Al} values, it is a proof for the appropriate peak separation. In ^{27}Al NMR spectra of Al^{3+}-$cP_3(NH)_n^{3-}$ ($n=1, 2$) mixture solutions at 22 ± 2 °C, the peaks of the monodentate and bidentate complexes can be separated into two and two peaks ($n=1$) and two and three peaks ($n=2$), respectively, and these spectra have been separated into four ($n=1$) and five ($n=2$) Lorentzian curves. In these spectra, the peaks of the tridentate complex have not been appeared. The determined δ_{Al} values are plotted against the C_P/C_{Al} values in Fig. 4-8.

It should be pointed out that, an additivity law has been reported on the ^{27}Al NMR measurement of successive complexation of Al^{3+} ion in aqueous solution. The ^{27}Al NMR chemical shift values, δ_{Al}, of the stepwise coordination in the series of cyclic phosphate ligand systems are plotted against the number of the non-bridging oxygen atoms, i, coordinated with Al^{3+} ion in Fig.4-9[3]. It is shown that corresponding to $[AlX_i(H_2O)_{6-i}]$ ($i=0-3$) type complexes give ^{27}Al chemical shift values varying proportionally to i upon exchanging H_2O molucule by X atom. The shift change is approximately 3 ppm up-field upon coordination with one phosphate moiety. Further, the $\delta_{Al,int}$ values in the Al^{3+}-$cP_3(NH)_n^{3-}$ ($n=1-3$) systems are plotted against the number of coordinating atoms with Al^{3+} ion, i, as shown in Fig. 4-10. In this figure, the slope of dotted line is equals to that of straight line in Fig. 4-9. It shows that these chemical shift values are due to O- or O,O-coordination, respectively. We can see that the "new additivity law" observed in the ^{27}Al NMR chemical shift change upon binding Al^{3+} ion

with the imino groups in the imidopolyphosphate ligand molecules. The intrinsic chemical shift value, $\delta_{Al,\,int}$, can be expressed in the additive form as,

$$\delta_{Al,\,int} = i\ \delta(\text{P-O}^-) + j\ \delta(\text{P-N}) + (6 - i - j)\ \delta(\text{H}_2\text{O}) \qquad (4\text{-}3)$$

where $\delta(\text{P-O}^-)$, $\delta(\text{P-N})$, and $\delta(\text{H}_2\text{O})$ are the intrinsic chemical shift values corresponding to the coordination due to monodentate phosphate group and imino group, and water molecules. The value of $\delta(\text{P-O}^-)$ is estimated previously as ca. -3.2 ppm and $\delta(\text{H}_2\text{O})$ is 0 ppm from its definition. By estimating the $\delta(\text{P-N})$ value equal to -4.2 ppm, all the $\delta_{Al,int}$ values for respective coordination structures are calculated. From this "new additivity law" it can be estimated that the peak corresponding to the tridentate ligand complex observed in the Al^{3+}-$cP_3(NH)_3{}^{3-}$ system can be assigned to N, N, O- or N, N, N-coordination.

From these experimental evidences, we can conclude that some Al^{3+} ions are bound to nitrogen atoms as well as oxygen atoms of $cyclo$-μ-imidotriphosphate anions to form mono-, bi-, and tridentate complexes in aqueous solutions. This N, N, N-coordination can only be explained by the position of Al^{3+} ion bound on the $cP_3(NH)_3$ molecules, where an Al^{3+} ion is bound at the center of the three equivalent nitrogen atoms, because the reaction of Al^{3+} ion with $cP_3(NH)_3$ ligand has been intramolecular reaction, and it is the most significant finding.

The structures of Al^{3+}-$cP_3(NH)_n{}^{3-}$ (n=0-3) complexes can be estimated by ^{27}Al NMR measurement, by the preceding discussion, and the analysis of the ^{31}P NMR spectra of the corresponding sample solutions are facilitated. The respective ^{31}P NMR spectra of Al^{3+}-$cP_3(NH)_n{}^{3-}$ (n=0-3) complexation systems shown in Fig. 4-11, it is notable that the number of the peaks due to complexation in the Al^{3+}-$cP_3(NH)_3{}^{3-}$ system are quite small compared with other systems, even though multidentate ligand complexation is apparently observed in the ^{27}Al NMR spectra. Because of ^{31}P NMR chemical shift shows upfield shift upon direct phosphate-Al^{3+} ion binding, such small shifts upon complexation are unexplainable, if we assume the complexation is due to the coordination of Al^{3+} ions with the non-bridging oxygen atoms. Another binding mode specific for the Al^{3+}-$cP_3(NH)_3{}^{3-}$ system should be taken into account, $i.e.$, Al^{3+}-N direct binding.

REFERENCES

1. M. Komiya, T. Miyajima, S. Sato, M. Watanabe, *Phosphorus Res. Bull.*, **1**, 137 (1991).

2. T. Miyajima, H. Maki, M. Sakurai, S. Sato, M. Watanabe, *Phosphorus Res. Bull.*, **3**, 31 (1993).

3. T. Miajima, R. Kakehashi, *Phosphorus Res. Bull.*, **1**, 101 (1991).

4. F. L. Conde, L. Prat, *Anal. Chim, Acta,* **16**, 473(1957).

5. J. J. Delpuech, M. R. Khadder, A. A. Peguy, and P. R. Rubin, *J. Am. Chem. Soc.*, **97**, 3373(1975).

6. T.Miyajima, H.Maki, M.Sakurai, S.Sato, M.Watanabe, *Phosphorus. Res. Bull.*, **3**, 31(1993).

7. T.Miyajima, H.Maki, M.Sakurai, M.Watanabe, *Phosphorus. Res. Bull.*, **5**, 155(1995).
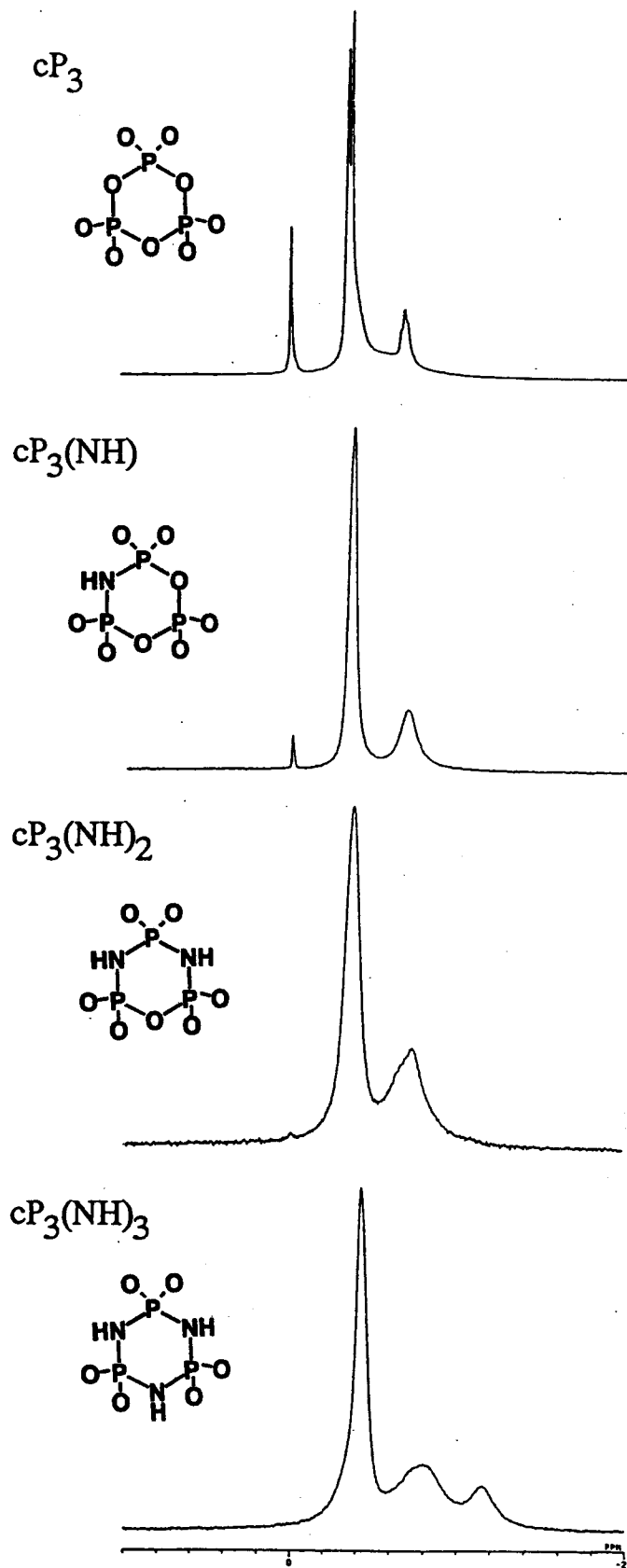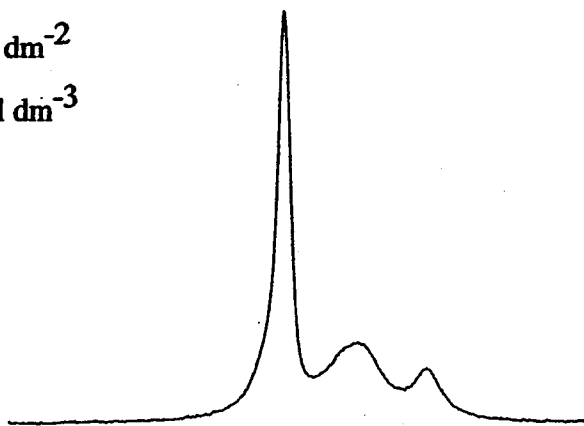
Fig. 4-1 Representative ^{27}Al NMR spectra of Al^{3+}-cP$_3$(NH)$_n$ (n=0-3) systems. $C_P = 3.33 \times 10^{-2}$ mol dm^{-3}, $C_{Al} = 2.00 \times 10^{-2}$ mol dm^{-3}.

$C_p = 3.33 \times 10^{-3}$ mol dm^{-2}

$C_{Al} = 2.00 \times 10^{-2}$ mol dm^{-3}

$C_p / C_{Al} = 1.67$

$C_p = 1.67 \times 10^{-3}$ mol dm^{-2}

$C_{Al} = 5.00 \times 10^{-3}$ mol dm^{-3}
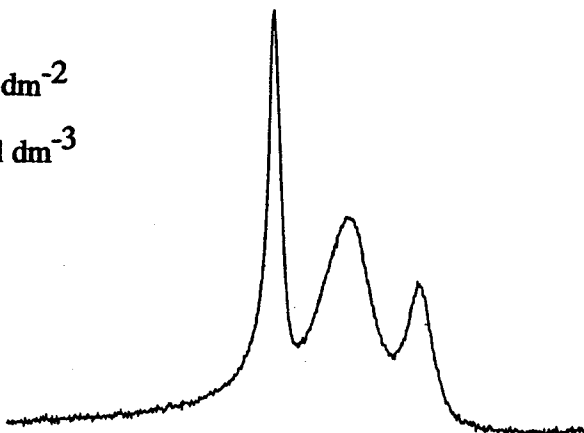
$C_p / C_{Al} = 3.33$

$C_p = 1.00 \times 10^{-2}$ mol dm^{-2}

$C_{Al} = 5.00 \times 10^{-3}$ mol dm^{-3}

$C_p / C_{Al} = 3.33$
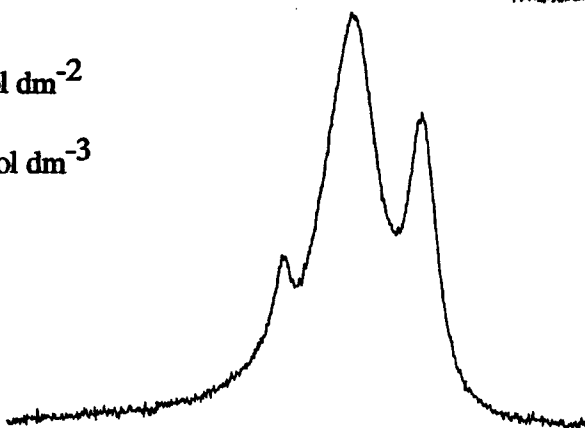
$C_p = 3.33 \times 10^{-3}$ mol dm^{-2}

$C_{Al} = 5.00 \times 10^{-3}$ mol dm^{-3}

$C_p / C_{Al} = 6.67$
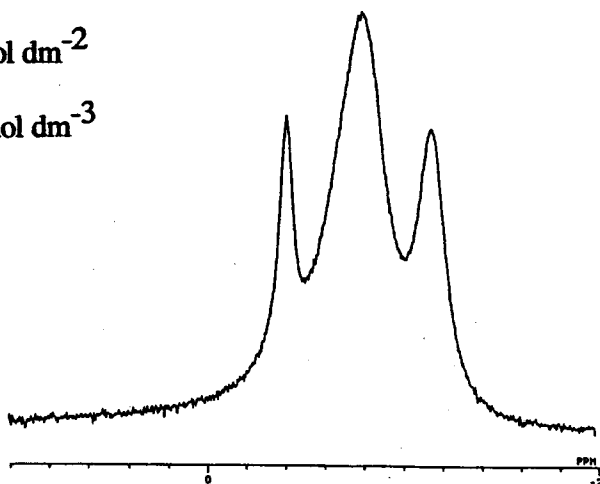
Fig. 4-2 Representative ^{27}Al NMR spectra of Al^{3+}-cP$_3$(NH)$_3$ systems.
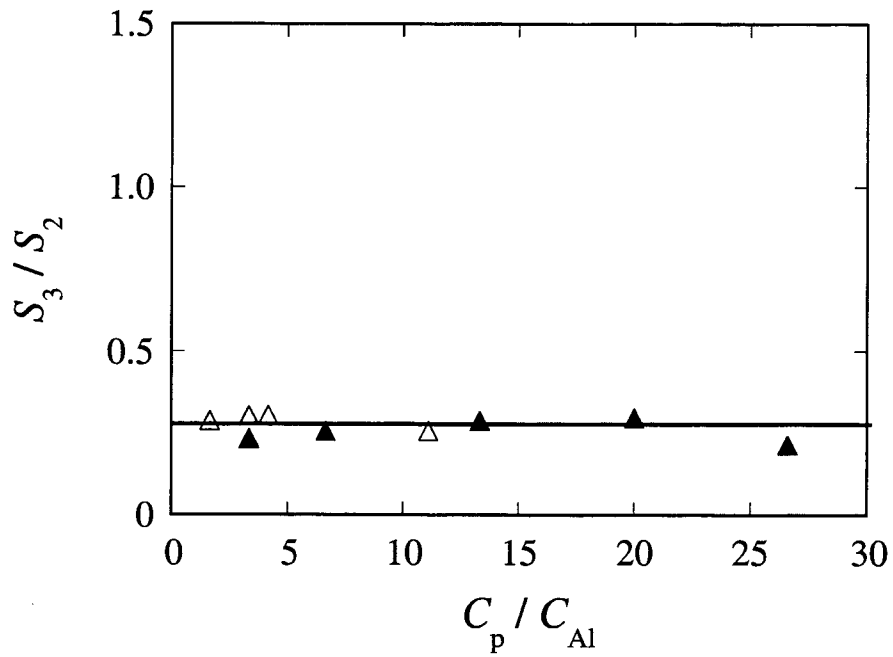
Fig.4-3 The plot of S_3/S_2 vs.C_p/C_{Al}.
   solid line; The constant value in the all region.
   open; C_{Al} is constant at 0.005 mol dm^{-3}.
   closed; C_p is constant at 0.033 mol dm^{-3}.
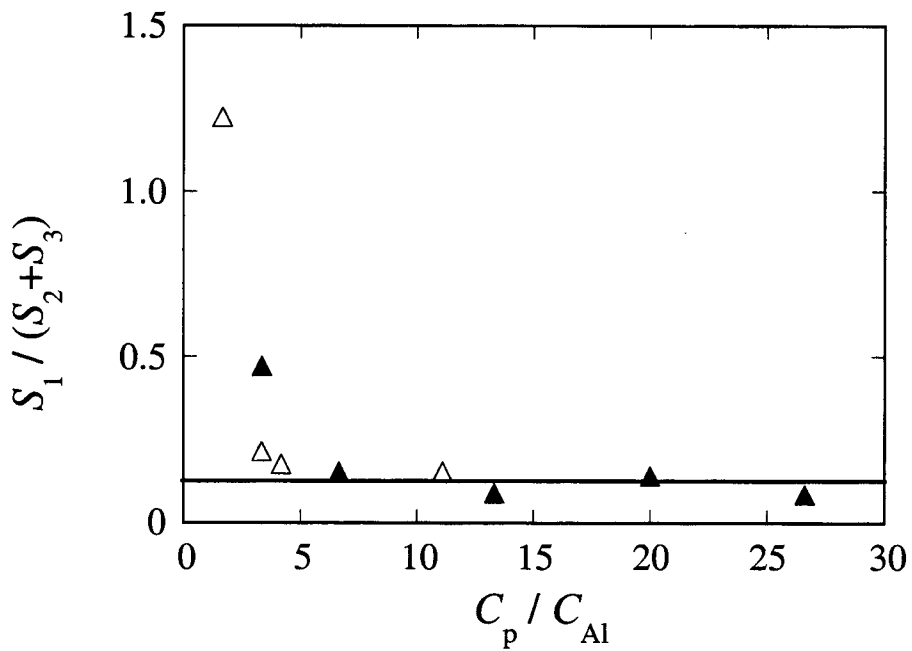
Fig.4-4 The plot of $S_1/(S_2+S_3)$ vs.C_p/C_{Al}.
   solid line; The constant value at $C_p/C_{Al}>6.7$.
   open; C_{Al} is constant at 0.005 mol dm^{-3}.
   closed; C_p is constant at 0.033 mol dm^{-3}.
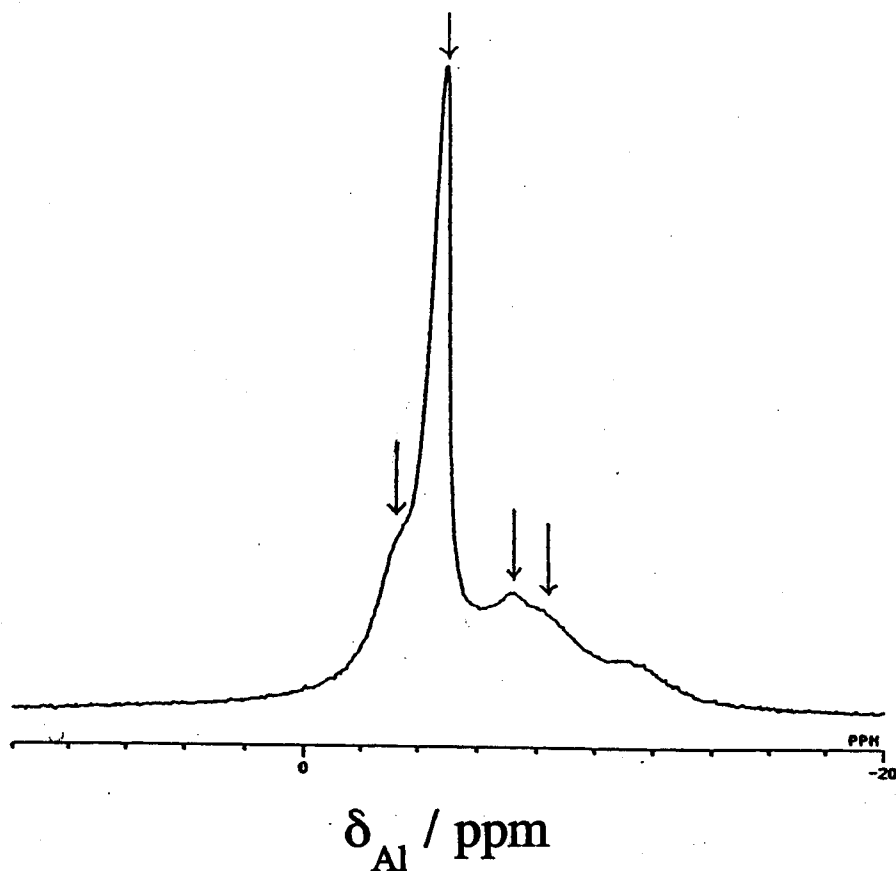
Fig. 4-5 ^{27}Al NMR spectrum of Al^{3+}-$cP_3(NH)_3$ mixtures at 0°C.
$C_P = 3.33 \times 10^{-2}$ mol dm^{-3}, $C_{Al} = 2.00 \times 10^{-2}$ mol dm^{-3}.
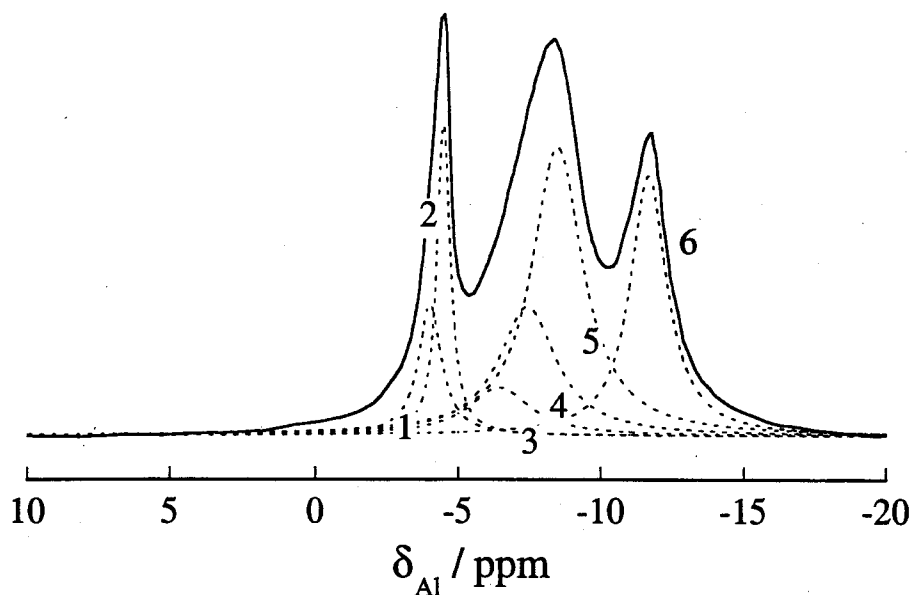
Fig.4-6 Representative peak separation of ^{27}Al NMR spectrum.
0.01 mol dm^{-3} Al^{3+} + 0.033 mol dm^{-3} $cP_3(NH)_3$, pH 4.63
1; O-coordination, 2; N-coordination, 3; O,O-coordination
4; O,N-coordination, 5; N,N-coordination, 6; tridentate complex.
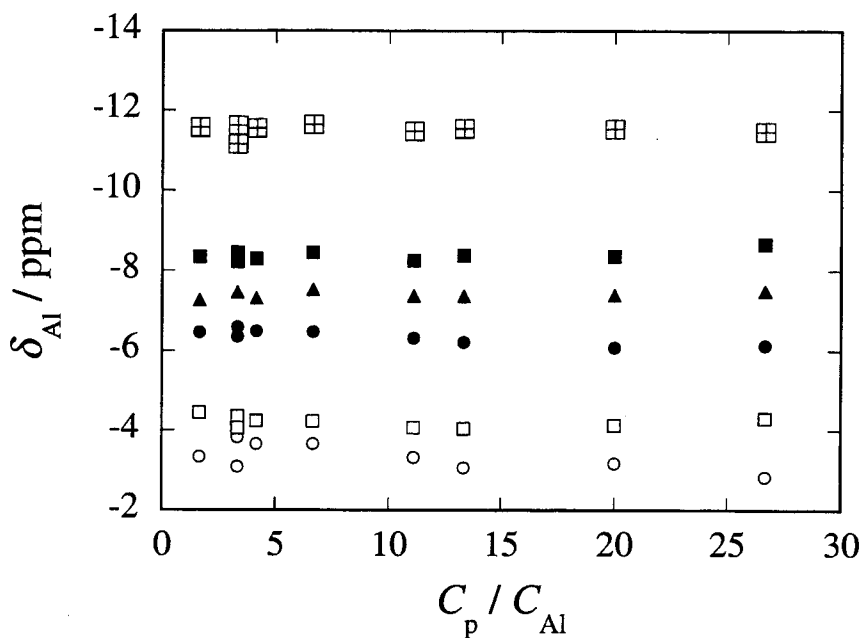
Fig.4-7 The plots of δ_{Al} vs. C_p/C_{Al} in Al^{3+}-$cP_3(NH)_3$ system.
(○); O-coordination,(□); N-coordination,(●); O,O-coordination,
(▲); O,N-coordination,(■); N,N-coordination,
(□); tridentate complex.
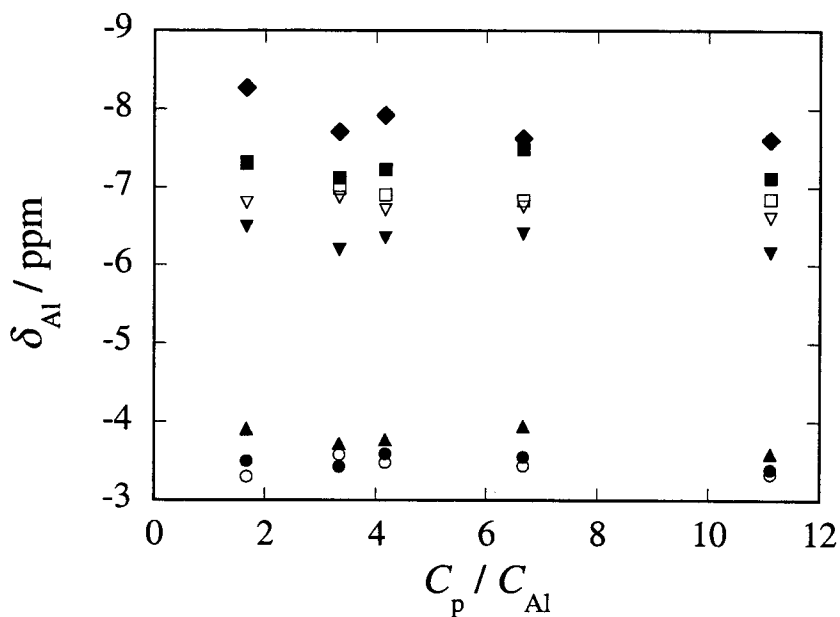
Fig.4-8 The plots of δ_{Al} vs. C_p/C_{Al} in Al^{3+}-$cP_3(NH)_n$ (n=1, 2) systems.
(○); O-coordination,(△); N-coordination, (▽); O,O-coordination,
(□); O,N-coordination, (◇); N,N-coordination.
open; Al^{3+}-$cP_3(NH)$ system, closed;Al^{3+}-$cP_3(NH)_2$ system.
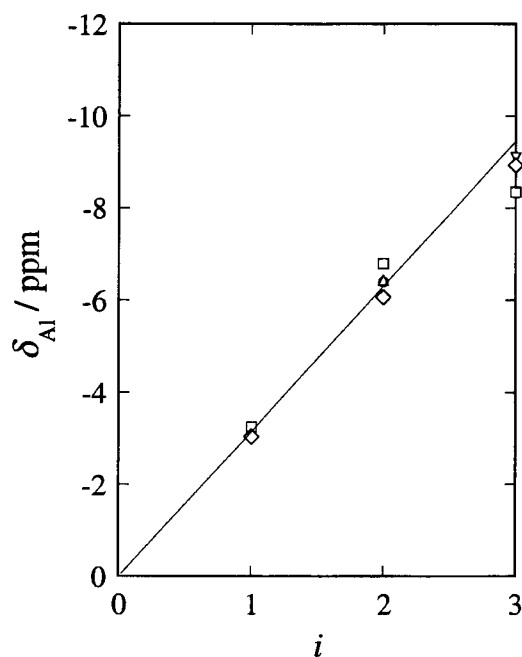
Fig.4-9 Additivity law of the respective intrinsic
chemical shift values δ_{Al} for the Al^{3+}-
cP_n^{n-} (n=3, 4, 6, 8) and -PP⁻ systems.
(◯); cP_3, (△); cP_4, (▽); cP_6, (□); cP_8,
(◇); long-chain polyphosphate.
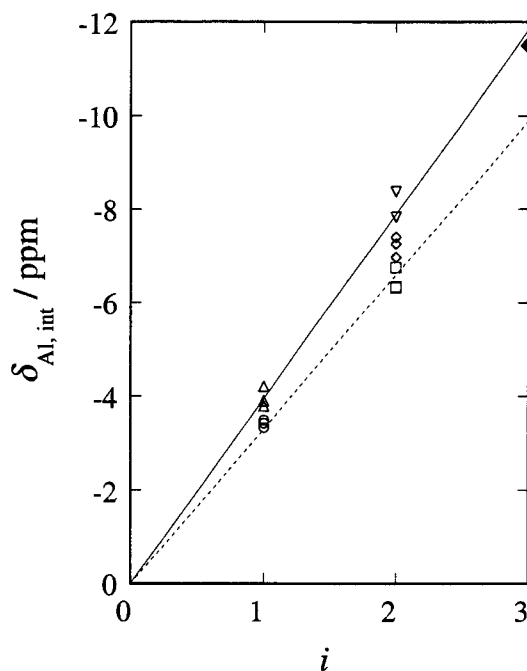
Fig.4-10 Additivity law of the respective intrinsic
chemical shift values $\delta_{Al, int}$ for the Al^{3+}-
$cP_3(NH)_n$ (n=1-3) systems.
(◯) ; O-coordination for n=1-3,
(△) ; N-coordination for n=1-3,
(□) ; O,O-coordination for n=1-3,
(◇) ; O,N-coordination for n=1-3,
(▽) ; N,N-coordination for n=2, 3,
(◆) ; tridentate complex for n=3.

4-14
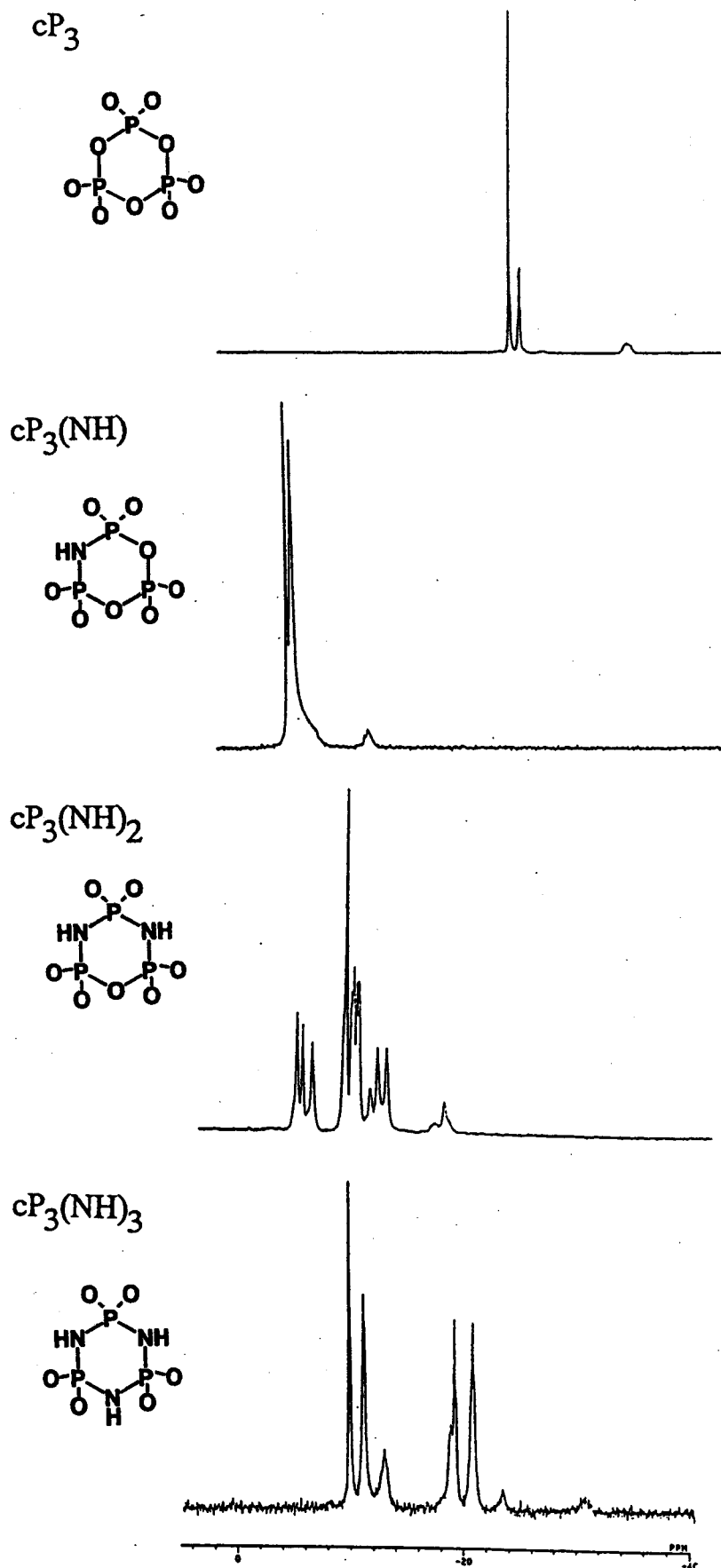
Fig. 4-11 Representative ^{31}P NMR spectra of Al^{3+}-$cP_3(NH)_n$ (n=0-3) systems. $Cp = 3.33 \times 10^{-2}$ mol dm^{-3}, $C_{Al} = 2.00 \times 10^{-2}$ mol dm^{-3}.

CHAPTER 5

^{9}Be and ^{31}P NMR analyses on Be^{2+} complexation with *cyclo*-tri-μ-imidotriphosphate anions in aqueous solution.

ABSTRACT

Microscopic information on complexation of Be^{2+} with *cyclo*-tri-μ-imido triphosphate anions in aqueous solution has been gained by both ^{9}Be and ^{31}P NMR techniques at -2.3 °C. Separate NMR signals corresponding to free and complexed species have been observed in both spectra. Based on an empirical additivity rule, *i.e.*, proportionality observed between the ^{9}Be NMR chemical shift values and the number of coordinating atoms of ligand molecules, the ^{9}Be NMR spectra have been deconvoluted. By the precise equilibrium analyses, the formation of mono- and bidentate complexes coordinated with non-bridging oxygen atoms has been verified, and the formation of complexes coordinating with nitrogen atoms of the cyclic framework in the ligand molecule has been excluded. Instead, the formation of one-to-one (ML) complexes, one-to-two (ML$_2$), together with two-to-one (M$_2$L) complexes has been disclosed, whose formation constants have been evaluated $K_{ML} = 10^{3.87 \pm 0.03}$ (mol dm^{-3})$^{-1}$, $K_{ML2} = 10^{2.43 \pm 0.03}$ (mol dm^{-3})$^{-2}$, and $K_{M2L} = 10^{1.30 \pm 0.02}$ (mol dm^{-3})$^{-2}$, respectively. ^{31}P NMR spectra measured concurrently have verified the formation of the complexes estimated by the ^{9}Be NMR measurement. Intrinsic ^{31}P NMR chemical shift values of the phosphorus atoms belonging to ligand molecules complexed with Be^{2+}, together with the coupling constants have been determined.

INTRODUCTION

In chapter 4, ^{27}Al NMR study on the multidentate complexation behavior of Al^{3+}-cP$_3$(NH)$_n^{3-}$ (n=0-3) system has been indicated direct coordination of Al^{3+} ions to imino nitrogen atoms. It has also been revealed that cP$_3$(NH)$_3^{3-}$ anions form various complexes from monodentate to tridentate coordination, and that imino nitrogen coordination has been much more favored than oxygen coordination for each complexes. This result does not agree with the simple prediction based on HSAB trends that Al^{3+} ions coordinate to not the softer bridging

nitrogen atoms but the harder non-bridging oxygen atoms. Several complex formation systems which Al^{3+} ions coordinate to not only oxygen donor atom but also nitrogen donor atom have been reported [1-5], and these peculiar coordination behavior are remarkably dependent on the high structural suitability, namely how well Al^{3+} ion fits into the cavity that the nitrogen donor atoms can provide for it.

The charge/ionic radius ratio for Be^{2+} ion (= 6.5 $Å^{-1}$) is greater than for any other cation except for H^+ and B^{3+}, so Be^{2+} ion is one of the hardest cations by an HSAB scale. The closest ratio is that for Al^{3+} (= 6.0 $Å^{-1}$) and some chemical similarities between Be^{2+} and Al^{3+} ions exist [6]. If the high structural suitability affects the coordination behavior of Al^{3+}- and Be^{2+}-$cP_3(NH)_3^{3-}$ systems, hence the ionic radius of Al^{3+} ion (0.51 Å) and Be^{2+} ion (0.35 Å) is different for about 1.5 times, it seems to observe some differences between both coordination behavior. In recent years, beryllium metal has utilized as material for beryllium copper which is excellent in conductivity, corrosion resistance and spring characteristics. However, despite strong carcinogenicity, only few attempts have so far been made at the chemical properties of beryllium compounds and the complexation behavior of Be^{2+} ions in aqueous solutions. In this study, it has been expected that various multidentate complexation behavior such as the direct coordination structure of "hard" Be^{2+} ions to the imino nitrogen atoms which is interested in solution chemistry. Although the previous study [7] has been suggested the direct coordination of Be^{2+} ions to the imino nitrogen atoms in the Be^{2+}-$cP_3(NH)_3^{3-}$ complex formation system by ^9Be NMR measurement, the complex stability has not been interpreted because the concentration range of Be^{2+} ion and $cP_3(NH)_3^{3-}$ ligand in the sample solution have limited very much. It is necessary to investigate a complex formation equilibrium over wide range of the concentrations of chemical species in order to indicate the thermodynamic stability of the coordination structure of the complex in aqueous solution.

In order to quantitatively evaluate the complex formation behavior, the complex stability constants which have been determined by a thermodynamic technique have been frequently applied. However, it has limited very much the directly observable species in many species which present in a solution by a thermodynamic technique, for example, such as the potentiometric titration which is widely employed has merely observed only the concentration of free cation, so it is difficult to directly determine the multidentate complex structure and the

coordination atoms of metal ions. On the other hand, the resolution in frequency and time domains of FT NMR are quite high, and the ability of distinction between the different chemical species is superior [8], so the complex structure in equilibrium systems can be obtained directly and simultaneously. In particular, the [9]Be NMR signal due to the free ion and the successive multidentate complexes [9,10] , since the ligand exchange rate of Be^{2+} ion is much slower than the NMR time scale as well as that of Al^{3+} ion, so FT NMR is a powerful tool for the investigation about the complicated multidentate complex structures. NMR peak area almost proportional to the number of nuclei, that is, the concentration of a species, and it leads to the quantitative information about a chemical equilibria. In the research applying NMR peak area, a particularly well studied system is that of the determination of the hydration number of cations [11-13], in addition, the investigations about the formation mechanism and the thermodynamic stability can be also applied [14-16]. In this study, the intricate multidentate coordination behavior of Be^{2+} ions with $cP_3(NH)_3$ ligands has been investigated quantitatively by [9]Be NMR and the peak deconvolution analysis of the NMR spectra.

In the Be^{2+}-$cP_3(NH)_3^{3-}$ system, ^{31}P nuclei in a $cP_3(NH)_3$ molecule is also high-sensitive NMR active nuclei, and by taking a high-resolution ^{31}P NMR technique one together, the multidentate coordination behavior which is obtained from [9]Be NMR spectra will become firmer.

EXPERIMENTAL

Chemicals

Trisodium *cyclo*-tri-μ-imido triphosphate tetrahydrate, $Na_3P_3O_6(NH)_3 \cdot 4H_2O$, was prepared according to the method in chapter 2 in this thesis. The purity of the ligand was determined by HPLC and ^{31}P NMR, and was found to be over 98%. The moisture content was determined colorimetrically with a Mo(V)-Mo(VI) reagent[17]. The stock solution of BeCl2 was determinated by the EDTA complexometry with [Co(NH3)6]Cl3[18]. Other reagents used in this work were of analytical grade.

NMR measurements

All NMR titrations were carried out by adding a portion of cP3(NH)3 sodium salt solution of 0.2 mol dm-3 to a 3.00 cm3 portion of BeCl2 solution contained in an NMR sample tube with a micro-syringe. Since Be^{2+} is highly hydrolyzable, *i.e.*, log $K_{Be(OH)}$ = 8.3[19], and the pK_{a1} value of cP3(NH)3 is 3.22±0.01[19], the pH of the sample solutions was kept between 2.3 and 2.7 throughout the NMR titration experiment by adding 0.1 mol dm-3 HCl solution. The initial BeCl2 concentrations, C_M^0, of the sample solutions of three titration series were 0.005, 0.01, and 0.02 mol dm-3. For all the titration series, the ratio of total concentrations of cP3(NH)3^{3-} to Be^{2+}, C_L/C_M, was varied from 0.1 to 4. Supporting electrolyte was not added to the sample solutions. All NMR spectra were recorded on a Bruker DPX-250 (5.87 T) Fourier-transform pulse NMR spectrometer with a tunable broad-band probe. ^{9}Be NMR spectra were recorded at an operating frequency of 35.147 MHz, and were applied a sweep width of 2500 Hz (71.130 ppm); the data acquisition time was 0.4 - 0.8 sec, and the data number during the free induction decay were collected in 2000 - 4000 points; *i.e.*, the resolution of the spectra on a frequency region was 1.25 - 2.50 Hz (0.0356 - 0.0711 ppm). The Lorentzian line-broadening factor of 1.0 Hz was applied to the total free induction decay prior to Fourier transformation. The relaxation delay between each scan of 0.1 sec was employed. Since it was confirmed that further extension of the relaxation delay did not change the intensity of ^{9}Be NMR spectra, it was concluded that the ^{9}Be NMR peak area was nearly proportional to the number of ^{9}Be nuclei producing the NMR resonance. ^{31}P NMR spectra were recorded at an operating frequency of 101.258 MHz; the data acquisition time was 2.0 sec, and the Lorentzian line-broadening factor was 1.5 Hz. A relaxation delay between each scan was 0.5 sec. The NMR chemical shifts were recorded against external standards of 0.1 mol dm-3 BeCl2 + 0.1 mol dm-3 HCl in 10% D2O for ^{9}Be, and 75% H3PO4 in 10% D2O for ^{31}P measurements, respectively. All sample solutions did not contain D2O for a field-frequency locking, because it was suspected that D2O would change the chemical atmosphere of the solvent. All the spectra were recorded with non-^{1}H decoupling. They were obtained at - 2.3°C[7,20-22]; the refrigeration was carried out by an inflow to an NMR probe of dried N2 gas which was cooled by liquid N2. The temperature was calibrated by using 1,2-ethanediol[23,24], whose accuracy was ±1K or better, and the reproducibility was lower than 0.2K.

RESULTS AND DISCUSSION

^9Be NMR analysis

A series of ^9Be NMR spectra obtained by the titration series of $C_M^0 = 0.01$ mol dm^{-3} are shown in Fig. 5-1. With an increase in ligand concentration, free Be^{2+} ([Be(H$_2$O)$_4$]$^{2+}$) peak, peak(1), and additional two peaks corresponding to complexes, peaks(2) and (3), appeared successively at 0, -0.6, and -1.2 ppm, respectively. Since ^9Be is a quadrupolar nuclei ($I = 3/2 > 1$), low symmetric environment around a complexed Be^{2+} ion produces a high electric field gradient at the ^9Be nuclei leading to unusually broad line width in the NMR spectrum[25]. According to our previous work on Be^{2+}-inorganic polyphosphate anion complexation systems[9], a proportionality holds between the ^9Be chemical shift values and the number of coordinating non-bridging oxygen atoms. Based on this empirical additivity rule, the peaks at -0.6 ppm and -1.2 ppm are assigned to monodentate and bidentate complexes, respectively. Since all ^9Be NMR spectra obtained in this work consist of broad signals comprising overlapping resonances, the area of each peak has been calculated by deconvolution of all ^9Be NMR spectra into some resonances. The calculation was carried out with a personal computer by the non-linear least squares procedure using a Newton-Gauss algorithm within the frequency range from 3 to -4 ppm. Since the NMR data were treated only digitally from the NMR measurements to the peak deconvolution of the spectra, the accuracy of the NMR measurements was retained perfectly.

An NMR peak can be expressed by the Lorentzian curve in the extreme nallowing region[26,27], and the intensity of the Lorentzian signal, I_δ, at a certain chemical shift, δ, can be expressed by eqn 5-1.

$$I_\delta = \frac{I_{max}}{1 + (\delta_0 - \delta)^2 / W_{1/2}^2} \tag{5-1}$$

where I_{max}, δ_0, and $W_{1/2}$ indicate the maximum intensity, the center chemical shift, and the half-height width of the Lorentzian peak, respectively. The peak area of the Lorentzian signal, S, can be calculated by the definite integral as follows;

$$S = \int_{\delta_A}^{\delta_B} \frac{I_{max}}{1 + (\delta_0 - \delta)^2 / W_{1/2}^2} \, d\delta$$

$$= I_{max} \cdot W_{1/2} \arctan\left(\frac{\delta_A - \delta_0}{W_{1/2}}\right) - I_{max} \cdot W_{1/2} \arctan\left(\frac{\delta_B - \delta_0}{W_{1/2}}\right) \qquad (5\text{-}2)$$

In this study, the integral range, δ_B - δ_A, has been designated 10 ppm (351 Hz) frequency domain which is *ca.* 10 times of $W_{1/2}$ of the Lorentzian signal. The representative calculated spectra (in solid lines) are shown in Fig. 5-2 together with the deconvoluted peaks indicated in dotted lines.

The ^{9}Be chemical shift, δ_{Be}, of the deconvoluted spectra is expressed in Fig. 5-3 as a function of C_L/C_M for the respective titration. It is notable that the shift values corresponding to free Be^{2+},(a), and bidentete complexes,(c), remain constant irrespective of the charge in C_L/C_M, whereas δ_{Be} assigned to monodentate complexes,(b), apparently shifts downfield upon C_L/C_M increase. This unexpected tendency in the monodentate complexes can also be observed in the apparent wider width of half peak height, $W_{1/2}$, of the monodentate complexes compared with free Be^{2+} and bidentate complexes, which can be seen in Fig. 5-1.

$W_{1/2}$ of a Lorentzian signal is related to the transverse relaxation rate, R_2, as follows;

$$R_2 = \pi \cdot W_{1/2} \qquad (5\text{-}3)$$

and is highly sensitive to both the chemical exchange processes and the electrical symmetry around the coordination sphere of the central metal ions. Free Be^{2+} ions, *i.e.*, $[Be(H_2O)_4]^{2+}$, with a highly symmetrical coordination environment give rise to a low electric field gradient around the central ^{9}Be nuclei, leading to a narrow NMR resonance, *i.e.*, the transverse relaxation rate, R_2, is slow. In an asymmetric system, such as coordination with phosphate ligand atoms, however, the interaction of the nuclear quadrupole moment with a high electric field gradient results in fast relaxation rate, yielding a broad NMR resonance. The R_2 values for the successive complexation observed in the present study is expected to follow the order, $[Be(H_2O)_4]^{2+}$ < monodentate complex < bidentate complex, since the electric field gradient will increase with the decrease in symmetry around the coordination sphere due to the successive complex formation. However as shown in Fig. 5-4, where the R_2 values of free Be^{2+},

monodentate, and bidentate complexes are plotted against C_L/C_M, those for monodentate complexes are comparable with those for bidentate complexes in magnitude. In addition, the R_2 value for monodentate complexes is variable with C_L/C_M, though those values for free Be^{2+} and bidentate complexes remain constant irrespective of the change in C_L/C_M.

These unexpected characteristics observed in the peak at *ca.* -0.6 ppm, assigned to monodentate complexes, leads us to assume the presence of more than one complexation mechanism for monodentate complexes. By assuming two peaks at *ca.* -0.6 ppm, the ^9Be NMR spectra have been deconvoluted once again in order to examine the possibility of coexistence of two complexation modes corresponding to the peak at *ca.* -0.6 ppm. Fig. 5-5 shows the newly deconvoluted spectra (in dotted line), where the original spectra are indicated in solid line for comparison. Two peaks (2) and (3), appear as monodentate complexes, whose δ_{Be} values are plotted against C_L/C_M in Fig. 5-6. It is apparent by comparing with Fig. 5-3-(b), constancy with respect to C_L/C_M is obtained for the two peaks. Also the respective R_2 values are plotted in Fig. 5-7 against C_L/C_M. It can be seen that the R_2 values for the two monodentate complexes are constant and are always much smaller than those for bidentate complexes, which is quite in agreement with expectation.

Based on the discussions mentioned above, the concurrent coordination modes for the monodentate complexation in Be^{2+}-$cP_3(NH)_3^{3-}$ system has been verified, even though bidentate complexation has been attributed to simultaneous binding of a Be^{2+} ion to two non-bridging oxygen atoms belonging to different ligand molecules. Two possible coordination mechanisms can be postulated for the monodentate complexation. One plausible mechanism is participation of one imino nitrogen atom in addition to one non-bridging oxygen atom of $cP_3(NH)_3$ ligand molecule, which has been suggested previously by several researchers[28-32]. In this case, the ratio of the amount of the two complexes, *i.e.*, $(Be^{2+}$-$O_-)$ and $(Be^{2+}$-$NH)$, should remain constant irrespective of the change in C_L nor C_M since the exchange reaction of the coordination structure between the complexes $(Be^{2+}$-$O_-)$ and $(Be^{2+}$-$NH)$ is an intramolecular reaction. Another possible mechanism is the parallel formation of two-to-one complexes, M_2L, with one-to-one complexes, ML. In both cases a Be^{2+} ion coordinates with one non-bridging oxygen atom, giving rise to the similar δ_{Be} values in the ^9Be NMR spectra, where the ratio of the amount of ML to ML_2 should be varied with the change in C_M and C_L.

A straightforward approach to selecting the most probable mechanism is, therefore, comparison of the ratio of the peak areas appearing at the chemical shifts of monodentate complexes in the newly deconvoluted spectra. Here, the monodentate complexes corresponding to $\delta_{Be} = -0.54$ ppm and $\delta_{Be} = -0.67$ ppm are designated as complex A and complex B, respectively, and the fractions of monodentate complexes, bidentate complexes, and free Be^{2+} ion, have been calculated based on the peak area measurement. The fractions, f, of free ion ($[Be(H_2O)_4]^{2+}$ ion), monodentate complex A and B, and bidentate complex, to total amount of Be^{2+} are plotted in Fig. 5-8 against C_L/C_M. As expected the fraction of free Be^{2+} decreases drastically and that of bidentate complex increases gradually with a C_L increase for the three titration series. The most enlightening gained in these three figures is the distinct distribution change in monodentate complexes A and B with respect to C_L increase. As discussed above, if complexes A and B are simply assigned to 1) coordination with non-bridging oxygen atom, and 2) coordination with bridging imino nitrogen atom, then the peak area ratio of the two peaks should remain constant. However, when $C_M^0 = 0.005$ mol dm^{-3}, the fraction of complex A simply increases with C_L/C_M whereas the fraction of complex B first increases to approach a maximum and then decreases. Also, when $C_M^0 = 0.01$ or 0.02 mol dm^{-3}, the fraction of complex A first increases and then gradually decreases after showing the maxima, and the fraction ratio of complexes A and B remarkably changes with respect to C_L/C_M. In the previous study, we suggested that a Be^{2+} ion coordinates directly with bridging imino nitrogen atom contrary to the empirical expectation by the HSAB rule[33,34]. However, the inconsistency of the fraction ratio of complexes A and B which observed in this study certifies the impossibility of the direct coordination of Be^{2+} ion to imino nitrogen atom. As increasing C_M^0, the magnitude of the decrease in free Be^{2+} fraction becomes appreciable in parallel with the outstanding increase in bidentate complex fraction. This trend strongly indicates the formation of two-to-one complex(M_2L), *i.e.*, two Be^{2+} ions bind simultaneously to one ligand molecule, which is composed of three phosphate units. Based on the complexation analysis mentioned above, a microscopic complexation equilibrium scheme in the $Be^{2+} - cP_3(NH)_3^{3-}$ complexation system can be postulated as follows.

The proposed mechanisms can be validated by the equilibrium analysis due to the peak area measurement. According to the peak assignment, the concentration ratios of respective

chemical species can be replaced by the fraction of the peak areas (*S*), and respective equilibrium constants, corresponding to $M + L \rightleftarrows ML$ (K_{ML}), $M + ML \rightleftarrows M_2L$ (K_{M2L}), and $L + ML \rightleftarrows ML_2$ (K_{ML2}), can be calculated by the following analytical procedures.
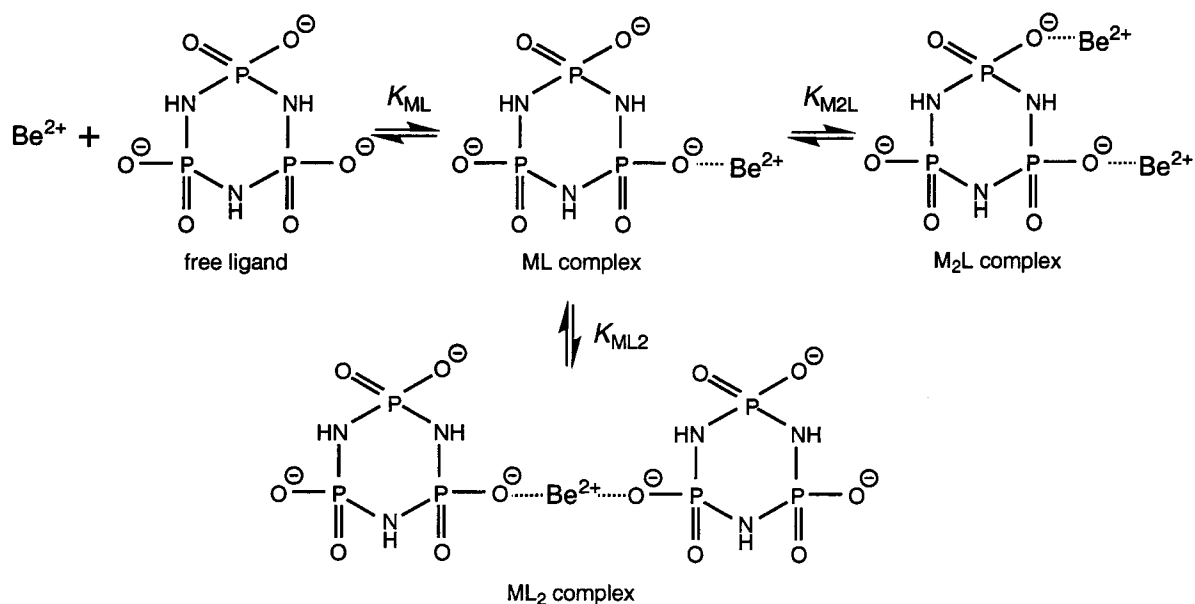
Scheme 5-1

$$K_{ML} = \frac{[ML^-]}{[M^{2+}]\cdot[L^{3-}]} = \frac{S_{1,A}}{S_0}\cdot[L^{3-}]^{-1} \qquad (5\text{-}4)$$

$$K_{M_2L} = \frac{[M_2L^+]}{[M^{2+}]\cdot[ML^-]} = \frac{S_{1,B}}{S_{1,A}}\cdot[M^{2+}]^{-1} \qquad (5\text{-}5)$$

$$K_{ML_2} = \frac{[ML_2^{4-}]}{[ML^-]\cdot[L^{3-}]} = \frac{S_2}{S_{1,A}}\cdot[L^{3-}]^{-1} \qquad (5\text{-}6)$$

where the free ligand concentration, $[L^{3-}]$, and the free Be^{2+} concentration, $[M^{2+}]$, can be calculated as follows,

$$[L^{3-}] = C_L - C_M \cdot \left(\frac{S_{1,A}}{\Sigma(S_i)} + \frac{S_{1,B}}{2\,\Sigma(S_i)} + \frac{2\,S_2}{\Sigma(S_i)} \right) \qquad (i = 0 - 2) \qquad (5\text{-}7)$$

$$[M^{2+}] = C_M \cdot \frac{S_0}{\Sigma(S_i)} \qquad (i = 0 - 2) \qquad (5\text{-}8)$$

where i indicates the coordination number of a Be^{2+} ion for the ligand. The $S_{1,A}/S_0$, $S_{1,B}/S_{1,A}$, and $S_2/S_{1,A}$ values thus calculated are plotted in Fig. 5-9 against $[L^{3-}]$, $[M^{2+}]$, and $[L^{3-}]$, respectively. As can be found in this figure, the plots determined from different titration series converge to straight lines for all the systems examined, indicating that the equilibrium constants, K_{ML}, K_{M2L}, and K_{ML2} can be calculated by the slopes of the respective straight line. From the linearities observed in the figures, we can conclude that the complexation mechanism indicated in Scheme 5-1 is most plausible. The equilibrium constants thus evaluated by the peak area measurement are tabulated in Table 5-1, together with the δ_{Be} values of respective complexed species.

It should be pointed out here that the Be^{2+} coordination with imino nitrogen atom has now been excluded, even though direct coordination of divalent metal ions with nitrogen atoms of imidopolyphosphate anions has been proposed by several researchers[28-32]. Tautomerism between phosphate group (P-O$^-$) and imino group (P-NH-P) may endow negative charge on the nitrogen atom, which facilitates direct metal ion coordination with nitrogen atoms[33]. However, as can be predicted by the HSAB rule, hard Be^{2+} ion is expected to bind to harder oxygen atom rather than nitrogen atom of imidopolyphosphate anions, and the present analyses verify this expectation. Further verification can be gained by a ^{31}P NMR measurement carried out concurrently, which will be discussed below.

31P NMR analysis

Due to slow chemical exchange upon complexation, separate peaks corresponding to phosphorus atoms belonging to coordinating or non-coordinating phosphate groups appear in the ^{31}P NMR spectra. Representative ^{31}P NMR spectra of the complexation system are shown in Fig. 5-10, which are obtained for the mixture sample solutions whose compositions are quite similar to those obtained for the [9]Be NMR spectra shown in Figs. 5-1, 5-2, and 5-5.

Compared with the ^{9}Be NMR spectra, where the chemical shift value changes upfield successively with increasing the number of coordinating phosphate groups, no regularity has been found in ^{31}P NMR chemical shift change upon complexation with inorganic polyphosphate ligands. However, by the careful examination of the peak height change with comparing the corresponding ^{9}Be NMR spectra, and by the ^{31}P-^{31}P coupling behavior, the complexation mechanism illustrated in Scheme 5-1 may be elucidated.

In the series of ^{31}P NMR measurements, at most 7 peaks have been observed as shown in Fig. 5-10-(a), where each peak can be signified as (1) - (7) from the low magnetic field. By knowing that the peak (3) corresponds to free $cP_3(NH)_3^{3-}$, the remaining 6 peaks are assigned to phosphorus atom belonging to complexed species. By increasing C_L, the peak height of respective peak changes in different ways; however, the heights of three pairs, (1)-(2), (4)-(7), and (5)-(6), change synchronously, indicating that these three pairs correspond to respective complexed species. Small, but apparent change in the chemical shift upon C_L increase observed for the peaks (2) and (4) may be attributed to the change in the binding strength between Be^{2+} ion(s) and phosphate oxygen atom upon C_L increase. By comparing the corresponding ^{9}Be and ^{31}P NMR spectra, the pairs of the peaks (1)-(2), (4)-(7), and (5)-(6), are assigned to the complexes, ML_2, M_2L, and ML, respectively, which is proposed by the present ^{9}Be NMR study. Respective peak has been assigned to phosphorus atoms α and β, where α and β indicate phosphorus atoms belonging to coordinating and non-coordinating phosphate groups, respectively. The final assignment of the ^{31}P NMR peaks is ensured by examining the ^{31}P-^{31}P coupling behavior, as shown in Fig. 5-10-(a), the peaks (4) and (5) are doublet and triplet, respectively, though other peaks are apparently singlet. In Fig. 5-11, additional ^{31}P NMR spectrum obtained under extremely high C_L/C_M is shown in order to indicate that the peaks (1) and (2) are originally doublet and triplet, respectively. By taking these coupling behavior of each peak into account, the pairs of the peaks (1) and (2), (4) and (7), and (5) and (6), are assigned to the complexes of ML_2, M_2L, and ML, respectively. Furthermore, the peaks (1) and (2) are assigned to phosphorus atoms, β and α of ML_2; (4) and (7) to atoms α and β of M_2L; (5) and (6) to atoms α and β of ML, respectively. The ^{31}P NMR peak assignments are summarized in Scheme 5-2, and the eigen values of the ^{31}P chemical shifts, δ_P, as well as the coupling constants, $^1J(^{31}P\text{-}^{31}P)$, are listed in Table 5-2.

Through the ^{31}P NMR measurements the complexation mechanism proposed by the ^{9}Be NMR study can be confirmed.
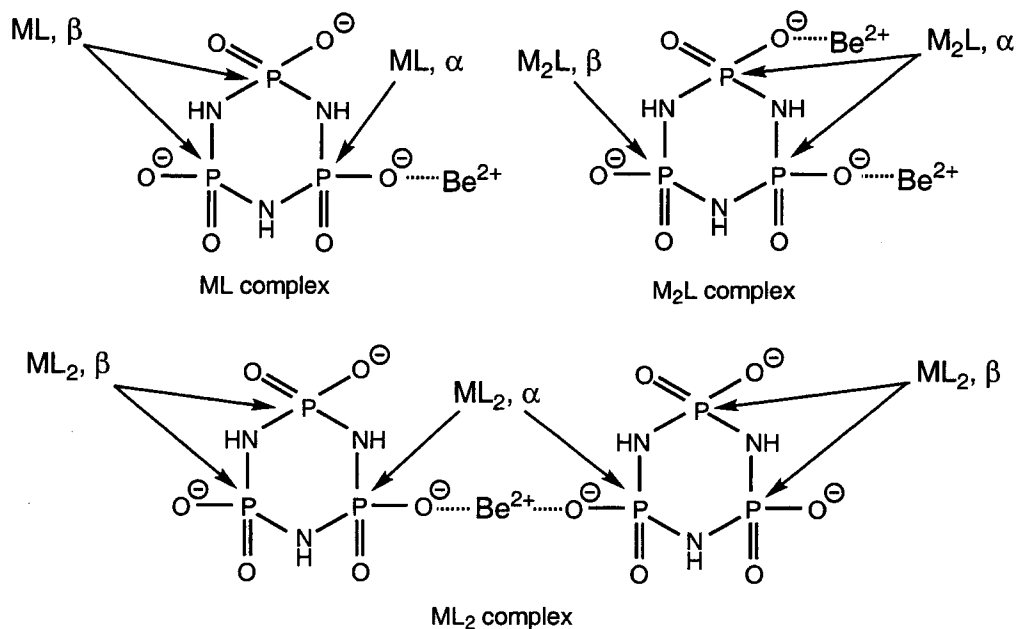
Scheme 5-2

CONCLUSIONS

Complexation equilibrium analyses of Be^{2+}-cP$_3$(NH)$_3{}^{3-}$ mixture solutions, whose C_M was changed from 0.005 to 0.02 mol dm^{-3} and C_L was increased up to 4 folds of C_M, have excluded the possibility of direct coordination of Be^{2+} to imino nitrogen atoms of the ligand molecule. Instead, simultaneous formation of M$_2$L and ML$_2$ type complexes in addition to ML type complexes has been revealed. Coexistence of the complexes of these three complexation modes is expected to produce a Be^{2+} ion bridged polymerized structure as indicated in Scheme 5-3. Indeed, the ^{31}P NMR peaks corresponding to a phosphorus atoms belonging to M$_2$L and ML$_2$ type complexes are shifted and are broadened upon C_M and C_L increase as can be seen in Fig. 5-10, though the peaks corresponding to β atoms of the complexes as well as a atoms of ML type complex do not shift at all upon the change in C_M and C_L. In order to investigate

further the particular coordination behavior of Be^{2+} ions with inorganic polyphosphate ligands, the Be^{2+} complexation with the analogs of the ligand investigated by the present study, such as *cyclo* triphosphate, *cyclo*-mono-μ-imido triphosphate, and *cyclo*-di-μ-imido triphosphate are now being investigated in our laboratory.
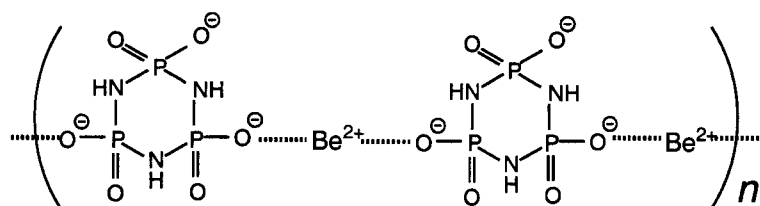
Scheme 5-3

REFERENCES

1. S. Liu, S. J. Rettig, and C. Orvig, *Inorg. Chem.*, **31**, 5400(1992).

2. R. Delgado, Y. Sun, R. J. Motekaitis, and A. E. Martell, *Inorg. Chem.*, **32**, 3320(1993).

3. A. Lycka, P. Rys, and P. Skrabal, *Magn. Reson.*, **36**, 279(1998).

4. J. Ashenhurst, G. Wu, and S. Wang, *J. Am. Chem. Soc.*, **122**, 2541(2000).

5. R. A. Kovar and G. L. Morgan, *J. Am. Chem. Soc.*, **92**, 5067(1970).

6. F. A. Cotton and G. Wilkinson, in *Advanced Inorganic Chemistry*, John Wiley & Sons, Inc., New York, 4th edn., 1980, ch. 8.1.

7. K. Komiya, T. Miyajima, M. Sakurai, S, Sato and M. Watanabe, *Phosphorus Res. Bull.*, **2**, 33(1992).

8. J. W. Akitt, in *NMR and Chemistry: An Introduction to Modern NMR Spectroscopy*, Chapman & Hall, London, 3rd edn., 1992, ch. 6.3.

9. T. Miyajima and R. Kakehashi, *Phosphorus Res. Bull.*, **1**, 101(1991).

10. F. W. Wehrli and S. L. Wehrli, *J. Magn. Reson.*, **47**, 151(1982).

11. M. Alei, Jr. and J. A. Jackson, *J. Chem. Phys.*, **41**, 3402(1964).

12. T. J. Swift, O. G. Fritz, Jr., and F. A. Stephenson, *J. Chem. Phys.*, **46**, 406(1967).

13. T. J. Swift and W. G. Sayre, *J. Chem. Phys.*, **44**, 3567(1966).

14. Y. Miyazaki, G. Kura, H. Tsuzuki, and H. Sakashita, *Bull. Chem. Soc. Jpn.*, **69**, 1955(1996).

15. I. Dellavia, J. Blixt, C. Dupressoir, and C. Detellier, *Inorg. Chem.*, **33**, 2823(1994).

16. M. P. Lowe, S .J. Rettig, and C. Orvig, *J. Am. Chem. Soc.*, **118**, 10446(1996).

17. F. L. Conde, L. Prat, *Anal. Chim, Acta*, **16**, 473(1957).

18. S. Misumi, T. Taketatsu, *Bull. Chem. Soc. Japan*, **32**, 593(1959).

19. G. Schwarzenbach,; H. Wenger, *Helv. Chim. Acta.*, **52**, 644(1969).

20. F. W. Wehrli, S. L. Wehrli, *J. Magn. Reson.*, **47**, 151(1982).

21. M. Munakata, S. Kitagawa, Yagi, F., *Inorg. Chem.*, **25**, 964(1986).

22. M. J. B. Ackerman, J. J. H. Ackerman, *J. Phys. Chem.*, **84**, 3151(1980).

23. A. L. Van Geet, *Anal. Chem.*, <u>40</u>, 2227(1968).

24. Braun, S.; Kalinowski, H. O.; Berger, S. In *150 and More Basic NMR Experiments*, VCH Publishers: New York, 1998; ch. 5.2.

25. J. W. Akitt, In *NMR and Chemistry: An Introduction to Modern NMR Spectroscopy*, Chapman & Hall: London, 3rd edn., 1992, ch. 4.3.

26. F. Bloch, *Phys. Rev.*, **70**, 460(1950).

27. A. R. Davis, R. B. Roden, A. J. Weerheim, Irish, D. E., *Applied Spectroscopy*, **26**, 384(1972).

28. S. Tran-Dinh, Roux, M. *Eur. J. Biochem.*, **76**, 245(1977).

29. M. A. Reynolds, J. A. Gerlt, P. C. Demou, N. J. Oppenheimer, G. L. *J.* Kenyon, *Am. Chem. Soc.*, **105**, 6475(1983).

30. M. P. Lowe, S. J. Rettig, C. Orvig, *J. Am. Chem. Soc.*, **118**, 10446(1996).

31. K. Sawada, T. Ichikawa, K. Uehara, *J. Chem. Soc. Dalton Trans.*, **21**, 3077(1996).

32. K. Sawada, T. Araki, T. Suzuki, K. Doi, *Inorg. Chem.*, **28**, 2687(1989).

33. H. Maki, M. Tsujito, H. Nariai, M. Watanabe, M. Sakurai, T. Miyajima, *Phosphorus Res. Bull.*, **12**, 155(2001).

34. H. Maki, M. Tsujito, H. Nariai, M. Watanabe, M. Sakurai, T. Miyajima, *Phosphorus Res. Bull.*, **12**, 161(2001).
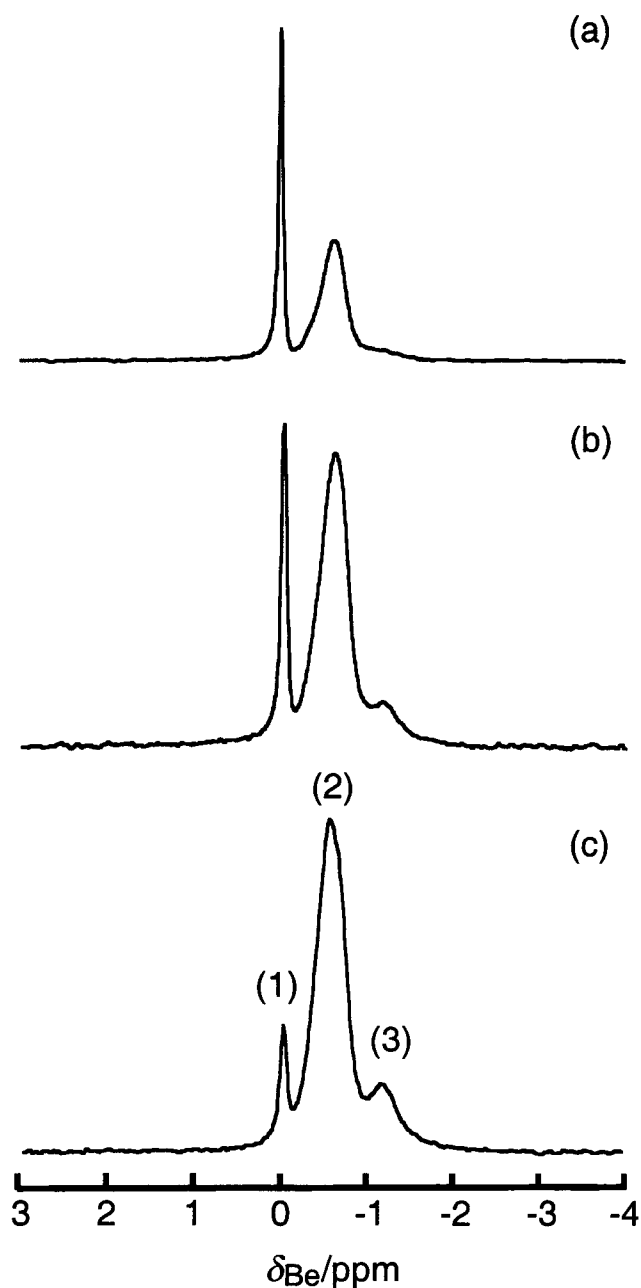
Fig. 5-1 Representative ^{9}Be NMR spectra of Be^{2+}-$cP_3(NH)_3{}^{3-}$ mixture solutions measured at

35.147 MHz in the absence of ^{1}H decoupling.

(a); $C_L = 4.80 \times 10^{-3}$ mol dm^{-3}, $C_M = 9.87 \times 10^{-3}$ mol dm^{-3} ($C_L/C_M = 0.486$), (b);

$C_L = 7.86 \times 10^{-3}$ mol dm^{-3}, $C_M = 9.72 \times 10^{-3}$ mol dm^{-3} ($C_L/C_M = 0.809$), (c); $C_L =$

1.23×10^{-2} mol dm^{-3}, $C_M = 9.48 \times 10^{-3}$ mol dm^{-3} ($C_L/C_M = 1.30$).

The three resonances arise from (1); $[Be(H_2O)_4]^{2+}$, (2); monodentate complex, and

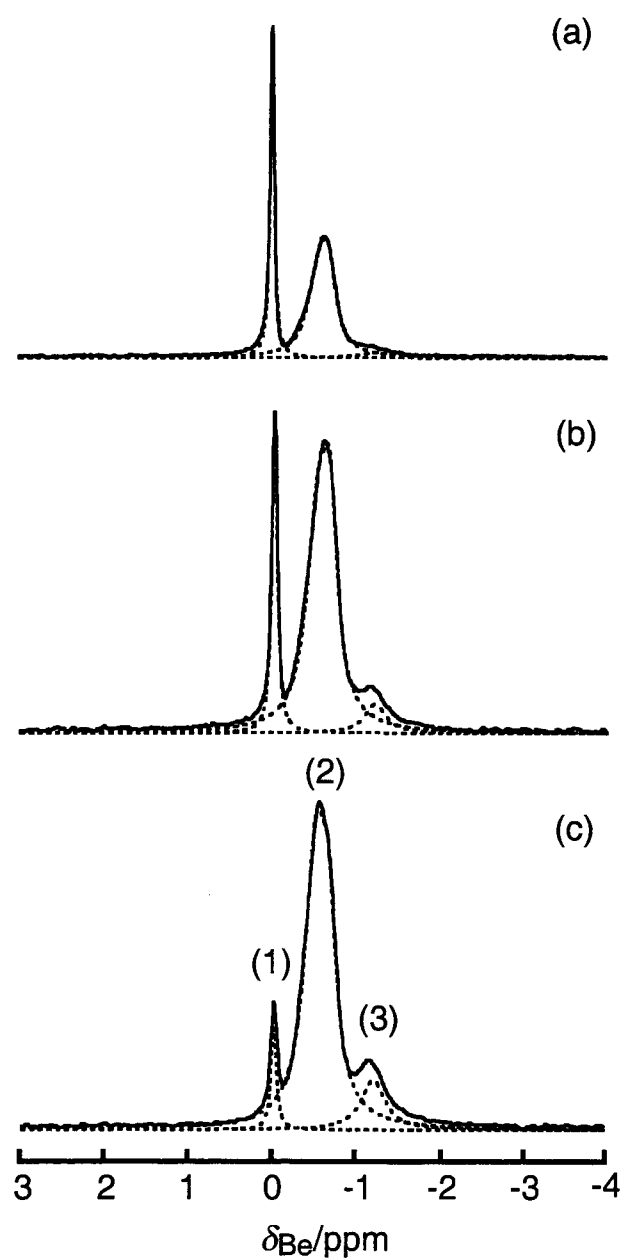(3); bidentate complex. The details for each resonance assignment are given in the text.

5-15

Fig. 5-2 Representative peak deconvolution of ^9Be NMR spectra of Be^{2+}-$cP_3(NH)_3^{3-}$ mixture solutions. The solution compositions and the assignments of the three resonances are shown in the caption of Fig. 5-1.
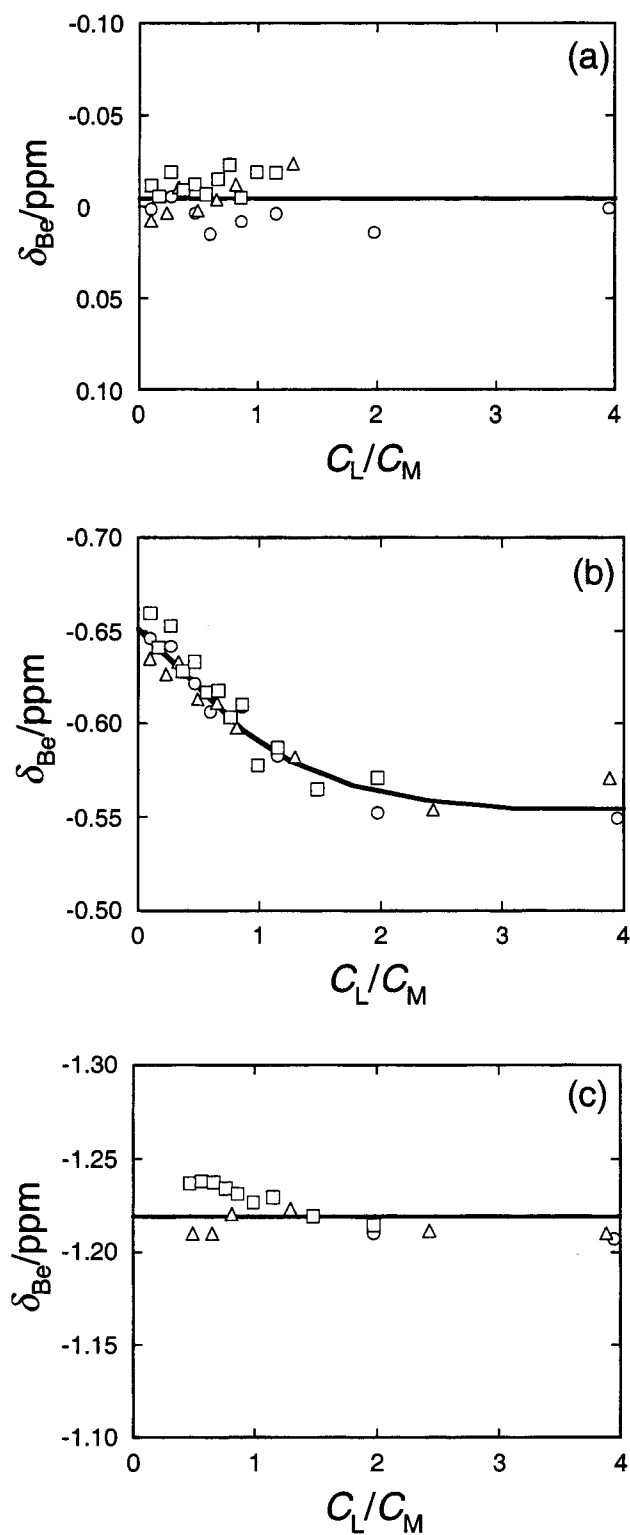
Fig. 5-3 Dependence of ^{9}Be NMR chemical shift on C_L/C_M, where (a), (b), and (c) correspond to (a); $[Be(H_2O)_4]^{2+}$, (b); monodentate complex, and (c); bidentate complex, respectively: ($\bigcirc$); $C_M{}^0 = 0.005$ mol dm^{-3}, ($\triangle$); $C_M{}^0 = 0.01$ mol dm^{-3}, ($\square$); $C_M{}^0 = 0.02$ mol dm^{-3}.

5-17
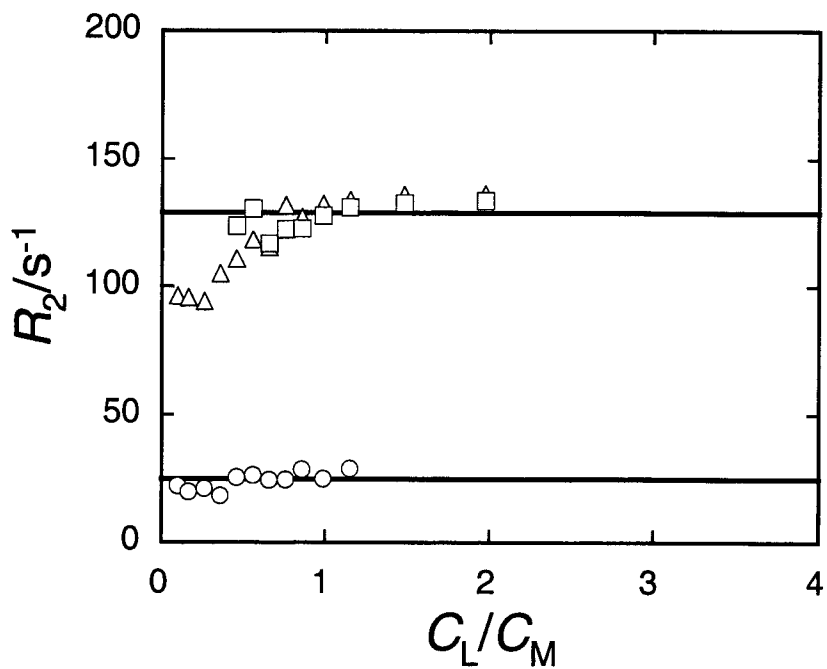
Fig. 5-4 Dependence of the transverse relaxation rate on C_L/C_M; $C_M{}^0 = 0.02$ mol dm^{-3}: (◯);

free [Be(H$_2$O)$_4$]$^{2+}$ ion, (△); monodentate complex, (□); bidentate complex.
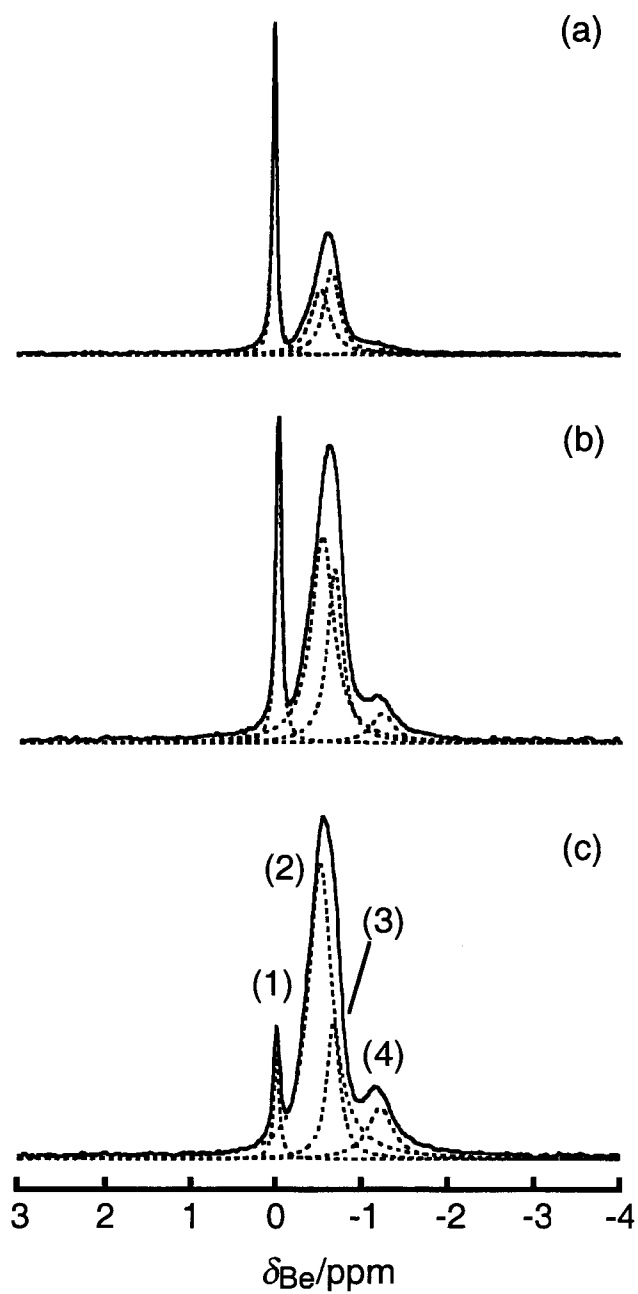
5-18

Fig. 5-5 Representative peak deconvolutions by assuming two complexation modes for monodentate complexes. The solution compositions are shown in the caption of Fig. 5-1. The four resonances arise from (1); free Be^{2+}, (2); monodentate complex A, (3); monodentate complex B, and (4); bidentate complex.
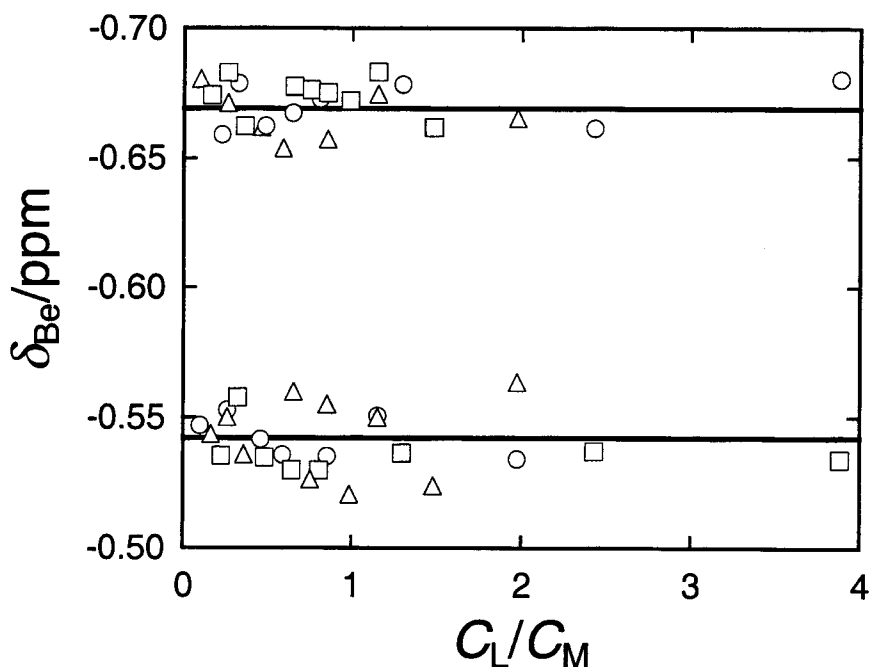
Fig. 5-6 Dependence of ^{9}Be NMR chemical shifts of two modes for monodentate complexation on C_L/C_M. ($\bigcirc$); $C_M^0 = 0.005$ mol dm^{-3}, ($\triangle$); $C_M^0 = 0.01$ mol dm^{-3}, ($\square$); $C_M^0 = 0.02$ mol dm^{-3}.
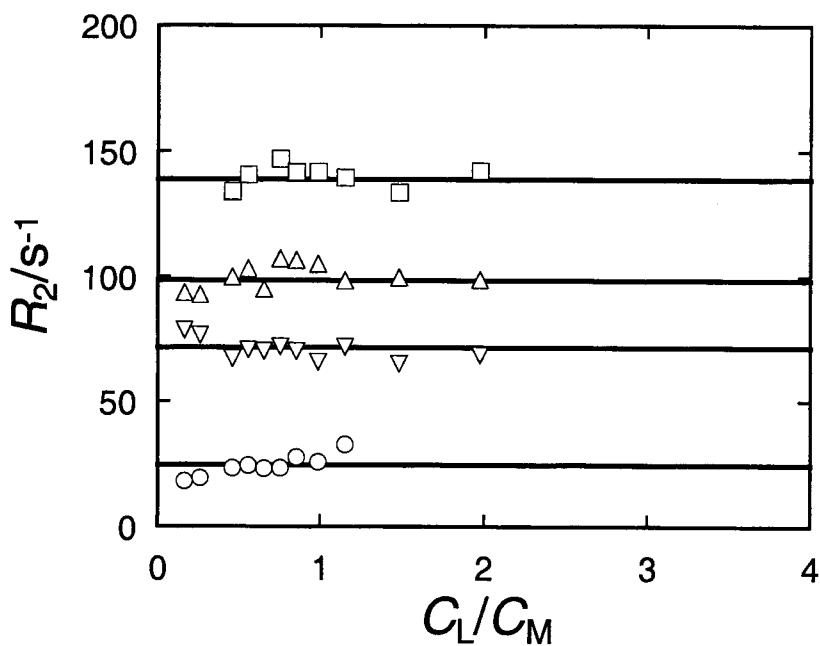
Fig. 5-7 Dependence of the transverse relaxation rate of two modes for monodentate complexation on C_L/C_M; $C_M^0 = 0.02$ mol dm^{-3}: ($\bigcirc$); free [Be(H$_2$O)$_4$]$^{2+}$ ion, ($\triangle$); monodentate complex A, ($\triangledown$); monodentate complex B, ($\square$); bidentate (ML$_2$) complex.
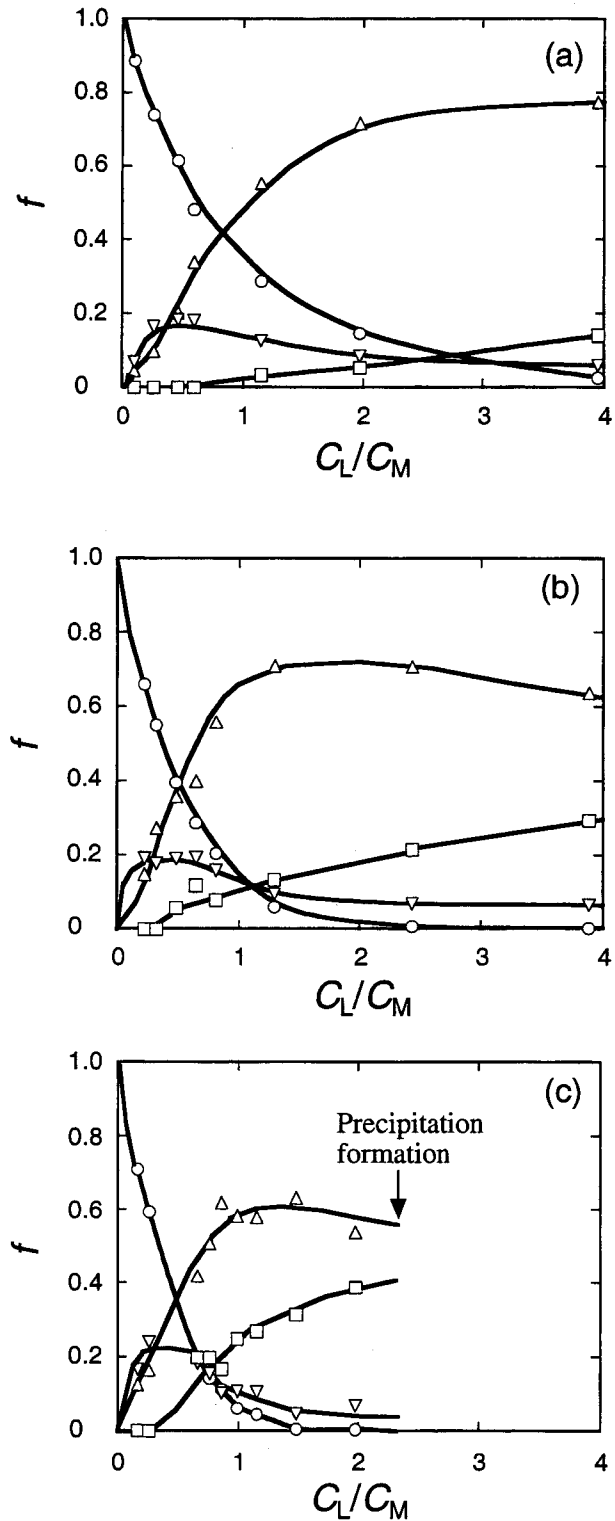
Fig. 5-8 Fractions of free $[Be(H_2O)_4]^{2+}$ ion ($\bigcirc$), monodentate complex A ($\triangle$), monodentate complex B ($\triangledown$), and bidentate (ML_2) complex ($\square$), expressed as a function of C_L/C_M. (a); $C_M{}^0 = 0.005$ mol dm^{-3}, (b); $C_M{}^0 = 0.01$ mol dm^{-3}, (c); $C_M{}^0 = 0.02$ mol dm^{-3}.
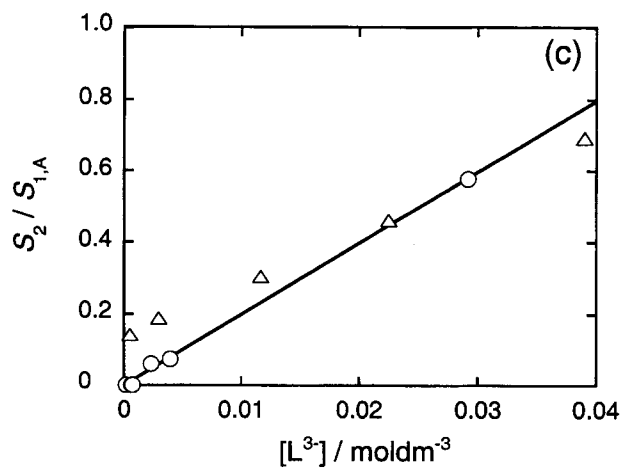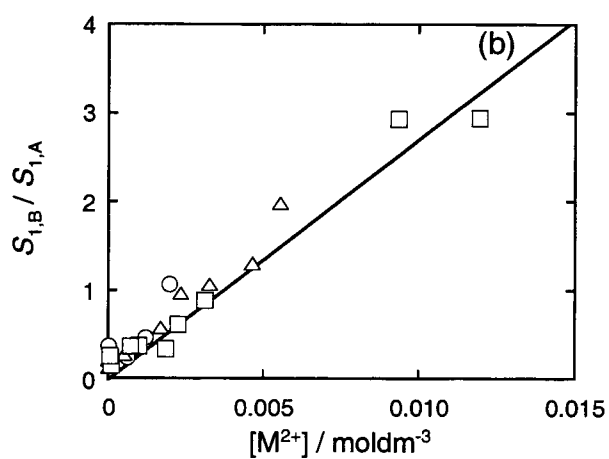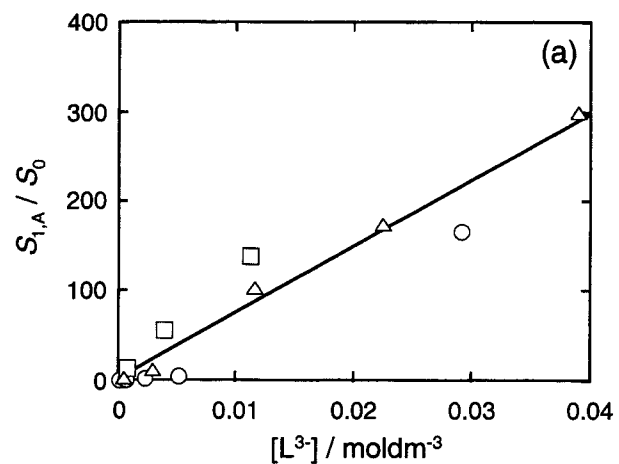
Fig. 5-9 Relationships of (a)$S_{1,A}/S_0$ vs. [L^{3-}], (b)$S_{1,B}/S_{1,A}$ vs. [M^{2+}], and (c)$S_2/S_{1,A}$ vs.

[L^{3-}]. K_{ML}, K_{M2L}, and K_{ML2} values can be determined from the slopes of these plots.

(◯); $C_M^0 = 0.005$ mol dm^{-3}, (△); $C_M^0 = 0.01$ mol dm^{-3}, (□); $C_M^0 = 0.02$ mol dm^{-3}.
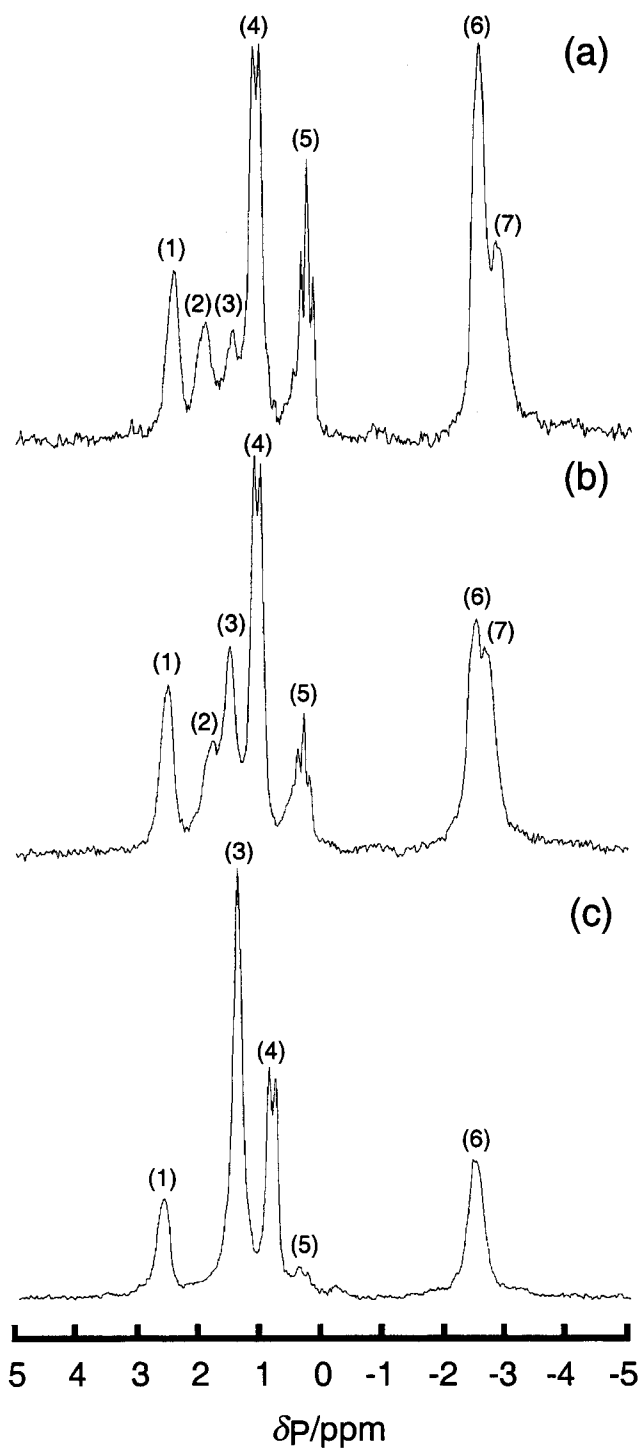
Fig. 5-10 Representative ^{31}P NMR spectra of Be^{2+}-$cP_3(NH)_3^{3-}$ mixture solutions measured at 101.258 MHz in the absence of ^1H decoupling. (a); C_L = 4.76 × 10^{-3} mol dm^{-3}, C_M = 9.64 × 10^{-3} mol dm^{-3} (C_L/C_M = 0.494), (b); C_L = 7.68 × 10^{-3} mol dm^{-3}, C_M = 9.34 × 10^{-3} mol dm^{-3} (C_L/C_M = 0.823), (c); C_L = 1.18 × 10^{-2} mol dm^{-3}, C_M = 8.93 × 10^{-3} mol dm^{-3} (C_L/C_M = 1.32). The details for all resonance assignments and that about the labels on each signal are given in Table 2.

5-23
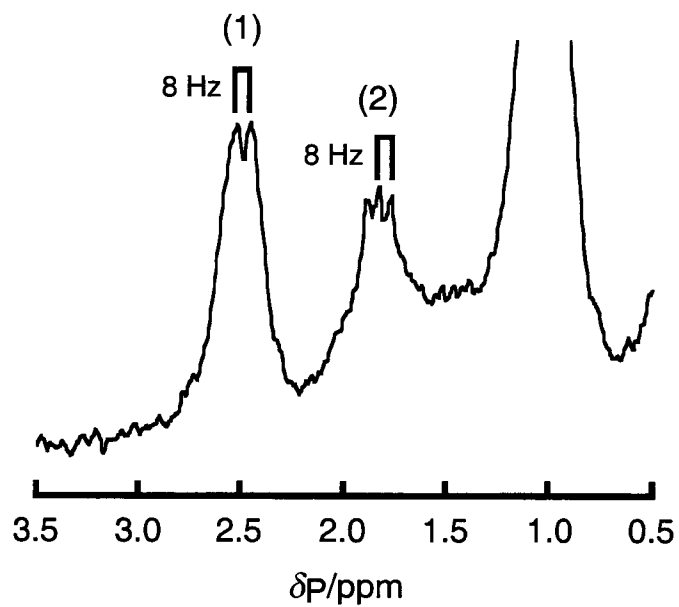
Fig. 5-11 Extended ^{31}P NMR spectrum of Be^{2+}-$cP_3(NH)_3^{3-}$ mixture solution. $C_L = 6.38 \times 10^{-3}$ mol dm^{-3}, $C_M = 1.94 \times 10^{-2}$ mol dm^{-3} ($C_L/C_M = 3.04$).

Table 5-1. Logatithmic stepwise complex formation constants[a] and intrinsic ^{9}Be NMR chemical shifts of Be^{2+} complexes with $cP_3(NH)_3$ evaluated by ^{9}Be NMR.

Complex	$\log K^a$	Chemical shift / ppm
ML^-	3.87 (0.05)	-0.54
M_2L^+	2.43 (0.03)	-0.67
ML_2^{4-}	1.30 (0.02)	-1.24

[a] Values in parentheses are standard deviations derived from the linear least squares approximation.

Table 5-2. ^{31}P NMR chemical shifts and ^{31}P-^{31}P spin-spin coupling constants due to successive complexes of Be^{2+}-$cP_3(NH)_3^{3-}$ system.

Atom[a]	δ_P / ppm	$^1J(^{31}P\text{-}^{31}P)$ / Hz[b]
Free $cP_3(NH)_3^{3-}$	1.5	none (s)
ML, α	0.3	10 (t)
ML, β	-2.5	broad
M_2L, α	1.0	10 (d)
M_2L, β	-2.8	broad
ML_2, α	1.9	8 (t)
ML_2, β	2.5	8 (d)

[a] Atom labelling refers to Scheme 5-2. [b] Symbols in parentheses, "s", "d", and "t", indicate "singlet", and "triplet", respectively.

CHAPTER 6

On the protonation behavior of several monothiophosphate anions.

ABSTRACT

The stepwise protonation constants of monothiomonophosphate, dithiomonophosphate, trithiomonophosphate and tetrathiomonophosphate anions have been determined by ^{31}P NMR chemical shift measurements in aqueous solution. In spite of the fast hydrolysis rate of the series of thiomonophosphate anions, the protonation processes of all thiomonophosphate anions may well be examined without any previous purification because the NMR signals corresponding to thiophosphate anions and hydrolysed residues can well be resolved. The successive protonation constants decrease with an increase in the number of sulfur atoms bound to center phosphorus atom. It has been revealed that the logarithms of the stabilities of the proton complexes of the series of thiomonophosphate anions decreases "linearly" with an increase in the number of sulfur atoms which constitute the anions. The intricsic ^{31}P NMR chemical shifts due to orthophosphate and tetrathiomonophosphate anions show up-field shifts upon the stepwise protonation of the anions, whereas the shifts due to mono-, di-, and trithiomonophosphate anions show low-field shifts upon that of the anions. Futhermore, an asymmetry of a molecule is related to the amount of the change of bond angles with a protonation and a complex formation, and it makes the nuclear screening drastically change. A symmetry of a molecular structure is related to the direction of the ^{31}P NMR chemical shift change due to the successive protonation of a ligand.

INTRODUCTION

The series of thiomonophosphate anions, *i.e.*, dithiomonophosphate anion, $H_nPO_2S_2^{(3-n)-}$ ($n = 0$-3), trithiomonophosphate anion, $H_nPOS_3^{(3-n)-}$ ($n = 0$-3), and tetrathiomonophosphate anion, $H_nPS_4^{(3-n)-}$ ($n = 0$-3), are very unstable in water. As previously described, the rate of the substitution of sulfur for water oxygen in the thiomonophosphate anions is fast[1], and so it is hard to measure the protonation constants of these anions with thermodynamical method, as a potentiometric titration method. Accordingly, in contradistinction to the well-known protonation behavior of polyphosphate anions, there is little work[2, 3] has been carried out on the protonation

equilibria of the series of the thiomonophosphate ligand molecules.

In recent years some studies have been made on monothiophosphate derivatives[4-6]. The Brönsted plot for the nonenzymatic hydroxide catalysed hydrolysis of a diethyl thiophosphate substrate showed a linear dependence between the pseudo-first-order rate constant and the pKa of the substrate[7], and the hydrolytic dethiophosphorylation and desulfurization of the 2'-, and 3'- and 5'-phosphoromonothioates have been investigated from the pH-Rate profiles for hydrolytic reactions and the acid-base properties of these anions[8]. B. Song $et~al.$, have been studied the protonation properties of adenosine 5'-O-thiomonophosphate in aqueous solution in detail[9]. R. K. O. Sigel $et~al.$, have been not only determined the 1:1 complex formation constants of 5'-O-thiomonophosphate but also considered the structures of these complexes by the application of the linear free energy relationships[10]. However, so far the study of the other thiophosphate, $i.e.$, di-, tri-, and tetrathiophosphates, derivatives have been scarce. It seems to be a cause that the acid-base properties and the complex formation behavior are hard to observe, since these thiophosphates are easy to hydrolyze in aqueous solution. This study is intended as an investigation of the protonation behaviors of not only a monothiophosphate anion but also di-, tri-, and tetrathiophosphates which are simple analogues of the several thiophosphate derivatives. It is considered that this information is useful for the interpretation of the protonation and the complex formation behavior of these derivatives. It is difficult to investigate the protonation behaviors of the thiophosphate anions by a general thermodynamic technique represented for the potentiometric titration because of hydrolyzation of the anions. To overcome this problem, ^{31}P NMR spectroscopy has been employed in this study. NMR is used extensively to monitor what is happening during chemical equilibria and is particularly useful in that, because starting materials, intermediate and side products may have resolved signals, then the progress of a reaction may well be fruitfully examined without any previous purification.

In the present study, the protonation constants together with intrinsic chemical shifts of the phosphorus nuclei belonging to the thiomonophosphate anions have been evaluated by means of the pH titration profiles of ^{31}P NMR chemical shifts of respective phosphorus nuclei. The direction and the magnitude of the shift changes of the respective phosphorus nuclei are compared with each other.

EXPERIMENTAL

Chemicals

Monothiomonophosphate dodecahydryde, $Na_3PO_3S \cdot 12H_2O$, was synthesized *via* a hydrolysis of P_2S_5[11, 12]. A 20 g of P_2S_5 was added gradually to 100 ml of 5 mol dm^{-3} NaOH aqueous solution, and reacted for 10 minutes below 50 °C with stirring. Precipitate was removed by suction filtration, and 40 ml of ethanol was added to the filtrate, cooled with ice. The reaction product was collected by suction filtration, washed with aceton, dried in air. About 40 g of the product was dissolved in 140 ml of water, heated to 70 °C, cooled immediately to 60 °C, and added 40 ml of ethanol, cooled with ice, filtered by suction. About 10 g of the precipitate was dissolved in 70 ml of water below 50 °C, filtered by suction. The filtrate was cooled gradually with ice, and 7.8 g of pure $Na_3PO_3S \cdot 12H_2O$ was prepared. The total yield was 11 %. The monothiomonophosphate salt was made sure that it had not hydrolyzed during preparation, since the aqueous solution of the salt produced an only singlet resonance in the ^{31}P NMR spectra.

Tetrathiomonophosphate octahydryde, $Na_3PS_4 \cdot 8H_2O$ was synthesized *via* an addition of P_2S_5 to $Na_2S \cdot 9H_2O$[4]. A 80 g of $Na_2S \cdot 9H_2O$ and a 8 g of P_2S_5 were mixed on a porcelain dish, and the intimate mixture were briefly melted at 1000 °C and reacted for 15 minutes. A 80 ml of boiling water was added to the melt, filtered immediately. After leaving for 1 day, the precipitate was collected by suction filtration, and 20 g of the reaction product was dissolved in 100 ml of 0.025 mol dm^{-3} Na_2S + 0.1 mol dm^{-3} NaOH aqueous solution. The solution was cooled with ice and 120 ml of ethanol was added, and 6.5 g of pure $Na_3PS_4 \cdot 8H_2O$ was prepared. The total yield was 24 %. All chemicals used in this work were of analytical grade (Wako Pure Chemicals).

^{31}P NMR measurements

All ^{31}P NMR spectra were recorded on a Bruker DPX-250 (5.87T) superconducting Fourier-transform pulse NMR spectrometer with a 10mm tunable broad-band probe was used at 101.258 MHz at 295.2 ± 1 °C. An acquisition time was 1.0 sec, and the FID were collected in 50000 data points, and was used a sweep width of 25 kHz, that is, the digital resolution in the frequency dimension was 1.0 Hz (0.0099 ppm). Extreme care was taken to avoid saturation of the

resonances. The NMR chemical shifts were recorded against an external standard of 85% H_3PO_4 in 10% D_2O. Since it has not added D_2O to all sample solutions in order to retain the solvent purity, the spectrometer were not field-frequency locked during the measurement of all sample solutions. All spectra were recorded in the absence of ^{1}H decoupling. A 3 ml quantity of *ca.* 0.01 mol dm^{-3} $Na_3PO_{4-n}S_n$ (*n*=1-4) added to the 10 mm ϕ NMR tube as an equilibrium reaction cell. Small aliquots of HNO_3 or $NaOH$ aqueous solution was added by a micro syringe in order to define the pH of the solutions, and the pH meter readings were recorded just before the ^{31}P NMR measurements. The pH meter readings were carried out with an Orion 250A instrument. In the case of monothiomonophosphoric anion, which hydrolyzes not so rapidly, the standard acid or standard base was added stepwisely, in the case of other thiomonophosphoric anions, which hydrolyzes very rapidly, the sample solutions were prepared newly every NMR measurements. In this work, a supporting electrolyte, *e.g.*, $NaNO_3$, has a tendency to accelerate the hydrolyzation of the di-, tri-, and tetrathiomonophosphoric anions, so that was not added to the sample solutions.
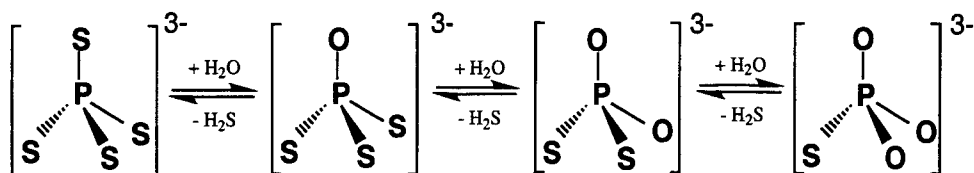
Potentiometric titrations

Stepwise protonation constants of a monothiomonophosphate anion were also determined by potentiometric titrations in a thermostating titration cell at 298.2 ± 1 °C. A potentiometer (an Orion 701A Ionalyzer) equipped with a glass electrode (an Orion 91-01) and a single junction reference electrode (an Orion 90-01) was used for a potentiometric titration. Before and after the titrations of the sample solutions, the glass electrode was calibrated as a hydrogen concentration probe by titrating known amounts of HNO_3 with CO_2-free $NaOH$ solution and determining the equivalence point by Gran's method[13] which allows one to determine the standard potential, E_0, and the liquid junction potential, *j*. Titrant solutions containing a 0.01 mol dm^{-3} Na_3PO_3S were titrated with a standard hydrochloric acid solution. All the titration procedures were carried out under N_2 atmosphere in 0.10 mol dm^{-3} $NaNO_3$ as a supporting electrolyte.
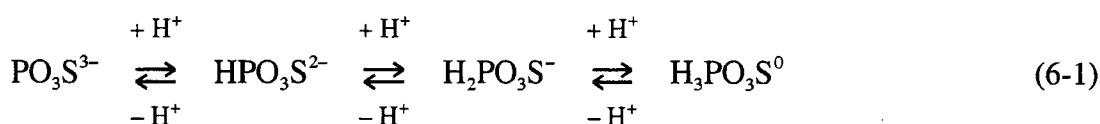
RESULTS AND DISCUSSION

Representative ^{31}P NMR spectra of Na_3PO_3S and Na_3PS_4 aqueous solutions are shown in Figs. 6-1 and 6-2, respectively; monothiomonophosphate anions in Na_3PO_3S aqueous solution

produced an only singlet resonance at any pH as shown in Fig. 6-1, whereas Na_3PS_4 aqueous solution produced three singlet resonances at any pH as shown in Fig. 6-2. It suggests that the sample aqueous solution contains at least three magnetically non-equivalent phosphorus nuclei. Maier and Van Wazer have been reported that the P-S linkages appear to be cleaved very quickly and that the sulfur atoms rapidly substituted by oxygen atoms from the water[13]. Klement suggests that tetrathiomonophosphate anions hydrolyze to tri-, di-, and monothiomonophosphate anions stepwisely in water, as shown in Scheme 6-1. A qualitative
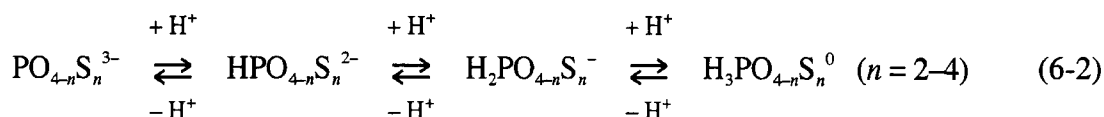
$$\left[\begin{array}{c} \text{S} \\ \text{S}\nwarrow\text{P}\searrow\text{S} \\ \text{S} \end{array}\right]^{3-} \underset{-\text{H}_2\text{S}}{\overset{+\text{H}_2\text{O}}{\rightleftarrows}} \left[\begin{array}{c} \text{O} \\ \text{S}\nwarrow\text{P}\searrow\text{S} \\ \text{S} \end{array}\right]^{3-} \underset{-\text{H}_2\text{S}}{\overset{+\text{H}_2\text{O}}{\rightleftarrows}} \left[\begin{array}{c} \text{O} \\ \text{S}\nwarrow\text{P}\searrow\text{O} \\ \text{S} \end{array}\right]^{3-} \underset{-\text{H}_2\text{S}}{\overset{+\text{H}_2\text{O}}{\rightleftarrows}} \left[\begin{array}{c} \text{O} \\ \text{S}\nwarrow\text{P}\searrow\text{O} \\ \text{O} \end{array}\right]^{3-}$$

Scheme 6-1

investigation of the hydrolysis of the tetrathiomonophosphate anion indicates a half life for this species of $ca.$ 20 min. in water at 25 °C[1]. The hydrolysis rate of dithiomonophosphate anions is relatively slow under experimental condition in this study, so the resonance due to monothiomonophosphate anions has not been detected on the spectra of Na_3PS_4 aqueous solutions as shown in Fig. 6-2. It follows from what has been discussed that the protonation equilibria for monothiomonophosphate anions may exist in Na_3PO_3S aqueous solution as follows:

$$PO_3S^{3-} \underset{-H^+}{\overset{+H^+}{\rightleftarrows}} HPO_3S^{2-} \underset{-H^+}{\overset{+H^+}{\rightleftarrows}} H_2PO_3S^- \underset{-H^+}{\overset{+H^+}{\rightleftarrows}} H_3PO_3S^0 \qquad (6\text{-}1)$$

and the equilibria for di-, tri-, and tetrathiomonophosphate anions coexist in Na_3PS_4 aqueous solution as follows:

$$PO_{4-n}S_n^{3-} \underset{-H^+}{\overset{+H^+}{\rightleftarrows}} HPO_{4-n}S_n^{2-} \underset{-H^+}{\overset{+H^+}{\rightleftarrows}} H_2PO_{4-n}S_n^- \underset{-H^+}{\overset{+H^+}{\rightleftarrows}} H_3PO_{4-n}S_n^0 \quad (n=2\text{--}4) \qquad (6\text{-}2)$$

In general, the change of the ^{31}P NMR chemical shift due to the variation in the electronegativity differences between the center phosphorus atom and its substituents, and the

6-5

decrease in the electronegativity of the adjacent substituents will cause a low-field shift of ^{31}P NMR resonances due to the center phosphate atom[14]. Hence the three resonances can be seen in Fig. 6-2, where the lowest-field resonance has been assigned to tetrathiomonophosphate anions, the highest-field resonance to dithiomonophosphate anions and a resonance to low field of the latter has been assigned as trithiomonophosphate anions.

As can be seen in Figs. 6-1 and 6-2, the changes with pH variations observed in the chemical shifts of the series of thiomonophosphate anions can be regarded by protonation of these thiomonophosphate anions. The pH titration profiles of the ^{31}P NMR chemical shifts due the phosphorus atoms belonging to these anions are shown in Fig. 6-3. In spite of the presence of many kinds of protonated species, H_nL ($n = 0$-3) of these anions, only sharp singlet resonances are observed in the ^{31}P NMR spectra over a wide range of pH. This fact indicates that the proton exchanges of these thiomonophosphate anions are very fast[15]. The additivity of the chemical shifts of NMR resonances of nuclei belonging to the anions, $H_nL^{(3-n)-}$ ($n = 0$-3), averaged by fast exchange over all species which are present in the equilibria (1) and (2) can be written in the following[16]:

$$\delta_P = (\delta_{L^{3-}}[L^{3-}] + \delta_{HL^{2-}}[HL^{2-}] + \delta_{H_2L^-}[H_2L^-] + \delta_{H_3L}[H_3L]) / C_L \qquad (6\text{-}3)$$
$$(L = PO_3S,\ PO_2S_2,\ POS_3,\ PS_4)$$

where C_L is the total concentration of the ligand in solution, δ_P, is the observed ^{31}P NMR chemical shift, and $\delta_{L^{3-}}$, $\delta_{HL^{2-}}$, $\delta_{H_2L^-}$ and δ_{H_3L} refer to the intrinsic chemical shifts of the phosphorus nuclei belonging to each species. In addition, the stepwise protonation constants of the thiomonophosphate anions, K_n, is defined as follows:

$$K_n = [H_nL^{(3-n)-}] / ([H^+][H_{n-1}L^{(2-n)-}]) \quad (n = 1\text{--}3) \qquad (6\text{-}4)$$

Using the mass action law for this system of equilibria, a suitable equation for the observed chemical shift can be expressed as following equation:

$$\delta_P = \left(\delta_{L^{3-}} + \sum_{i=1}^{3} K_1 \cdots K_i [H^+]^i \delta_{H_iL^{(3-i)-}}\right) / \left(1 + \sum_{i=1}^{3} K_1 \cdots K_i [H^+]^i\right) \qquad (6\text{-}5)$$

The values of the protonation constants and the intrinsic chemical shifts giving a minimum error-square sum of chemical shifts, $\Sigma(\delta_{P,obs} - \delta_{P,calc})^2$, were calculated by a non-linear least squares curve-fitting method with the aid of a computer. The logarithmic protonation constant, log Kn, and the intrinsic chemical shift of each species thus obtained from plots of δ_P $vs.$ pH (Fig. 6-3) are listed in Tables 6-1 and 6-2, respectively. Solid lines in Fig. 6-3 are calculated curves obtained by using the pertinent values listed in Tables 6-1 and 6-2 and show good agreement with the experimental results. The log Kn values of orthophosphate anions at 25 °C in Table 6-1 were referred from I. L. Khodakovskiy et $al.$[17], and the δ_P values of the anions at 27 °C in Table 6-2 were referred from M. M. Crutchfield et $al.$[18].

K. Moedritzer et $al.$ have measured the ^{31}P NMR chemical shifts due to the free PO_3S^{3-}, $PO_2S_2^{3-}$ and POS_3^{3-} ligands in aqueous solutions contain 3% Na_2S: $\delta_{PO_3S^{3-}}$ = 33.8 ppm, $\delta_{PO_2S_2^{3-}}$ = 61.9 ppm, $\delta_{POS_3^{3-}}$ = 86.5 ppm[19]. The above values are agree with the parameters in Tables 6-1 and 6-2. This fact justifies the NMR resonance assignment and the data treatment in this study.

The hydrolysis rate of monothiomonophosphate anions is relatively slow, so the log Kn values of monothiomonophosphate anions at 25 ± 0.5 °C and I = 0.10 ($NaNO_3$) by a potentiometric titration method. The average number of bound H^+ ions per monothiomonophosphate anion, $\bar{n}$, can be calculated by dividing the concentrations of bound H^+ ions, $[H^+]_b$, by the total concentration of ligand ions, C_L. Since $[H^+]_b$ is given as the difference of the total concentration of H^+ ions, C_H, and the free H^+ ion concentration of the equilibrium solution, $[H^+]$, $\bar{n}$ can be determined as,

$$\bar{n} = \frac{[H^+]_b}{C_L} = \frac{(C_H - [H^+])}{C_L} \tag{6-6}$$

$[H^+]$ can be measured by the electrochemical method. By use of eqn. 6-6, $\bar{n}$ can also be expressed as,

$$\bar{n} = \frac{K_1[H^+] + 2K_1K_2[H^+]^2 + 3K_1K_2K_3[H^+]^3}{1 + K_1[H^+] + K_1K_2[H^+]^2 + K_1K_2K_3[H^+]^3} \tag{6-7}$$

The $\bar{n}$ vs. log[H^+] plots obtained for monothiomonophosphate anions are shown in Fig. 6-4. The log K_n (n = 1-3) values have been obtained as log K_1 = 9.83 ± 0.02, log K_2 = 5.22 ± 0.05, and

log $K_3 = 0.83 \pm 0.08$, which determined by the non-linear least squares curve-fitting method. The solid line in Fig. 6-4 refers to the calculated curve by the use of the respective log K_n ($n = 1$-3) values, and show good agreement with the experimental results. It should be noted that the log K_n ($n = 2$-3) values determined by the ^{31}P NMR method and a potentiometric titration are almost in agreement with each other within the experimental error, despite the difference in principles of the two methods. This indicates the validity of the protonation constants as well as the intrinsic shift values evaluated by the present study. It can find slight difference between the log K_1 values which determined by both methods. This implies that Na^+ ions which are supporting cations form 1:1 complexes with thiomonophosphate anions. The complex formations reduce the partial negative charge of a center phosphorus atom, so the nucleophilic attack on the phosphorus atom from bulk water molecules may be facilitated, and the hydrolysis rates of thiomonophosphate anions has been accelerated, as shown in Scheme 6-2. This acceleration is remarkable in case of the di-, tri, and tetrathiomonophosphate anions and so the protonation constants of these anions under the supporting electrolyte existence could not be determined not only by a potentiometric titration but also by the ^{31}P NMR method.

As the previous reported by R. R. Irani *et al.* and by T. Miyajima *et al.*, the protonation constants of imidopolyphosphate and *cyclo*-imidopolyphophate anions increase with an increase in the number of imino groups which constitute the ligand molecules[20,21]. T. Miyajima *et al.* suggest that the increase in the basicity of the anions can be interpreted by the difference in the electronegativity of the bridging oxygen and nitrogen atoms[21]. On the other hand, the log Kn values decrease with an increase in the number of sulfur atoms neighboring the center phosphate atom as can be seen in Fig. 6-5, showing that the thiomonophosphoric acids become stronger acids because of the substitution from oxygen to sulfur. Since the difference in the electronegativity of the oxygen and sulfur atoms is larger than that of the oxygen and nitrogen atoms, the less affinity of thiomonophosphate anions for H^+ is not adequately explained by the difference. On the hard and soft acids and bases (HSAB) scale, a very basic negative donor forms complexes of high stability with "hard" cations such as H^+. Thio groups are not so "hard" in the HSAB sense, so the thiomonophosphate anions form complexes of low stability with H^+. It must be noted that the stabilities of the thiomonophosphate anions with H^+ are effected additionary by the less basic negativity of the anions, hence the log Kn values decrease linearly with an increase in

6-8

the number of sulfur atoms which constitute the anions.

The correlation of the intrinsic ^{31}P NMR chemical shifts of the series of thiomonophosphate anions and electric charge of the anions as shown in Fig. 6-6. The stepwise protonation of the thiomonophosphate anions results in a shift of the ^{31}P NMR resonances of the anions due to the decrease in the electronegativity of the coordination atom. It is noteworthy that the intricsic ^{31}P NMR chemical shifts (a) and (e) show up-field shifts upon the stepwise protonation of orthophosphate and tetrathiomonophosphate anions respectively, whereas the shifts
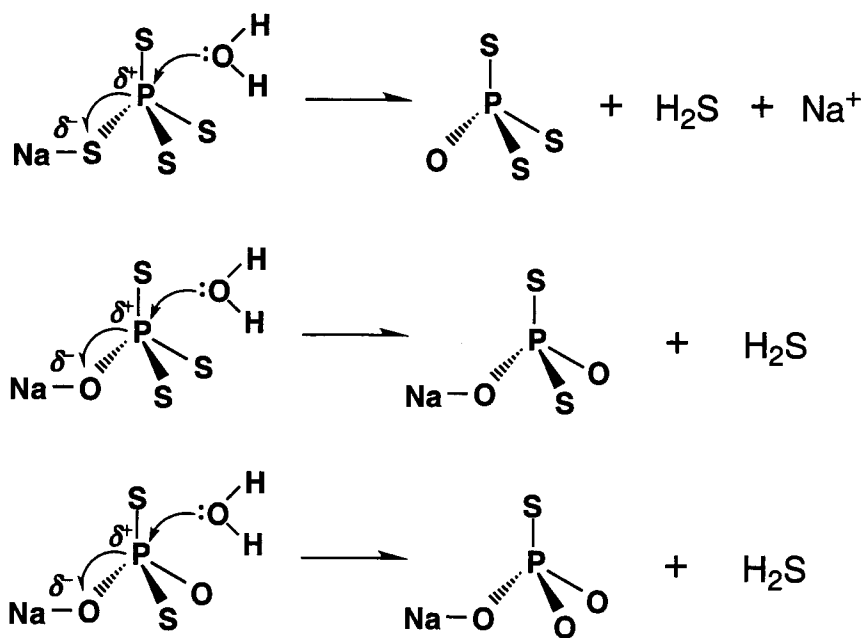
Scheme 6-2

(b), (c) and (d) show low-field shifts upon that of mono-, di-, and trithiomonophosphate anions respectively. Approximate quantum chemical calculations[22,23] have shown that the change in the chemical shift, $\Delta\delta$, for these anions may be treated by the relationship[24]

$$\Delta\delta = 180\Delta\chi_0 - 147\Delta n_\pi - A\Delta\theta \qquad (6\text{-}8)$$

where $\Delta\chi_0$ is the change in the effective electronegativity of PX$_4$ anion, Δn_π is the concomitant change in the phosphorus d_π-orbital occupation due to variation in the p character of the P-X bonds thus induced, and $\Delta\theta$ is any change in the XPX bond angle. Orthophosphate and tetrathiomonophosphate anions have only one kind of coordination atom, and all of P-O or P-S

bindings in the anions are equivalent. Therefore, the coordination atoms in these anions around the center phosphorus atom occupied positions at the corners of a regular tetrahedron unit in aqueous solution, which has ideal symmetry T_d. Since the exchange rate of the protons is much faster than the NMR timescale, each of the protonation properties of all coodination atoms is equivalent in the NMR time domain. It is obvious that the OPO or SPS bond angles of these anions does not change with successive protonation, and that the change of the electronegativity, the changes in $\Delta\chi_0$, which originates from the decrease in negative charge with the protonation almost certainly predominates for the up-field shifts observed for the phosphorus nuclei in the orthophosphate and tetrathiomonophosphate anions. On the other hand, mono-, di-, and trithiomonophosphate anions have two kinds of coordination atom, and all of bindings between a coordination atom and a center phosphorus atom in the anions are not equivalent. Therefore, it seems reasonable to suppose that the ^{31}P NMR signal due to these anions show drastic low-field shifts by the changes of the OPO, OPS, and SPS bond angles, *i.e.*, the contribution of the $\Delta\theta$ term, with successive protonation. It should be noted that an asymmetry of a molecule is related to the amount of the change of bond angles with a protonation and a complex formation, and it makes the nuclear screening drastically change.

Relationships of the intrinsic ^{31}P NMR chemical shifts and the number of sulfur atoms in the anions are shown in Fig. 6-7. It is noteworthy that the changes of the intrinsic ^{31}P NMR chemical shifts due to the anions with the stepwise protonation increase in the series of orthophosphate and tetrathiomonophosphate anions (less than 10 ppm) < monothiomonophosphate and trithiomonophosphate anions (ca. 15 ppm) < dithiomonophosphate anion (c.a. 30 ppm). Since the dithiomonophosphate anion contains two oxygen atoms and two sulfur atoms as coordination atoms, the molecular structure of the anion is the most asymmetric, so it seems that the change of the OPO, OPS, and SPS bond angles in the anion with the stepwise protonation is the most remarkable in the thiomonophosphate anions, and the nuclear screening in the anion is changed drastically by the contribution of $\Delta\theta$ term which dominates the screening. Thus changes in $\Delta\theta$ probably account for a major part of the screening changes observed phosphorus nuclei in a dithiomonophosphate anion.

REFERENCES

1. L. Maier and J. R. Van Wazer, *J. Am. Chem. Soc.*, **84**, 3057(1962).

2. O. Mäkitie and V. Konttinen, *Acta Chem. Scand.*, **23**, 1459(1969).

3. C. J. Peacock and G. Nickless, *Z. Naturforsch.*, **24**, 245(1969).

4. H. Kanehara, T. Wada, M. Mizuguchi and K. Makino, *Nucleosides and Nucleotides*, **15**, 1169(1996).

5. S. Tawata, S. Taira, H. Kikizu, N. Kobamoto, M. Ishihara and S. Toyama, *Biosci. Biotech. Biochem.*, **61**, 2103(1997).

6. A. Chive, B. Delfort, M. Born, L. Barre, Y. Chevalier and R. Gallo, *Langmuir*, **14**, 5355(1998).

7. S. B. Hong and F. M. Raushel, *Biochemistry*, **35**, 10904(1996).

8. M. Ora, M. Oivanen and H. Lonnberg, *J. Chem. Soc. Perkin Trans.*, **5**, 771(1996).

9. B. Song, R. K. O. Sigel and H. Sigel, *Chem. Eur. J.*, **3**, 29(1997).

10. R. K. O. Sigel, B. Song and H. Sigel, *J. Am. Chem. Soc.*, **119**, 744(1997).

11. R. Klement, *Z. Anorg. Allg. Chem.*, **253**, 237(1947).

12. G. Brauer, *Handbook of preparative inorganic chemistry*, 2nd edn, p. 569, Academic Press, New York (1963).

13. G. Gran, *Analyst*, **77**, 661(1951).

14. K. Moedritzer, *Inorg. Chem.*, **6**, 936(1967).

15. J. W. Akitt, *NMR and Chemistry: An Introduction to Modern NMR Spectroscopy*, 3rd edn, p. 139, Chapman & Hall, London (1992).

16. A. B. Kudryavtsev and W. Linert, *Physico-chemical Applications of NMR: A Practical Guide*, p. 145, World Scientific Publishing Co. Pte. Ltd., Singapore (1996).

17. I. L. Khodakovskiy, B. N. Ryzhenko and G. B. Naumov, *Geokhimiya*, **12**, 1205(1968).

18. M. M. Crutchfield, C. F. Callis, R. R. Irani and G. C. Roth, *Inorg. Chem.*, **1**, 815(1962).

19. K. Moedritzer, L. Maier and L. E. D. Groenweghe, *J. Chem. Eng. Data*, **7**, 307(1962).

20. R. R. Irani and C. F. Callis, *J. Phys. Chem.*, **65**, 934(1961).

21. T. Miyajima, H. Maki, M. Sakurai, and M. Watanabe, *Phosphorus Res. Bull.*, **5**, 149(1995).

22. J. H. Letcher and J. R. Van Wazer, *J. Chem. Phys.*, **44**, 815(1966).

23. J. H. Letcher and J. R. Van Wazer, *J. Chem. Phys.*, **45**, 2916(1966).

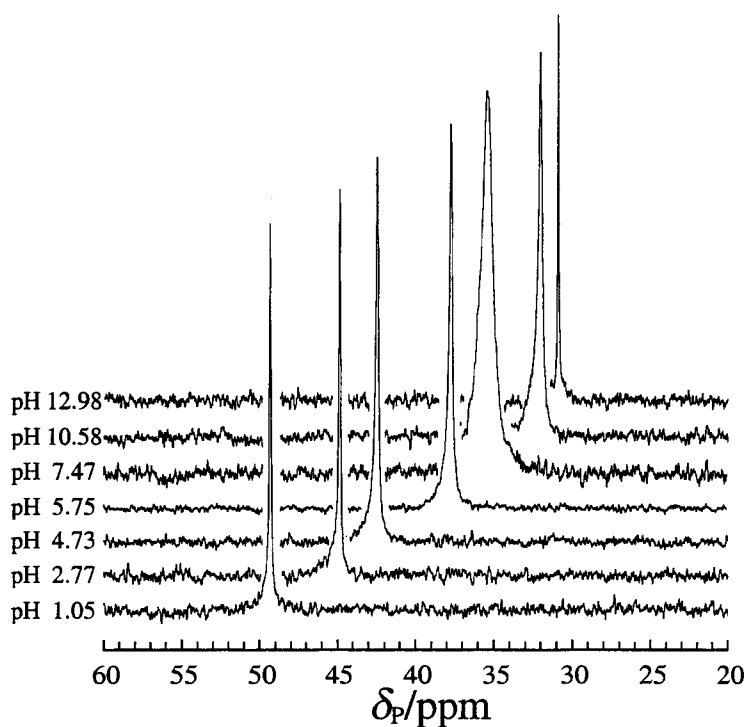24. P. Haake and R. V. Prigodich, *Inorg. Chem.*, **23**, 457(1984).

Fig. 6-1 Representative ^{31}P NMR spectra of a ca. 0.01 mol dm^{-3} Na$_3$PO$_3$S aqueous solution at 101.258 MHz in the absence of ^{1}H decoupling. All resonances are singlets.
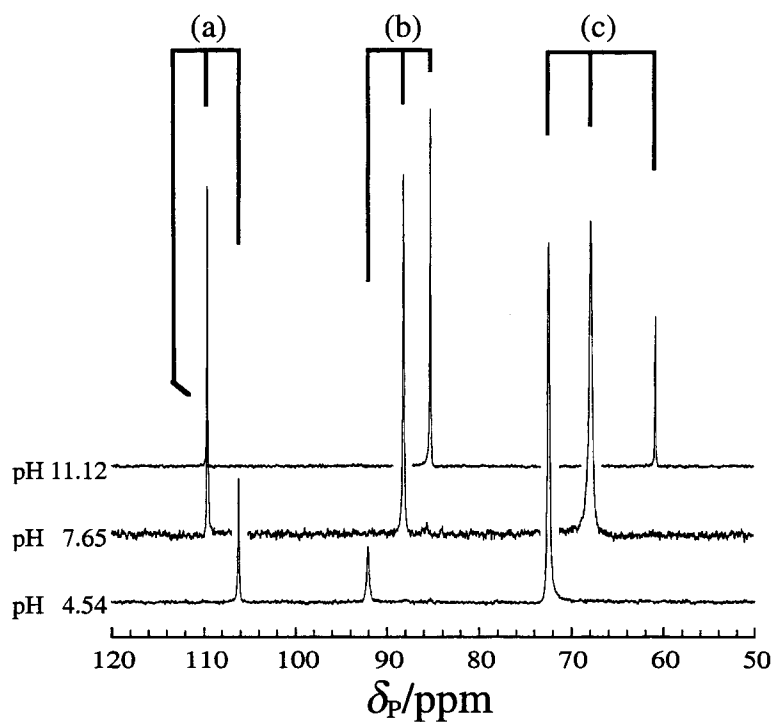

Fig. 6-2 Representative ^{31}P NMR spectra of a ca. 0.01 mol dm^{-3} Na$_3$PS$_4$ aqueous solution at 101.258 MHz in the absence of ^{1}H decoupling. All resonances are singlets. The three resonances arise from (a); tetrathiophosphoric anions, (b); trithiophosphoric anions, (c); dithiophosphoric anions.
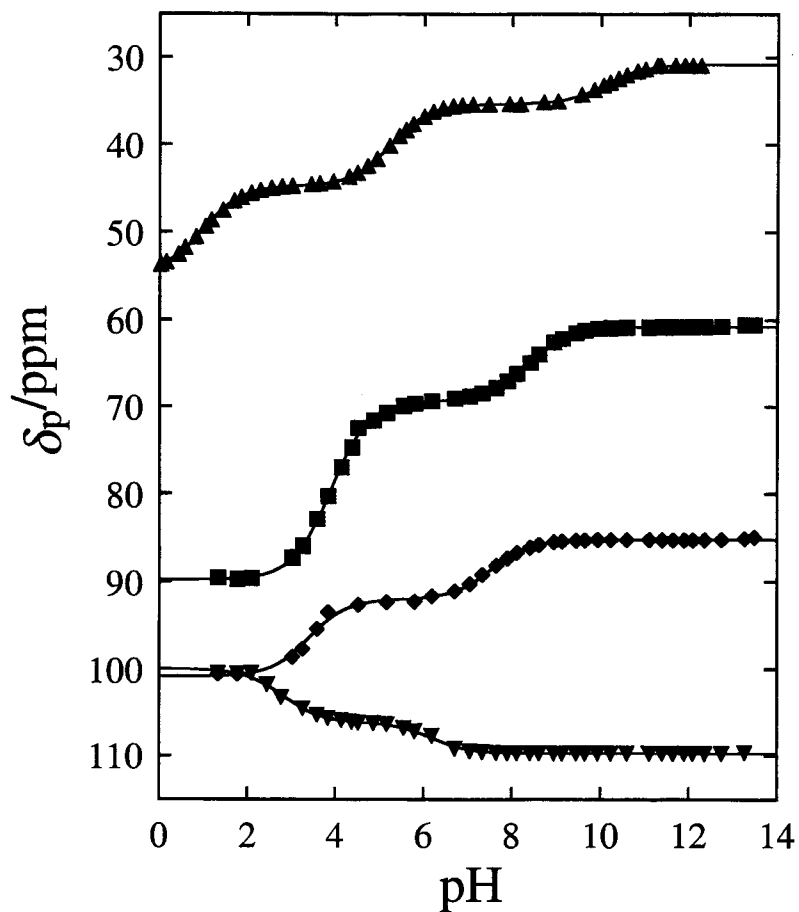
Fig. 6-3 ^{31}P NMR chemical shifts of various thiophosphoric anions as a function of pH at 22 ± 1 °C. Solid lines refer to the calculated curves by the use of the pertinent parameters of Tables 6-1 and 6-2, see eqn.6-1.

(▲); monothiophosphoric anions, $H_nPO_3S^{(3-n)-}$ (n = 0-3), (■); dithiophosphoric anions, $H_nPO_2S_2^{(3-n)-}$ (n = 0-2), (◆); trithiophosphoric anions, $H_nPOS_3^{(3-n)-}$ (n = 0-2), (▼); tetrathiophosphoric anions, $H_nPS_4^{(3-n)-}$ (n = 0-2).
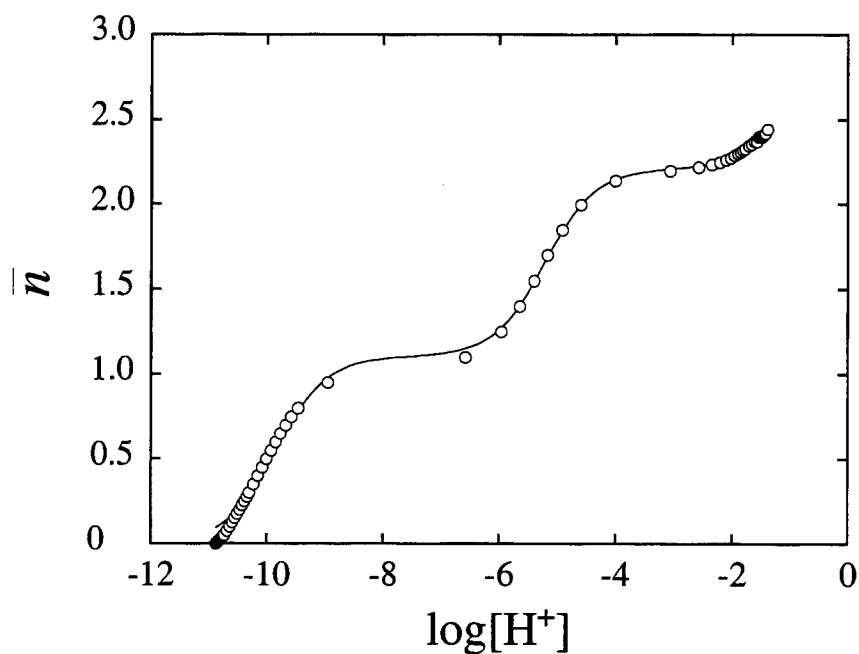
Fig. 6-4 Potentiometric titration curves of the protonation for a monothiophosphoric anions at 25 ± 0.5 °C and I = 0.10 (NaNO₃). Solid line refers to the calculated curve by the use of the pertinent parameters of log K_1 = 9.83, log K_2 = 5.22, and log K_3 = 0.83, see eqn.6-7.
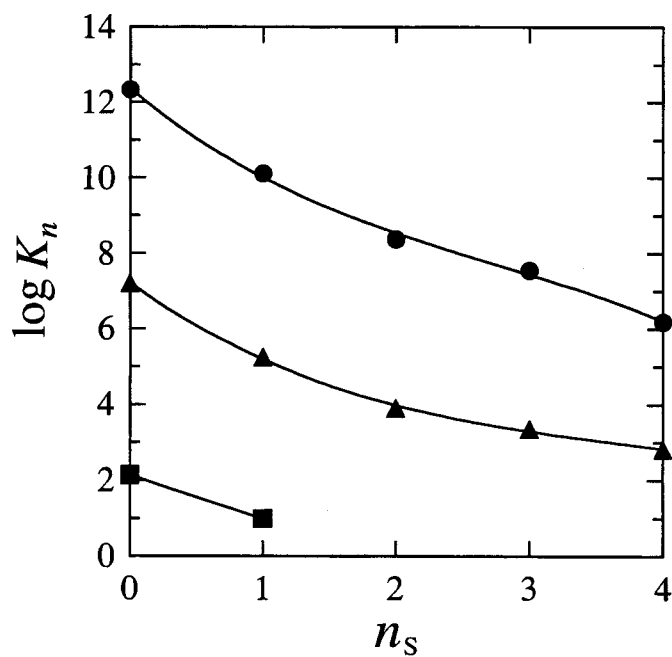
Fig. 6-5 Variation of the logarithmic successive protonation constants of various thiophosphate anions at 22 ± 1 °C against the number of sulfur atoms attached to the center phosphorus atom of the anions. (●); log K_1, (▲); log K_2, (■); log K_3.

6-14
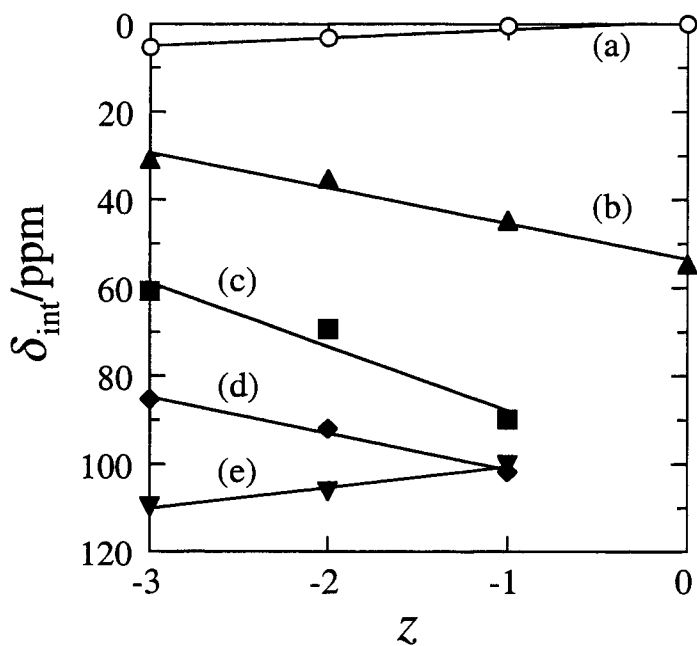
Fig. 6-6 Correlation of the intrinsic ^{31}P NMR chemical shifts of various thiophosphate anions and electric charge of the anions. ($\bigcirc$); orthophosphoric anions, $H_nPO_4^{(3-n)-}$ (n = 0-3), and the other symbols as in Fig. 6-3.
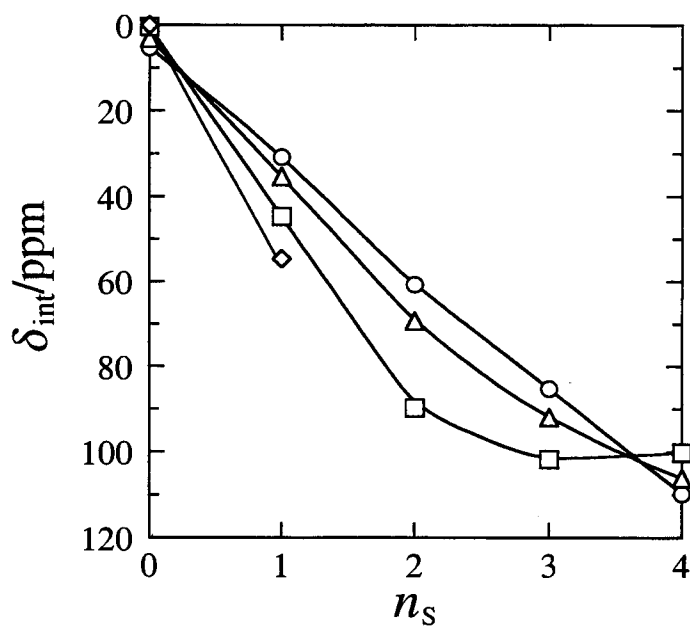

Fig. 6-7 Correlation of the intrinsic ^{31}P NMR chemical shifts of various thiophosphate anions and the number of sulfur atoms attached to the center phosphorus atom. ($\bigcirc$); free ligands, $PO_{4-n}S_n^{3-}$ (n = 0-4), ($\triangle$); monoprotonated anions, $HPO_{4-n}S_n^{2-}$ (n = 0-4), ($\square$); diprotonated anions, $H_2PO_{4-n}S_n^-$ (n = 0-4), ($\Diamond$); triprotonated anions, $H_3PO_{4-n}S_n^0$ (n = 0, 1).

6-15

Table 6-1 Logarithmic protonation constants of various thiophosphate anions[a] determined by the pH profiles of ^{31}P NMR chemical shifts of the anions at 22 ± 1℃ in aqueous solutions[b]. No supporting electrolyte was added.

	$H_n PO_4^{(3-n)-}$	$H_n PO_3 S^{(3-n)-}$	$H_n PO_2 S_2^{(3-n)-}$	$H_n POS_3^{(3-n)-}$	$H_n PS_4^{(3-n)-}$
$\log K_1$	12.33[c, d]	10.12 ± 0.02	8.37 ± 0.03	7.55 ± 0.05	6.19 ± 0.04
$\log K_2$	7.20[c, d]	5.25 ± 0.01	3.90 ± 0.01	3.35 ± 0.03	2.82 ± 0.03
$\log K_3$	2.15[c, d]	0.99 ± 0.01	–	–	–

[a]The errors given are *equimultiple* the standard deviation resulting from the non-linear least-squares calculations. [b] In the absence of D_2O for field-frequency locking. [c] From Ref. 17. [d] At 25 ℃, and no supporting electrolyte was added.

Table 6-2 Intrinsic ^{31}P NMR chemical shifts of various thiophosphate anions[a] determined by the pH profiles of ^{31}P NMR chemical shifts[b] of the anions at 22 ± 1℃ in aqueous solutions[c]. No supporting electrolyte was added.

	$H_n PO_4^{(3-n)-}$	$H_n PO_3 S^{(3-n)-}$	$H_n PO_2 S_2^{(3-n)-}$	$H_n POS_3^{(3-n)-}$	$H_n PS_4^{(3-n)-}$
$\delta_{L^{3-}}$/ppm	5.3[d, e]	30.83 ± 0.03	60.78 ± 0.06	85.25 ± 0.07	109.74 ± 0.02
$\delta_{HL^{2-}}$/ppm	3.1[d, e]	35.35 ± 0.03	69.36 ± 0.08	91.96 ± 0.13	106.17 ± 0.05
$\delta_{H2L^{-}}$/ppm	0.4[d, e]	44.75 ± 0.03	89.79 ± 0.11	101.77 ± 0.13	100.18 ± 0.09
δ_{H3L}/ppm	0[d, e]	54.71 ± 0.05	–	–	–

[a]The errors given as a footnote a of Table 6-1. [b] Referenced to external 85% H_3PO_4. [c] In the absence of D_2O for field-frequency locking. [d] Adapted from Ref. 18. [e] At 27 ℃, and saturated aqueous solution of Na_3PO_4 was used.

CHAPTER 7

General Conclusion

Protonation equilibrium studies by ^{31}P NMR chemical shift and potentiometry with a glass electrode have revealed the basicity of the non-bridging oxygen atoms of the $cP_3(NH)_n^{3-}$ ($n = 0\text{-}3$) molecules increases linearly with an increase in the number of imino groups which constitute the trivalent anion molecules, "n". The pronounced increase is not only due to the difference in the electronegativity of nitrogen and oxygen atoms, but also due to the tautomerism reaction between the phosphate units linked by the P-NH-P bonding. The intrinsic shift values of phosphorus nuclei in the $cP_3(NH)_n^{3-}$ ($n = 0\text{-}3$) molecules show good linearlity with the numbers of oxygen and/or nitrogen atoms bonded to the central phosphorus atoms, and the linearlity of the intrinsic shift values of protonated species is better than that of deprotonated species. It has been revealed that hydrogen bonding is formed among the phosphate groups belonging to the cyclic trimers, probably due to proximity of the neighboring phosphate units fixed to rigid rings.

By the metal complexation equilibrium studies, linearity has also been observed between the log β_1 values of the divalent metal ion complexes and the "n" value. By plotting the log β_1 values against the pK_a values, linear relationships have been observed in all complexation systems. The slope of the plots in the Cu^{2+} and Cd^{2+} ions systems are much higher than the Ca^{2+} system, which may indicate the direct participation of nitrogen atoms as well as oxygen atoms in the complexation. It was found that the complexation reaction in the Cu^{2+}- and Cd^{2+}-$cP_3(NH)_3^{3-}$ system is more endothermic than that in the Ca^{2+}-$cP_3(NH)_3^{3-}$ system, indicating that Cu^{2+} and Cd^{2+} ions bind electrostatically to the oxygen and/or nitrogen atoms of the $cP_3(NH)_3$ molecules.

The ^{27}Al NMR study has clarified the multidentate complexation profiles of the $cP_3(NH)_n$ ($n = 0\text{-}3$) molecules with Al^{3+} ions. The chemical shift values of respective peaks change upfield stepwisely with the number of the coordinating oxygen or nitrogen atoms of the $cP_3(NH)_n$ ($n = 0\text{-}3$) molecules. This "additivity law" between the intrinsic chemical shift values due to the stepwise multidentate complexes and the coordination number of the complex is obviously different from the additivity law which has been reported on the Al^{3+}-cP_n^{3-} ($n = 3, 4, 6, 8$) systems. We can see that the "new additivity law" observed in the ^{27}Al NMR chemical shift change upon binding Al^{3+} ion with the imino groups in the $cP_3(NH)_n$ ($n = 1\text{-}3$) molecules. From the peak area measurement

of the Al^{3+}-$cP_3(NH)_3^{3-}$ system, it was verified that the peak area ratio of the tridentate complex to didentate complex is unvaried. This ensures the successive complex formation is intramolecular reaction, whose equilibrium constant $K_{2\to3}$ is 0.27. By considering the ligand structure, it is anticipated the tridentate complexes of $cP_3(NH)_3^{3-}$ correspond to Al^{3+}-(N, N, N) and/or Al^{3+}-(N, N, O) type coordination. From these experimental evidences, we can conclude that the formation of tridentate complex found in the Al^{3+}-$cP_3(NH)_3^{3-}$ system, where an Al^{3+} ion is bound to the three equivalent nitrogen atoms. This result does not agree with the simple prediction based on HSAB trends that Al^{3+} ions coordinate to not the softer bridging nitrogen atoms but the harder non-bridging oxygen atoms. These peculiar coordination behavior are remarkably dependent on the high structural suitability, namely how well Al^{3+} ion fits into the cavity that the nitrogen donor atoms can provide for it.

In the Be^{2+}-$cP_3(NH)_3^{3-}$ system, separate NMR signals corresponding to free and complexed species have also been observed in both spectra. Based on an empirical additivity rule, the ^9Be NMR spectra have been deconvoluted. By the precise equilibrium analyses, the formation of mono- and bidentate complexes coordinated with non-bridging oxygen atoms has been verified. It was noteworthy that the formation of complexes coordinating with nitrogen atoms of the cyclic framework in the ligand molecule has been excluded in spite of some chemical similarities between Be^{2+} and Al^{3+} ions which originate from the closest charge/ionic radius. The high structural suitability affects the coordination behavior of Al^{3+}- and Be^{2+}-$cP_3(NH)_3^{3-}$ systems, hence the ionic radius of Al^{3+} ion (0.51 Å) and Be^{2+} ion (0.35 Å) is different for about 1.5 times, it seems to observe these difference between both coordination behavior. Instead, the formation of one-to-one (ML) complexes, one-to-two (ML_2), together with two-to-one (M_2L) complexes has been disclosed, whose formation constants have been evaluated $K_{ML} = 10^{3.87 \pm 0.03}$ (mol $dm^{-3})^{-1}$, $K_{ML_2} = 10^{2.43 \pm 0.03}$ (mol $dm^{-3})^{-2}$, and $K_{M_2L} = 10^{1.30 \pm 0.02}$ (mol $dm^{-3})^{-2}$, respectively.

The stepwise protonation constants of monothiomonophosphate, dithiomonophosphate, trithiomonophosphate and tetrathiomonophosphate anions have been determined by ^{31}P NMR chemical shift measurements in aqueous solution. In spite of the fast hydrolysis rate of the series of thiomonophosphate anions, the protonation processes of all thiomonophosphate anions may well be examined without any previous purification because the NMR signals corresponding to thiophosphate anions and hydrolysed residues can well be resolved. The successive protonation

constants decrease with an increase in the number of sulfur atoms bound to center phosphorus atom. It has been revealed that the logarithms of the stabilities of the proton complexes of the series of thiomonophosphate anions decreases "linearly" with an increase in the number of sulfur atoms which constitute the anions. The intrinsic ^{31}P NMR chemical shifts due to orthophosphate and tetrathiomonophosphate anions show up-field shifts upon the stepwise protonation of the anions, whereas the shifts due to mono-, di-, and trithiomonophosphate anions show low-field shifts upon that of the anions. Futhermore, an asymmetry of a molecule is related to the amount of the change of bond angles with a protonation and a complex formation, and it makes the nuclear screening drastically change. A symmetry of a molecular structure is related to the direction of the ^{31}P NMR chemical shift change due to the successive protonation of a ligand.

Acknowledgements